

THE PERFORMANCE OF LATERALLY LOADED
CROSS-BRACED TIMBER FRAMES

A report
submitted in partial fulfilment
of the requirements for the Degree
of
Master of Engineering
at the
University of Canterbury
by

B. L. DEAM

University of Canterbury
Christchurch, New Zealand.

1988

ABSTRACT

The overall behaviour of laterally loaded cross-braced timber frames is investigated. Frame behaviour is classified as ductile or non-ductile when subject to reverse cyclic loading. Individual Nailon plated joints were tested and a regression equation fitted to the load-displacement curves. The strength of Nailon plated joints loaded perpendicularly to the grain was investigated. Ten frames simulating diagonally braced light timber frame walls incorporating a variety of joint details were constructed and tested to failure. In addition, four diagonally braced frames with Nailon plated joints were tested. Two types of connection suitable for attachment of a frame to its supports were tested. A numerical model of Nailon plate was developed and used to predict the behaviour of a particular type of connector.

Toothplate connectors and light nailstrap bracing are identified as non-ductile elements in a frame. Frames constructed with Nailon plate are strong, stiff and ductile. Published design loads for nails in Nailon plate appear to be conservative. Frames must be detailed to prevent out-of-plane buckling of the timber members. Joints must be detailed to minimize the effects of combined perpendicular-to-grain tension and shear in the timber. More investigation is required on joints where this occurs.

ACKNOWLEDGEMENTS

The work described in this Thesis was carried out in the Department of Civil Engineering at the University of Canterbury and at Peter Stevens Limited of Christchurch. The author is grateful for the supervision of this project by Dr. J.A. Dean and Dr. A.H. Buchanan.

Financial assistance provided by The Earthquake and War Damages Commission is gratefully acknowledged.

The author also wishes to extend his gratitude to:

The Head of Department for the use of Departmental facilities and technical staff;

Peter Stevens Limited for the use of their floor space;

Peter Coursey for his help in the laboratory;

Stephen Coll of Gang-Nail N.Z. Ltd.;

Brian Rowland who contributed to the design and testing of the frames described in Chapter 4.

Marcus Edwards for his help with frame testing and draughting.

CONTENTS

CHAPTER	PAGE
ABSTRACT	i
ACKNOWLEDGEMENTS	ii
TABLE OF CONTENTS	iii
LIST OF NOTATION	v
I. INTRODUCTION	1
1. Timber as a construction material	1
2. Design approaches	2
3. Connection materials	3
4. Scope of this report	5
II. LOAD-DISPLACEMENT CURVES FOR NAILON PLATE	6
1. Introduction	6
2. Specimens	6
3. Test procedure	8
4. Test observations	8
5. Discussion	10
III. PERPENDICULAR-JOINT TESTS	22
1. Introduction	22
2. Specimens	22
3. Joint type 1	26
4. Joint type 2	26
5. Joint type 3	28
6. Joint type 4	28
7. Load-deflection curves	30
8. Discussion	32
IV. BRACED TIMBER FRAMES	33
1. Introduction	33
2. Frame F1	38
3. Frame F2	44
4. Frame F3	47
5. Frame F4	50
6. Frame F5	54
7. Frame F6	57
8. Frame F7	61

9. Frame F8	64
10. Frame F9	67
11. Frame F10	70
12. Discussion	72
V. NAILON PLATE FRAMES	73
1. Introduction	73
2. Frame 1	74
3. Frame 2	82
4. Frame 3	86
5. Frame 4	93
6. Discussion	97
VI. HOLD-DOWN TESTS	98
1. Introduction	98
2. Concrete fixing cleats	98
3. Prototype shearwall hold-down	104
4. Angle shearplate	108
5. Discussion	110
VII. NAILON PLATE JOINT MODEL	112
1. Introduction	112
2. Theory	112
3. Calibration of the model	115
4. Angle shearplate properties	118
5. Angle shearplate load-displacement curves	122
VIII. CONCLUSIONS AND RECOMMENDATIONS	124
1. Conclusions	124
2. Recommendations	125
REFERENCES	126
APPENDICES	127
A. Basic nail load computation	127
B. Program for computer model	129
C. Toothplated joint load computation	139

CHAPTER I

INTRODUCTION

Timber is one of the oldest construction materials but its properties and behaviour are still not well understood. Timber is the basic material used for the construction of most domestic dwellings and some larger commercial buildings in New Zealand. Research is necessary to determine the properties of this material before more effective use can be made of it in large structures. In contrast, steel and reinforced concrete are used for most large structures today. This is because they have consistent properties and have been subjected to intensive study.

1. TIMBER AS A CONSTRUCTION MATERIAL

Timber strength is variable, varying even between samples taken from the same tree. Timber is a brittle material in some directions. Failure can occur with little warning. These two properties suggest that a structure constructed with timber should be designed to prevent failure of the timber members. This is achieved by incorporating other materials into the structure which are ductile (to prevent brittle failure of the timber), and have a predictable strength.

Providing ductile connections between the timber members is a good design philosophy. Ductile connections provide weak-links which prevent failure of the timber through over-loading, and the required ductility of the structure. This enables the behaviour of the structure to be based upon the known behaviour of the connections.

2. DESIGN APPROACHES

Design of timber structures in New Zealand is regulated by two design codes of practice. NZS 4203:1984 [9] gives design loadings to be applied to the structure and NZS 3603:1981 [8] gives the methods for evaluating how the structure will resist those loads.

There are two methods for ensuring that a structure will not collapse. One method is to factor the loads on the structure to obtain a larger load and designing the structure to resist this. This is the strength method defined in the Loadings Code, NZS4203:1984. The 'Alternative method', NZS 4203:1984, factors the material strength down. The loads for this design method remain unchanged. This is the design method which the Timber Design Code, NZS 3603:1981, requires to be used.

Gravity loadings as defined by NZS4203:1984 are not considered in this project report as they have an easily predicted magnitude and are applied only in one direction. Wind or seismic (abbreviated wind/seismic) loading, however, places loads on the structure which have a less well defined magnitude, alternate in direction and are of a considerably shorter duration than dead loads.

The structure must be designed to resist the maximum possible wind load without excessive deformation or failure of any components.

Seismic loads are the least predictable. The design load is the equivalent static load on the structure resulting from the expected earthquake, assuming that the structure behaves elastically. This load may be reduced if the structure is expected to behave in a ductile manner. The size of this reduction is dependent on the expected ductility of the structure. The reduction increases as the ductility increases. Part of the scope of this report is to determine the ductility of timber frames .

Dean and Buchanan [1] have presented a method for establishing the seismic design loadings based the structural type. Two categories of structure were defined, according to whether the structure is ductile or non-ductile. This ductility is dependent on the external connections as well as the connections within the timber structure.

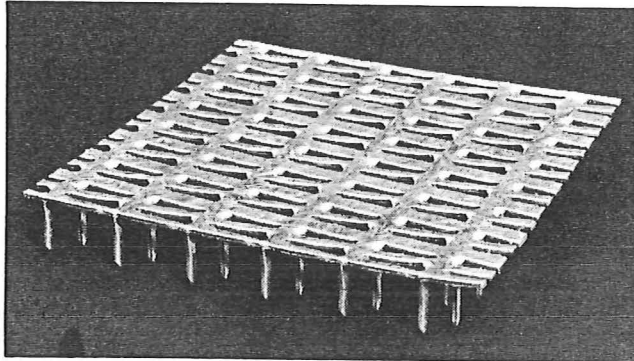
Two types of frame are described in this report, the first type (described in Chapter 4) is classified as non-ductile and the second type (described in Chapter 5) is classified as ductile. Reverse cyclic loading was applied to whole frames to determine their overall response.

The properties of the joints in a structure are important so individual joints were tested to determine their behaviour. This report describes the behaviour of both internal and external joints.

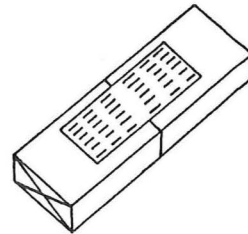
3. CONNECTION MATERIALS

There are two types of connection which are reasonably quickly and easily attached to timber members; toothplates with teeth integral with the plate material and Nailon plate with prepunched holes through which nails may be driven.

Toothplates, such as Gang-Nail GN10 [4] (fig. 1.1(a)), are galvanised steel plates which have teeth stamped out and bent perpendicular to the plate. The teeth are pressed into the timber members (fig. 1.1(b)) to form the connection. They are always used in pairs on opposite faces of the timber members. This type of plate has a high tooth density within the plate and is rapidly pressed into the timber with a large press. This connector is mostly used for light truss construction.



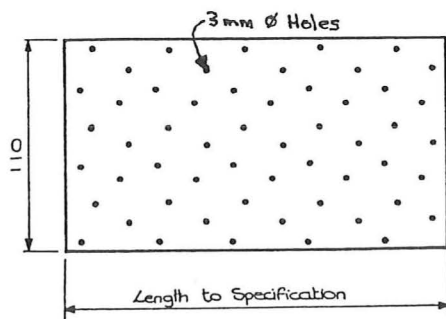
(a)



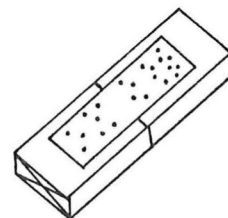
(b)

Figure 1.1 a) Toothplate connector and b) Resulting connection.

Nailon plate (fig. 1.2(a)) is thin steel plate, between 1 and 3mm thick, which has a series of pre-punched holes in it. Nails are driven with a hammer through the holes into the timber member (fig. 1.2(b)). Nailon plate [6] is 110 mm wide, 1 or 2 mm thick and accommodates 11 Nails per 40 mm of length.



(a)



(b)

Figure 1.2 a) Nailon plate and b) The resulting connection.

4. SCOPE OF THIS REPORT

The following is a summary of the following Chapters.

2. The load-displacement relationship for connections using Nailon plate is investigated. Six joints were tested and an empirical equation for individual nail behaviour is presented.
3. Four types of Nailon plated frame corner joint were tested. In each joint type one of the timber members was loaded perpendicularly to the grain. The effect of varying the placement of the nails within the timber member was investigated.
4. Ten 2 m x 2 m timber frames were constructed to simulate diagonally braced frames in light timber construction. The frames were tested to determine the response of the connectors to cyclic loading.
5. Four 2 m x 2 m diagonally braced timber frames with 150 x 50 mm timber members and Nailon plate joints were tested to determine the ductility of the connections.
6. Two commercial types of external "hold-down" connection were tested to determine the stiffness of these types of connection positioned between a frame and its supports.
7. A numerical model of a Nailon plate connector is developed and used to predict the behaviour of connections constructed with flat or folded Nailon plate.

CHAPTER II

LOAD-DISPLACEMENT CURVES FOR NAILON PLATE

1. INTRODUCTION

In this chapter the behaviour of the connection of Nailon plate to timber is described. The load-displacement behaviour of joints representative of a splice within a straight member and connections between perpendicular members were both tested.

The relationship between the joint load and the total joint displacement was obtained from the tests. Quantifying this relationship allows the analysis of a complete frame by superposition of the member and joint deformations.

Previous researchers [3, 5, 11] have obtained load vs displacement relationships for various types of nailed joint. They analysed timber to timber, plywood to timber and steel plate to timber connections. The latter relationships are not representative of joints formed with 1 mm thick Nailon plate because thicker steel plates (3-5 mm thick) were used. These thick plates provide clamping of the nail near the nailhead, forcing the nail into a double curvature bending mode. Out of plane deformations of the plate itself are more likely to develop in the Nailon plates than in plates over 3 mm thick.

2. SPECIMENS

Six specimens were constructed from ex 150 x 50 rough sawn, dry *Pinus Radiata*, and three of these were tested with parallel-parallel connections, where the grain and loading directions are the same for both pieces of timber (subsequently referred to as a 'parallel' connection, fig. 2.1(a)). The other three were tested with parallel-perpendicular connections (referred to as a 'perpendicular' connection, fig. 2.1(b)).

A 200 mm length of 110 x 1 mm Lumberlok Nailon plate was placed across the joint on both sides of the timber members and secured with ten 35 x 3.15 mm diameter galvanised flathead nails (Lumberlok 'product nails') [6] in each nailgroup (see Groups A,B,C,D in fig. 2.1). This gave a rated wind/seismic load of 10 kN for the joint based on Lumberlok data [6]. The rated wind/seismic load based on NZS 3603:1981 [8] is 8.0 kN. This load includes a factor of 1.25 (allowing an increased load because of the steel side plate) but not the reduction factor K_{13} (a reduction for joints with more than one nail).

Requirements for nail spacing according to NZS3603:1981 were not adhered to for the nail to edge-of-member distances, or along the grain in nailgroups C or D (fig. 2.1(b)). There was some variability of group nailing patterns between specimens, as only 10 of the available holes in the Nailon plate were filled, but it was not expected that this would significantly affect the overall behaviour of the joint.

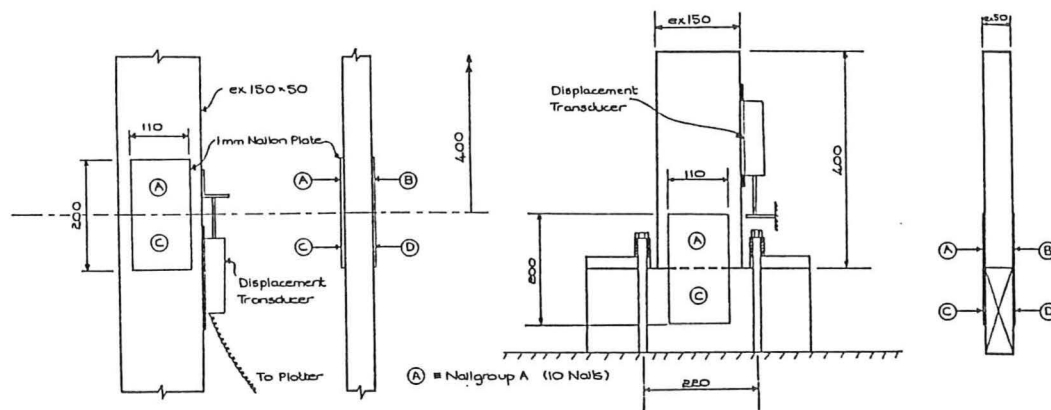


Fig 2.1 Construction Details of (a) parallel-parallel and (b) parallel-perpendicular specimens

3. TEST PROCEDURE

Testing was carried in a displacement-controlled machine at a rate of 2 mm/minute. Initially the joint was loaded in tension (assumed positive) to its computed target wind/seismic load, unloaded, loaded to an equal magnitude in compression and unloaded again to complete one loading cycle. A second loading cycle was then applied with the same target load as the first. The target load was then increased by an increment equivalent to wind/seismic load or half of wind/seismic load for each subsequent two loading cycles. The cycling was stopped when it was obvious that the specimen was displacing by a large amount with no increase (or even with a decrease) in sustained load.

The second two of the perpendicular tests were carried out monotonically in tension as it was evident that the cycling produced a bounding curve similar in shape to the expected monotonic curve.

4. TEST OBSERVATIONS

All of the specimens behaved in a similar manner. There was no significant separation between the plate and the timber until the displacement of the nailgroup reached about 10 mm (3 nail diameters), at which point the nails began withdrawing from the timber.

It was observed that the displacement of nailgroup A (fig. 2.1(a)) was different to that of C but that the proportion of displacement of group A to that of C remained constant for most of the test. A similar but slightly different proportional constant applied for groups B and D. This was not true, however, for large joint displacements where two of the nailgroups (either A and B or A and D) displaced no further, as all of the joint displacement took place in the other two groups.

In Parallel test 2, two of the nails were too close to the end of the timber and caused small pieces of timber to be pushed out into the gap between the ends of the timber members. These pieces then jammed between the timber members as the joint closed in compression.

The bent shape of the nails in all of the joints was similar, bending at a point approximately 4 nail diameters from the surface of the timber after a nailslip of 2 nail diameters was attained. Figure 2.2 shows the bent shape of the nails as the joint was cycled to increasing displacements. In the joints which were loaded to failure, the nails began to withdraw from the timber after displacing about 3 nail diameters at the surface. This caused separation between the Nailon plate and the timber, moving progressively from the end of the Nailon plate toward the centre of the joint, as the joint displacement increased.

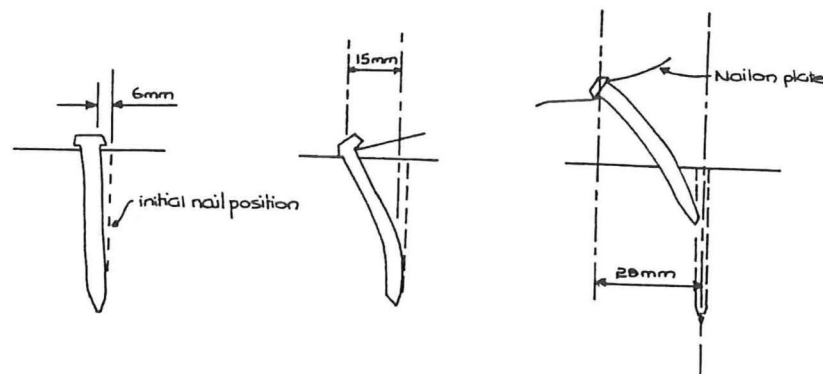


Figure 2.2 Nail behaviour in response to increasing deformation

Little curvature developed in the nail between the head and the point of bending for both parallel-to-grain and perpendicular-to-grain nailhead displacements. The deformation pattern of the timber around the nails was not similar, with the nails splitting the timber apart in the parallel case and tearing through the fibres in the perpendicular case (fig. 2.3).

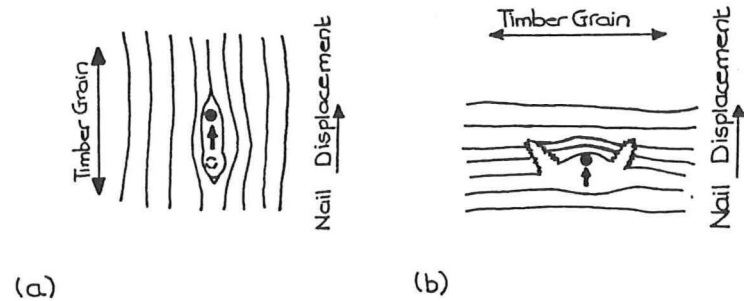
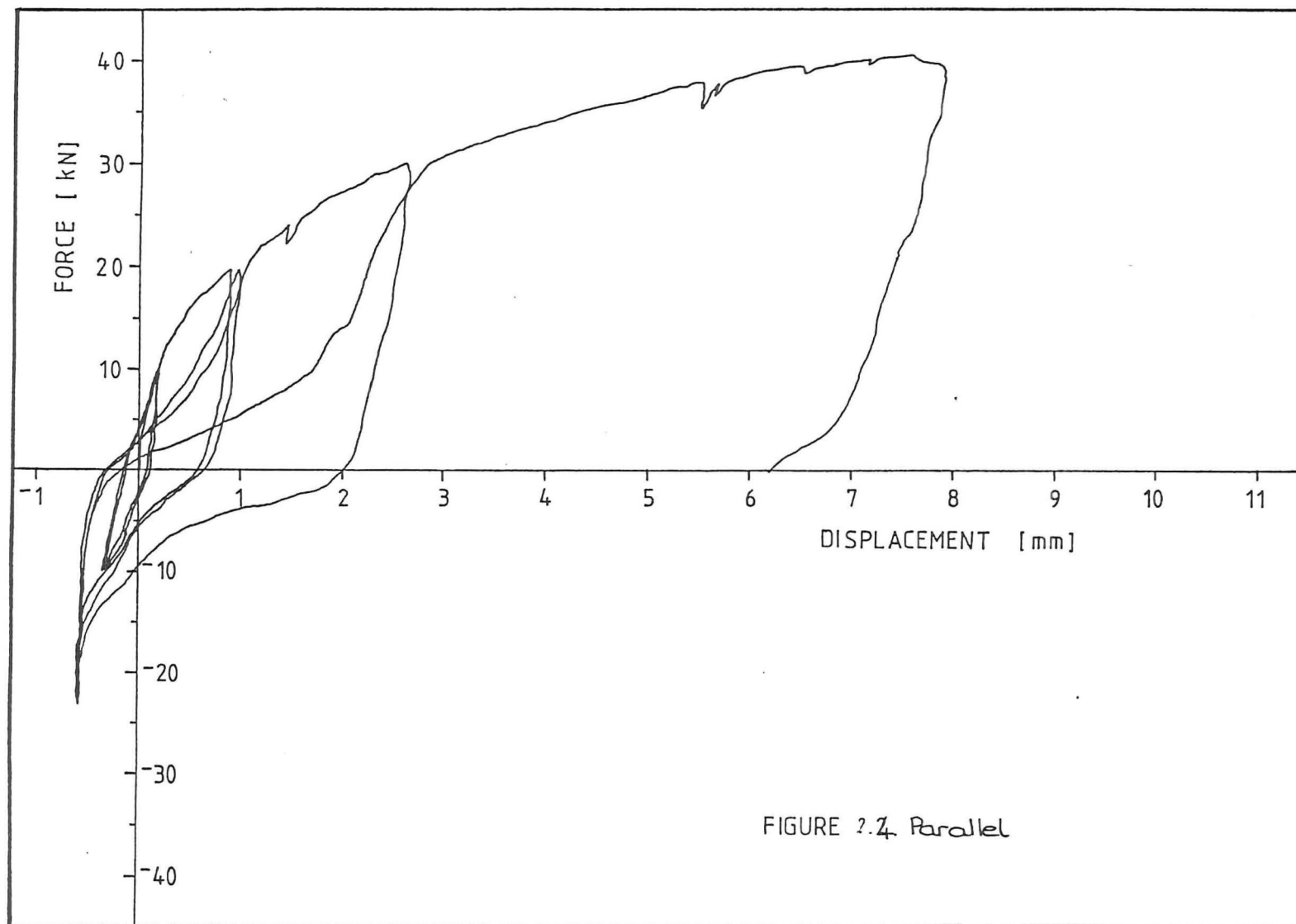
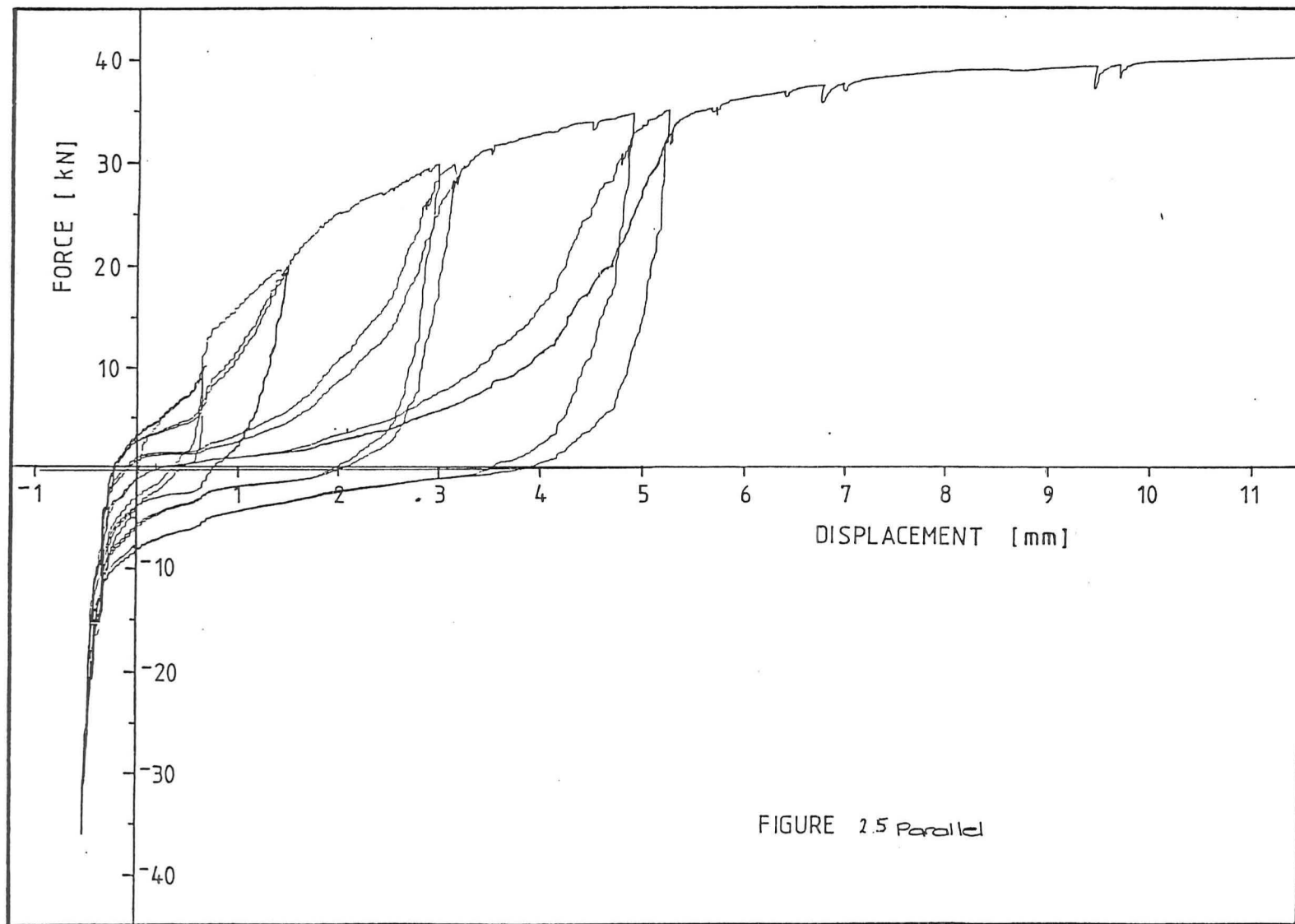


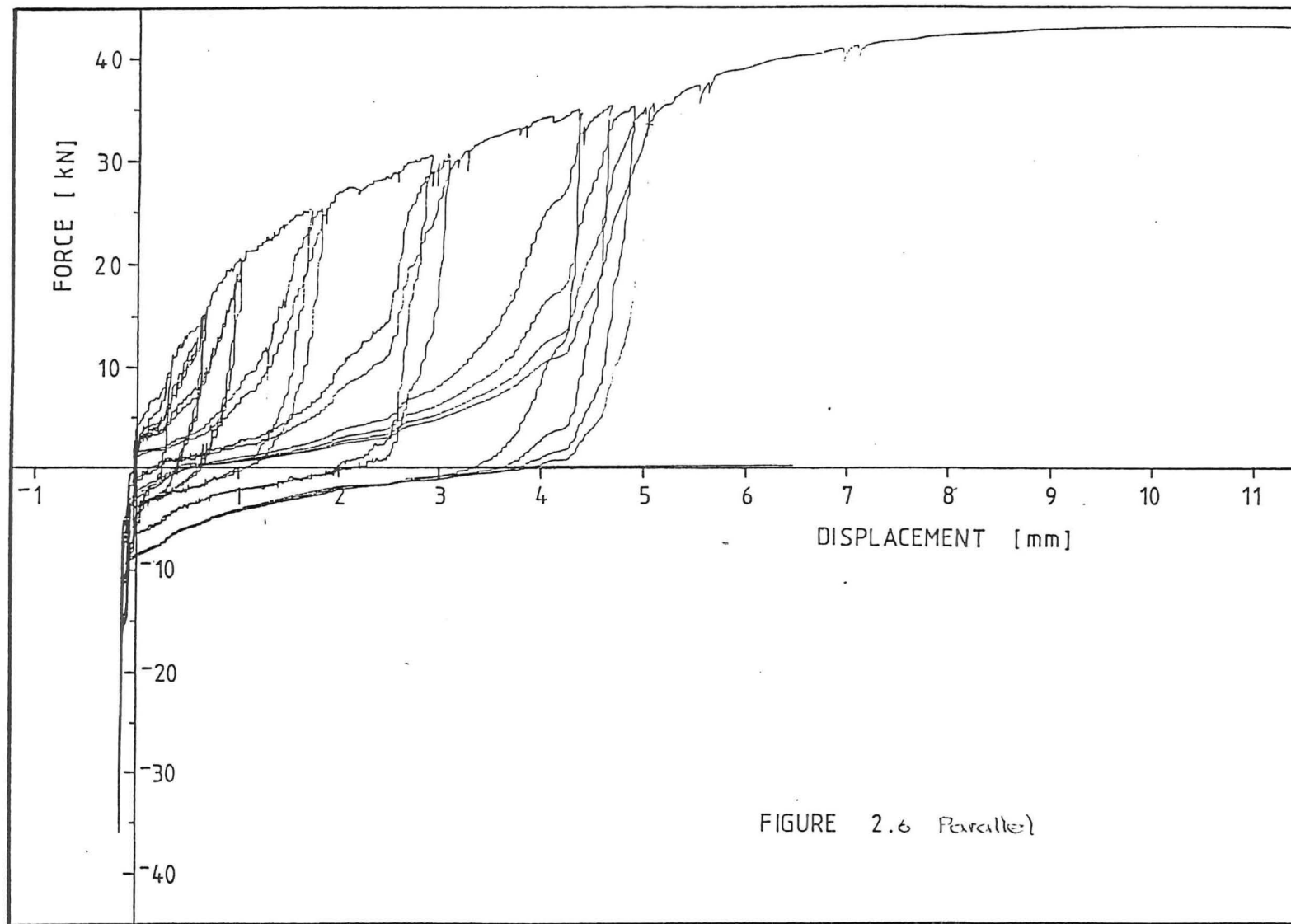
Figure 2.3 Timber behaviour with nail loaded a) parallel-to-grain and b) perpendicular-to-grain.

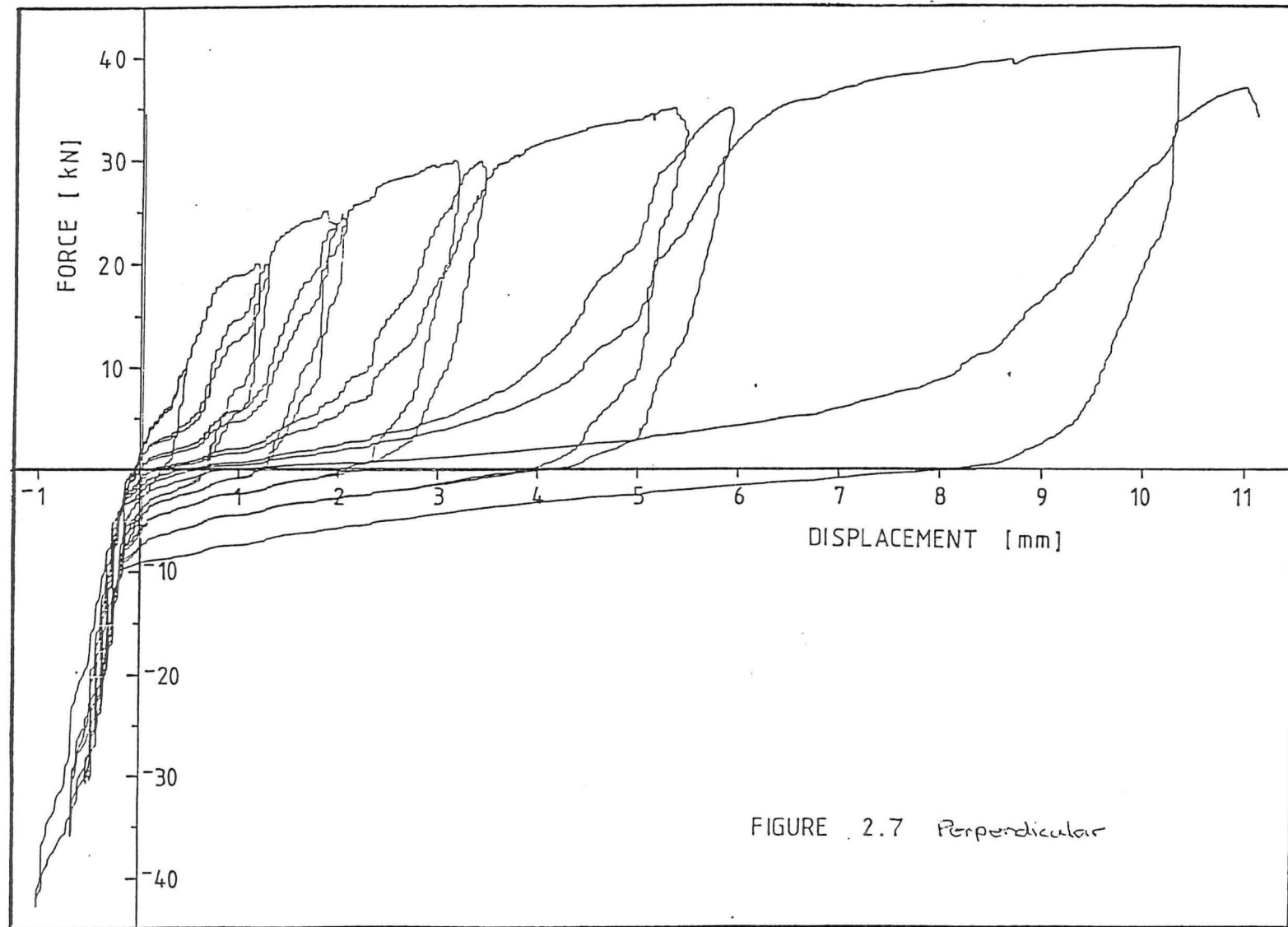
5. DISCUSSION

Figures 2.4 to 2.9 give the load-displacement plots for the six tests. The plots exhibit characteristics typical of nail-timber connections. The bounding curve, equivalent to the monotonic curve, has an initially high stiffness which decreases with increasing displacement, until a point is reached where the joint has reached its ultimate load. After this the load decreases for an increasing displacement. The monotonic curve is followed wherever the nails are being displaced further than any previous position attained in the history of the joint.









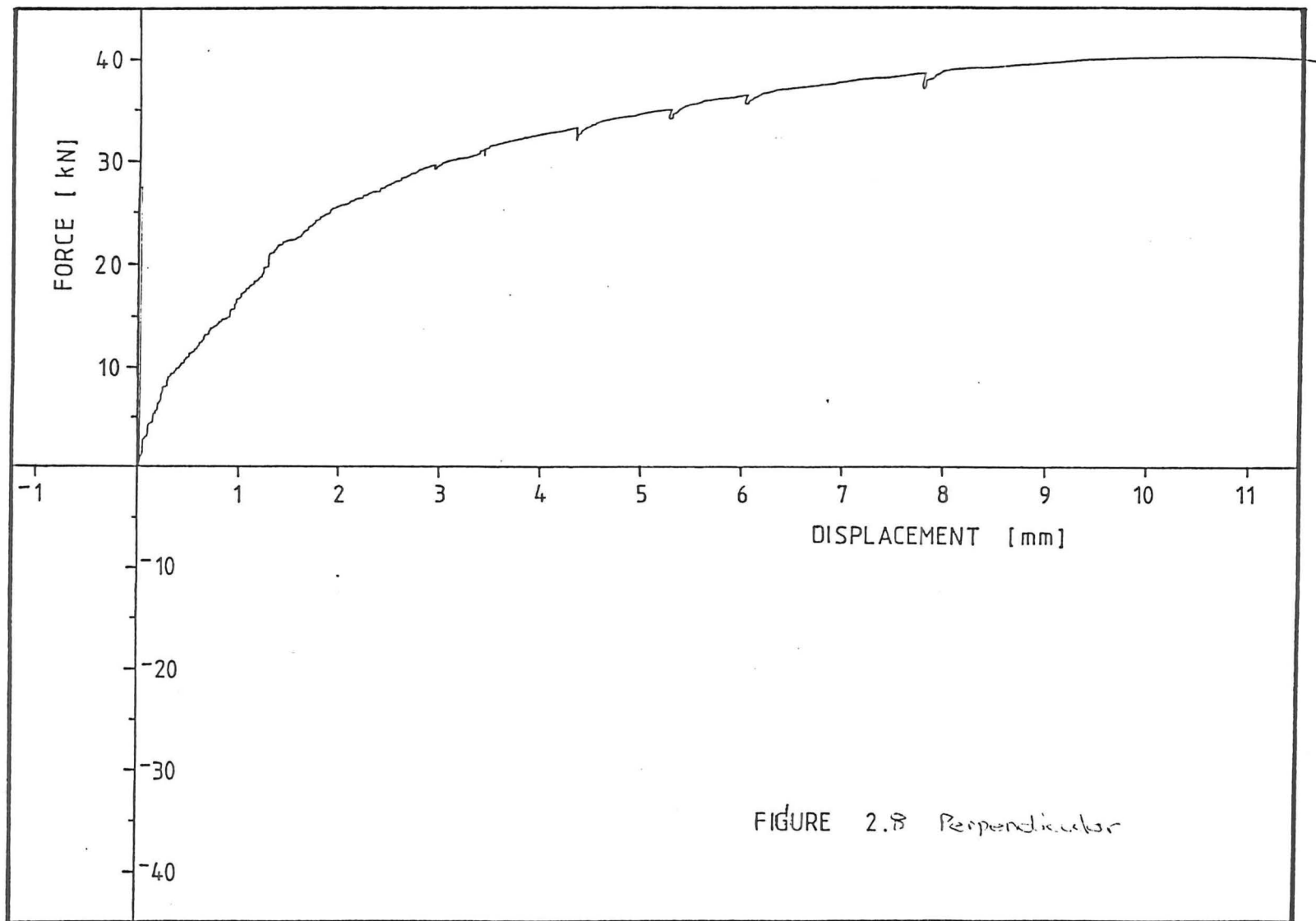
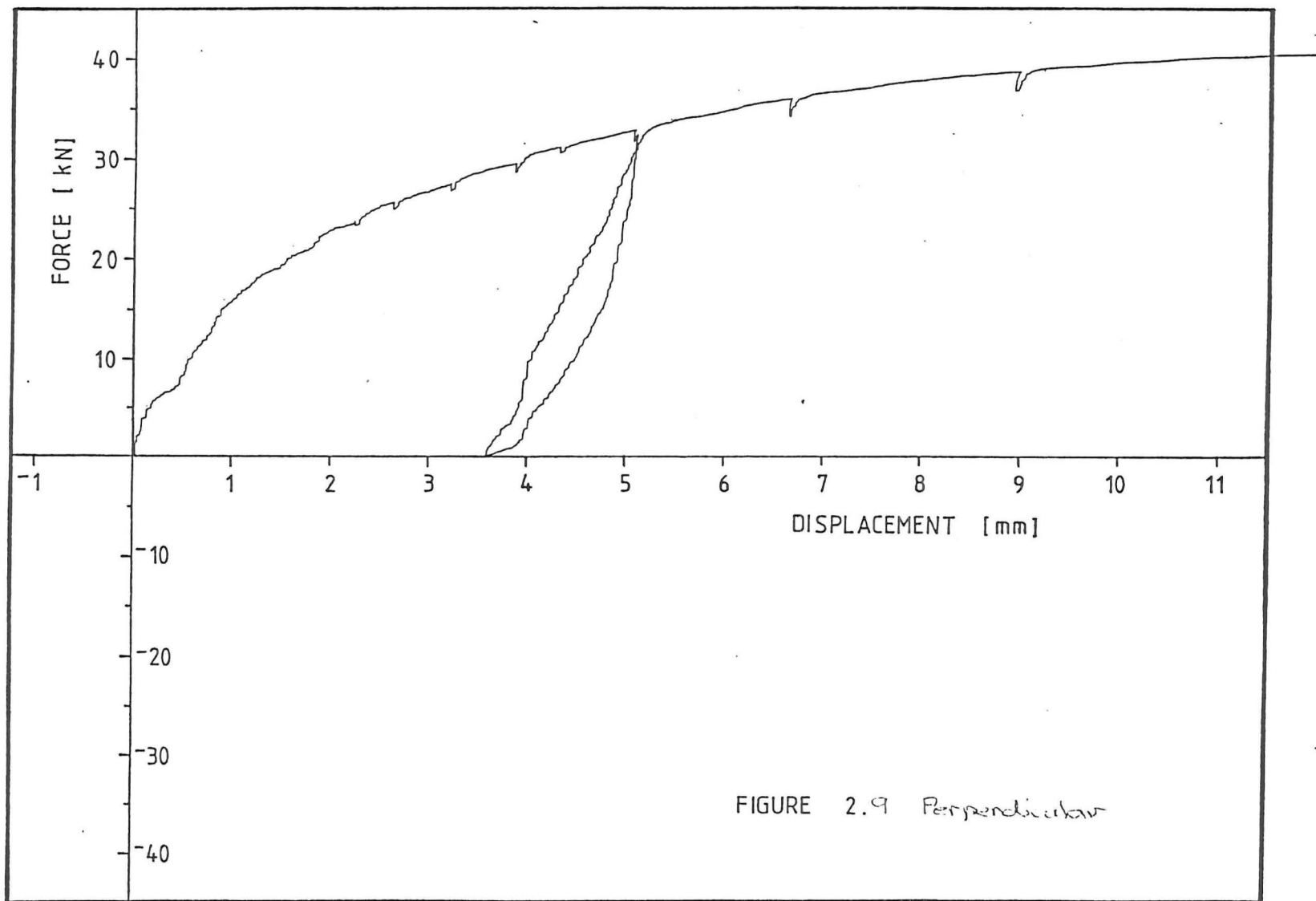


FIGURE 2.8 Perpendicular



The hysteresis loops, or plots of load-displacement for a complete loading cycle of positive and negative load, are also similar to those of ductile timber structures. During loading in the positive direction, the monotonic curve is followed unless the joint has been displaced further in a previous cycle. In this case, the stiffness is very much lower until a position is reached where the nails again bear against the timber, resulting in increased stiffness, almost attaining the initial tangent stiffness. The stiffness reduced again to follow the monotonic boundary curve as it is approached. As the load is released the joint returns elastically a small amount toward its initial position, the remainder of the deformation being irrecoverable.

This behaviour in structures has been idealized previously by Stewart et al. [2] as that of a slackness oscillator, i.e. a mass oscillating between two springs of equal stiffness (fig 2.10(a)). A single joint has a response more consistent with the oscillator shown in figure 2.10(b), but a complete frame will have some joints in tension and others in compression so that the Stewart model is a realistic model of the overall behaviour.

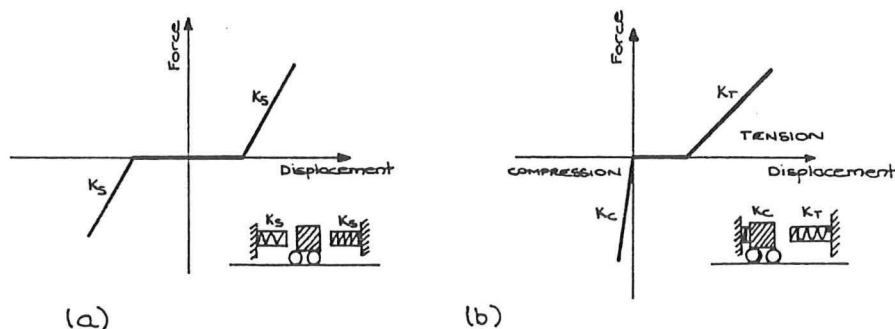


Fig 2.10 Idealized elastic responses incorporating slackness

(a) For the structure as a whole [2].

and (b) For an individual joint.

A two-part empirical regression curve (fig 2.11(a)) has been fitted as an average of all of the test plots (fig. 2.11(b)) and is used as a basis for the numerical model developed in chapter 6. Equation 2.1 gives the relationship between the force on one nail and the total joint displacement (Δ), and equation 2.2 relates the force to the nailgroup displacement (nailslip (x)) of the individual nails within a nailgroup (i.e. not that of the joint).

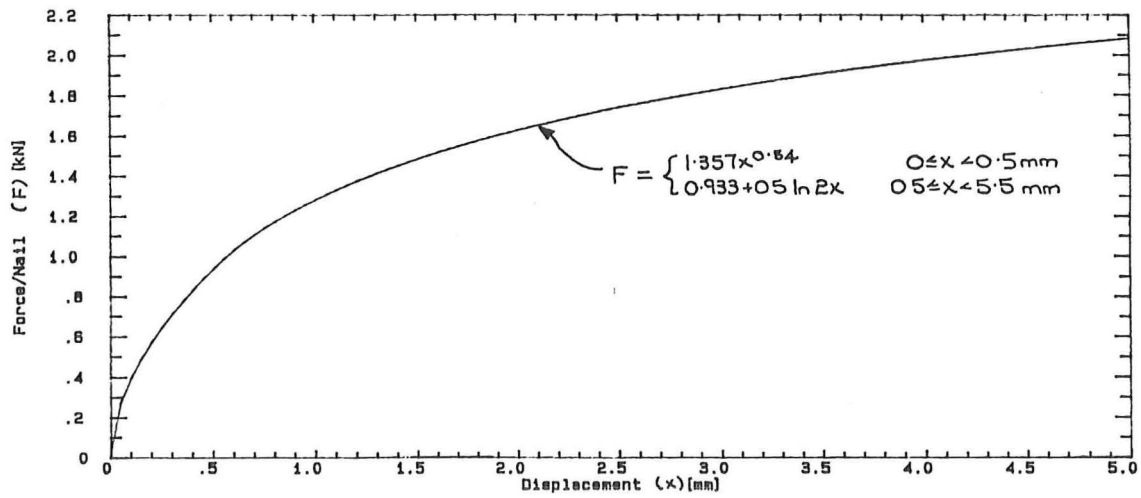
$$F = \begin{cases} 0.933 \Delta^{0.54} & 0 \leq \Delta < 1.0 \text{ mm} \\ 0.933 + 0.5 \ln \Delta & 1.0 \leq \Delta < 11 \text{ mm} \end{cases} \quad (2.1)$$

$$F = \begin{cases} 1.357 x^{0.54} & 0 \leq x < 0.5 \text{ mm} \\ 0.933 + 0.5 \ln 2x & 0.5 \leq x < 5.5 \text{ mm} \end{cases} \quad (2.2)$$

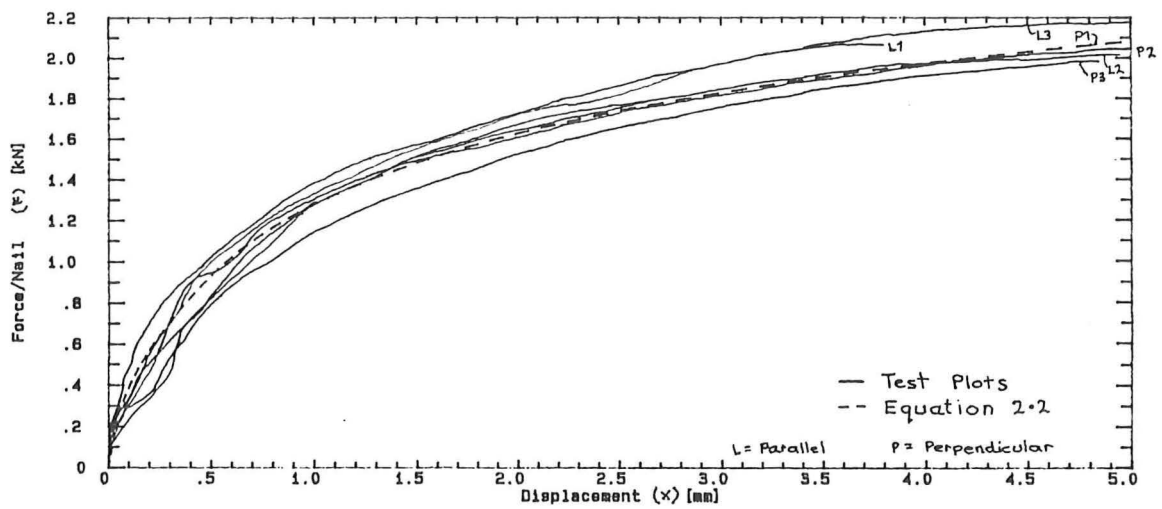
where F = load on one nail in kN
 Δ = total joint displacement in mm
 x = timber-plate nailslip in mm

The ultimate load of 2 kN / nail was attained at a nailslip (x) of 6 mm on average (i.e. 12 mm gap between the timber members). This would be an unacceptably large displacement for non-seismic loading situations. For this reason, some timber design codes require that the basic nail loads must be derived from the load for a nailslip of 0.4 mm, or a portion of the ultimate load, whatever is smaller.

The nail load at 0.4 mm nailslip lies in the range of 0.7 to 0.9 kN per nail within the nailgroup, with equation 2.2 giving 0.83 kN. For all 6 tests the individual nail loads reached 1.0 kN before 0.8 mm nailslip was attained. Table 2.1 gives the basic nail load computed according to the procedure in NZS 3603:1981 Appendix A, the basic load from Lumberlok [6] data and the NZS 3603:1981 nail load (NZS 3603:1981 Table 11 Basic working load of 214 N multiplied by 1.25 for metal sideplates). The calculations are presented in appendix A.



(a)



(b)

Figure 2.11 a) Empirical regression curve from Equ. 2.2.
b) Test plots.

Source	Basic N	Ultimate N
From this test series	580	2000
Lumberlok Catalogue	340	1500
NZS 3603:1981	268	--

Table 2.1 Comparison of nail loads for a 3.15 mm nail.

There appear to be large differences of allowable nail loads between the different sources of data.

The regression equation (Equ.2.2) is plotted again in figure 2.12 with the regression equations presented by Edwards [3] and Thurston [11] for comparison. The equations given by both researchers were for different nail diameters, so they have been scaled in Figure 2.12 to the common diameter of 3.15 mm. This scale factor was obtained as a simple ratio of the respective basic nail loads taken from NZS 3603:1981 e.g. the 2.80 mm nail (basic nail load 171 N) used by Edwards required that his equations be scaled by $214/171 = 1.25$ to obtain the equivalent load for the 3.15 mm nail (basic nail load 214 N).

The end distances of 15 to 25 mm between the nail and the end of the timber appeared to be adequate. The two nails closer than 15 mm did cause pieces of timber to push out into the gap, but it cannot be determined whether this has any detrimental effect on joint strength. These distances were smaller than the 38 mm (12 fastener diameters) minimum allowed by NZS 3603:1981. The timber members did not split. This may not be true of joints which are constructed with green timber and tested after allowing to dry.

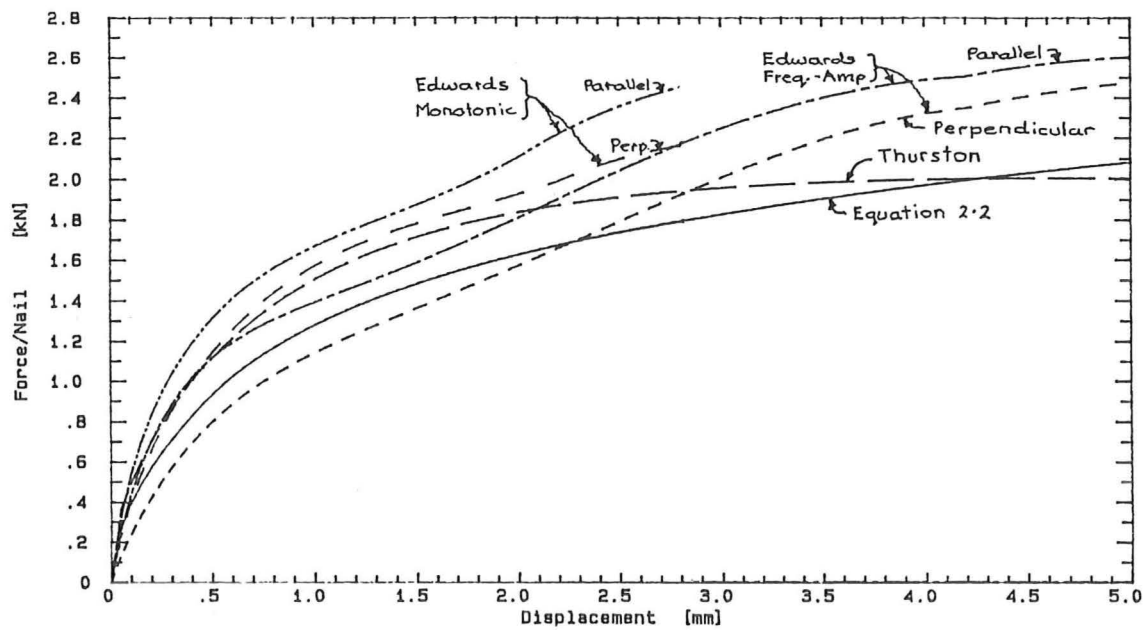


Figure 2.12 Comparison of regression equations.

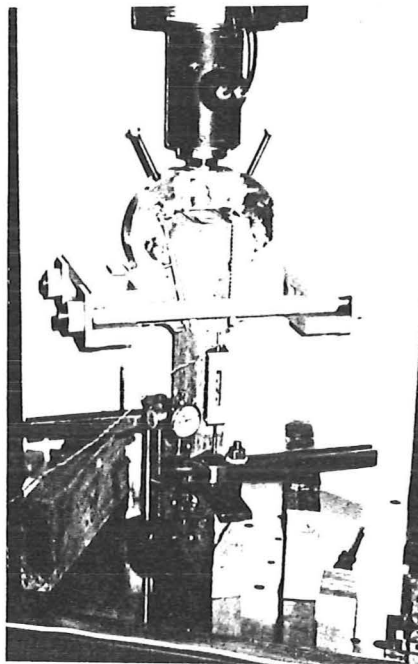


Plate 2.1 Testing a perpendicular joint.

CHAPTER III

PERPENDICULAR-JOINT TESTS

1. INTRODUCTION

This Chapter describes the testing of joints representing the corner joints of a diagonally braced frame with Nailon Plate connections. The testing procedure described in Chapter 2 for determining the perpendicular-to-grain load-displacement relationship gave results representing nail behaviour within the joint, but did not give an indication of how an actual joint might fail before the nails attained their ultimate load. The purpose of the series of tests described in this chapter was to determine how the joint behaved without the influence of the holding down plates, used in the tests described in Chapter 2, for the perpendicular timber member close to the joint.

The effect of the pattern and placement of the nails within the nailgroup in the perpendicular member was also investigated to determine which patterns may significantly reduce the strength or ductility of a joint.

2. SPECIMENS

Four pairs of test joints were incorporated into the loading frames shown in Figure 3.1. Two identical joints were incorporated within each frame because of the eccentric loading a single joint would have imposed on the testing machine. The same lower three members were used in all of the frames. The nails in the nailgroup being tested, and the top member were replaced for each new test. The 4 types of joint tested are summarized in Table 3.1 and the details of the joint construction are shown in Figure 3.2.

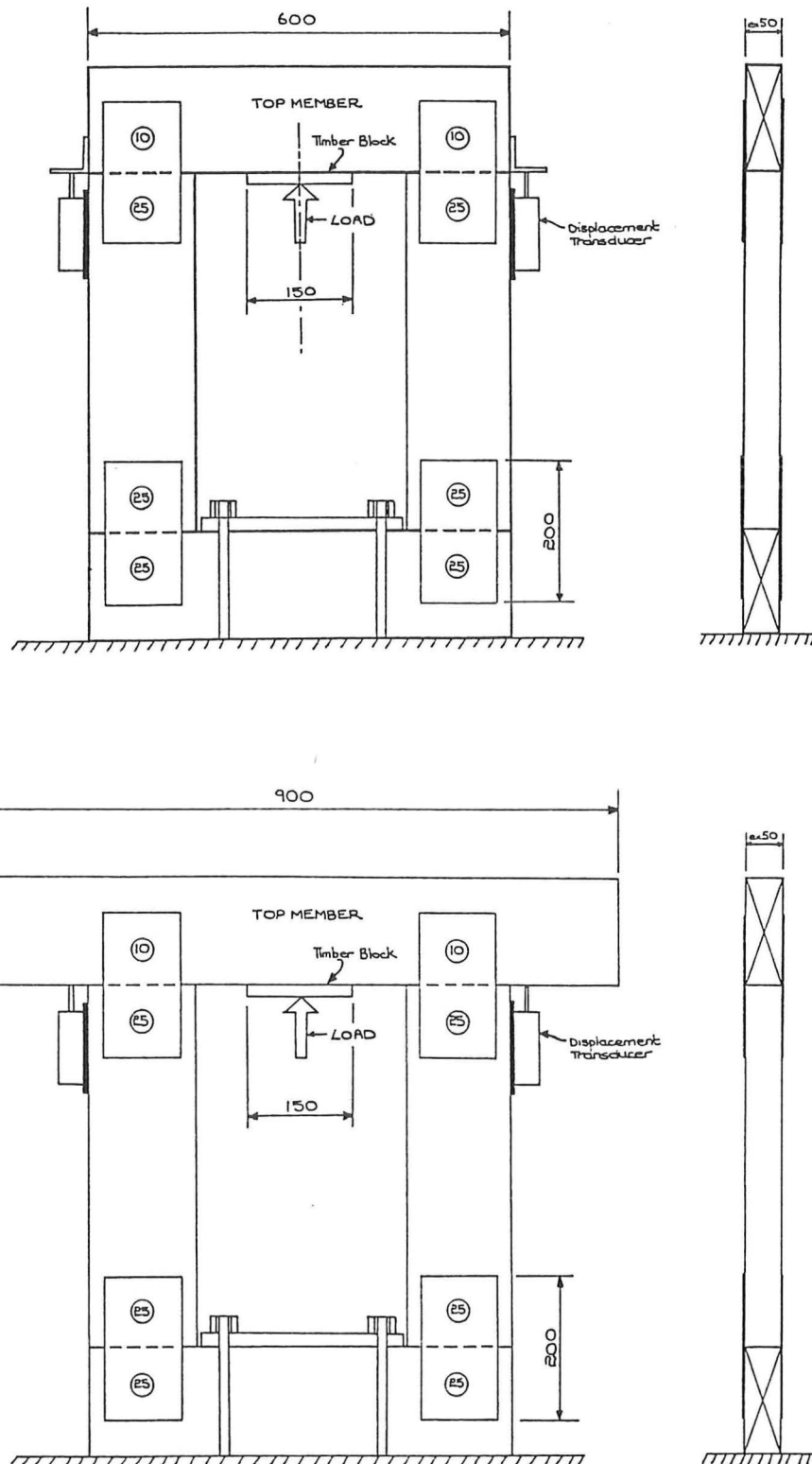


Figure 3.1 Loading frames

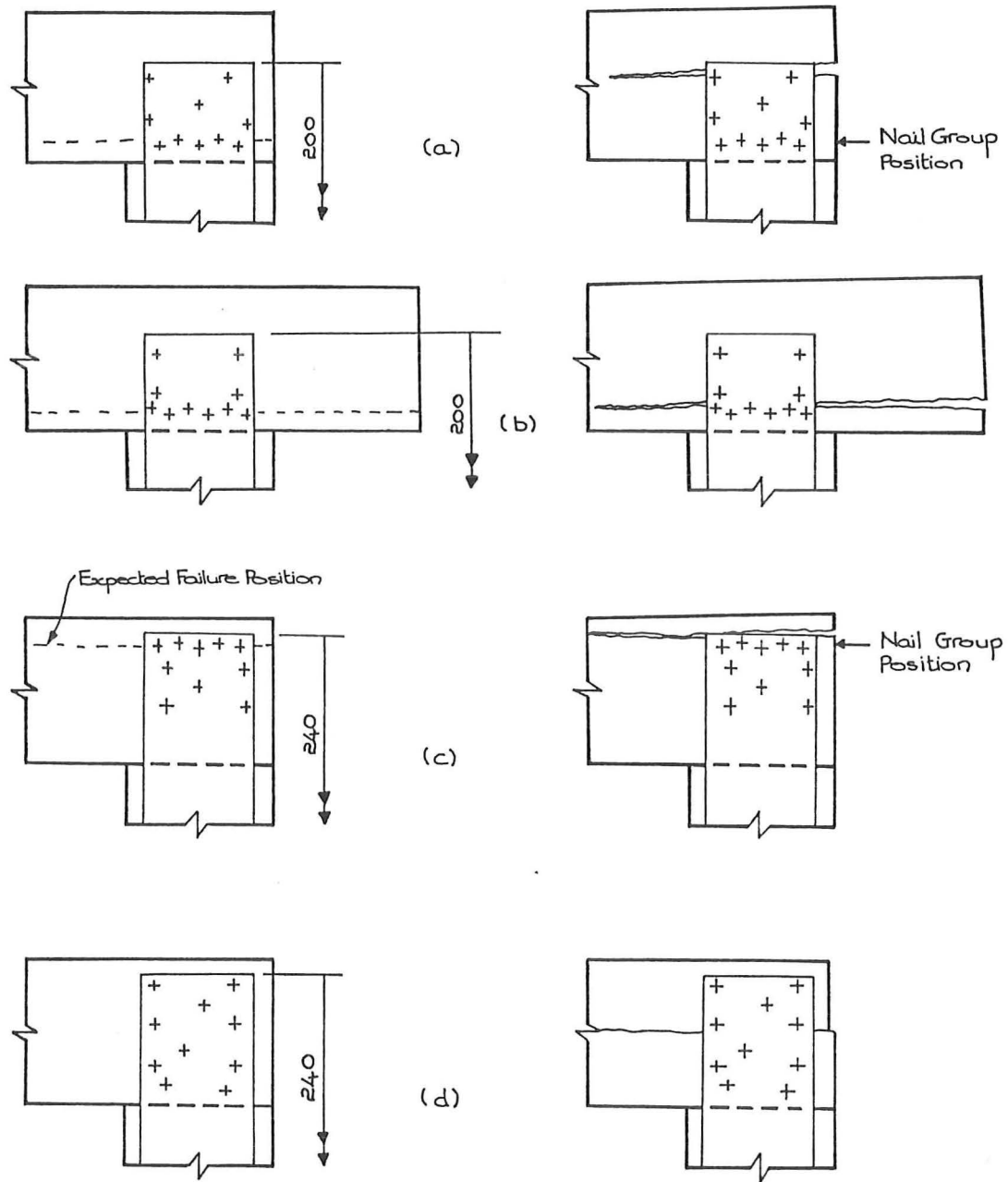


Figure 3.2 Joint construction and failure patterns.

Joint Type	Nail * Positions	Top member length	Nailon length
1	Bottom	600	200
2	Bottom	900	200
3	Top	600	235
4	Distributed	600	235

* Nail group position within depth of perpendicular member, see Figure 3.2

Table 3.1 Summary of joint types.

The timber used was from the same pack of ex 150 x 50 rough sawn dry Radiata Pine as the joints described in Chapter 2. For testing joint types 1 and 2, the same 200 mm lengths of 110 x 1 Nailon plate were used. These were then removed from the loading frame and 235 mm lengths nailed to the frame for testing joint types 3 & 4. Nailgroups in the joints being tested in the top perpendicular member incorporated 10 nails and there were 25 nails in the nailgroups within the other half of the top Nailon plates and the lower plates of the frame. This was done to ensure the test joints would fail before the other joints in the frame.

The Chapter 2 results indicate that the expected capacity of 20 nails is 40 kN. At this load, the bending stress in the outer fibres of the timber is 32 MPa. The NZS 3603:1981 Table 2 lower 5 percentile strength of No 1 Framing timber is 13.2 MPa. The timber used was free from major visible defects so it was expected that one of the pair of joints would fail before timber flexural failure. The effects of shear were neglected, as allowed by NZS 3603:1981, where the joint face was less than the depth of the beam from the inside face of the support.

Table 3.2 gives the Chapter 2 capacity load, the Lumberlok wind/seismic load and the load at which failure occurred for the four joint types.

Joint Type	Nail Capacity	Lumberlok wind/seismic	Joint Load
1	40	15	20
2	40	15	17
3	40	15	25
4	40	15	30

(kN)

Table 3.2 Joint types and loads

3. JOINT TYPE 1

This joint pair was constructed with 200 mm lengths of Nailon plate, with the top member extending between the outside faces of the vertical members (fig. 3.2(a)). Five of the 10 nails in each of the nailgroups in the top member were positioned close to the bottom edge of the timber member. It was expected that the nailing pattern would cause the bottom edge of the timber to split away from the remainder of the member as shown in Figure 3.2(a).

The failure of one joint at an applied load of 20 kN / joint (i.e. 40 kN on the joint pair) was sudden and without warning. The top member split along the grain through the position of the top nails in the joint (Plate 2.1). The load attained by this joint was only half of its Chapter 2 nail capacity load.

4. JOINT TYPE 2

This joint pair (fig 3.2(b)) was constructed in a similar manner to that of joint type 1 except the top member was extended beyond the edge of the vertical member to determine whether the extra length would change the manner in which the joint failed. In particular, the extra length of timber was expected to increase the load the timber would be able to sustain by increasing the area of timber stressed in tension perpendicular-to-grain. The expected failure pattern was as shown in Figure 3.2(b), similar to that of joint 1.

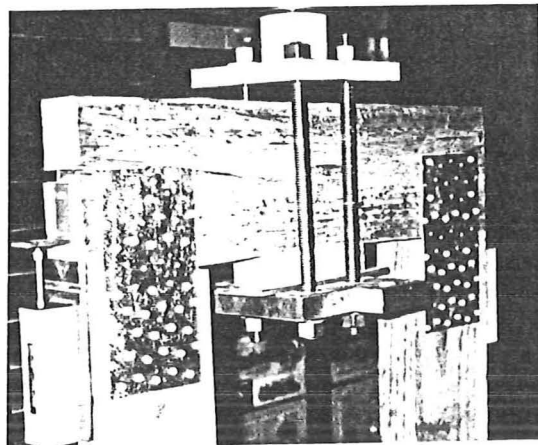


Plate 2.1 Failure of Joint Type 1.

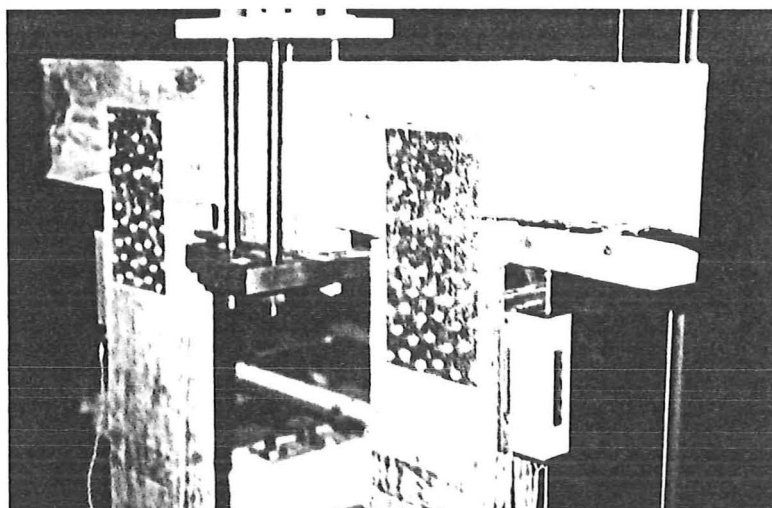


Plate 2.2 Failure of Joint Type 2.

The joint failed slowly, the timber in the vicinity of the joint splitting along a nail line while displacing with no increase in load. The section finally separated completely (Plate 3.2), with the load falling rapidly to zero. This joint only attained a load of 17 kN before failure, again lower than its Chapter 2 nail capacity load, and less than expected in comparison with joint type 1.

5. JOINT TYPE 3

For this joint pair 235mm lengths of Nailon plate were used, providing one more row of holes in the top of the plate (fig. 3.2(c)). Half of the total number of nails in the group were in the top row of holes in the Nailon plate. It was expected that this pattern would cause the joint to fail in a manner similar way to that of joint type 1.

The joints achieved a load of 25 kN / joint before failure of the timber member. The top timber member failed suddenly with a split passing through the position of the top nails in one plate (Plate 2.3) and the lower section of the timber was torn from the remainder of the member.

6. JOINT TYPE 4

The nails in nailgroups in this joint pair were distributed across the width of the top member, spaced as far apart as possible (fig. 3.2(d)). No particular failure pattern was predicted for this joint.

These joints attained a higher load than other joints, achieving 30 kN / joint before one failed. At failure, again suddenly, the timber split along the centre of the top member (Plate 3.4) and the lower section moved horizontally relative to the top section (exaggerated in fig. 3.2(d)). The calculated timber shear stress at 30 kN is 6 MPa (parabolic distribution assumed), compared to the shear stress allowed by NZS 3603:1981 of 1.9 MPa.

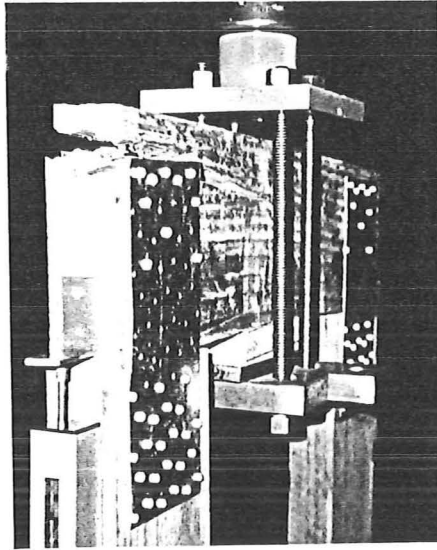


Plate 2.3 Failure of Joint Type 3.

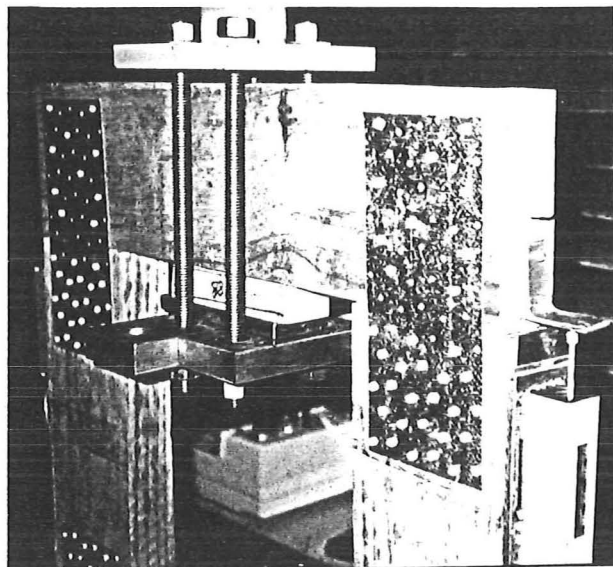


Plate 2.4 Failure of Joint Type 4.

7. LOAD-DEFLECTION CURVES

The Load-Deflection curves for all of the joints are given in Figure 3.3. The curve for the failed joint of each joint pair is indicated, this joint generally being the one with the greater deflection immediately before failure.

The testing machine loading head in the centre of the top member will have applied a rotational restraint to that member. The applied moment may have altered the load applied to each joint by up to 18%.

The load-deflection curves (fig. 3.3) may not be compared with those of the joints in Chapter 2. One reason for this is that the nailgroup of the test joint had 10 nails whereas the nailgroup in the other end of the Nailon plate had 25 nails, giving an average load-deflection curve which lies between those for groups of 10 and 25 nails. The second reason is that the second joint pair of each Nailon plate size (i.e. joint pairs 2 and 4) used the same Nailon plate and nailgroup of 25 as the first test. Thus the group of 25 was being loaded for a second time and would not be following the original monotonic loading curve.

The initially negative displacement for joint pairs 3 and 4 is due to rotation of the ends of the top member as it was being loaded. This is the result of bending of the top member and is recorded because of the position of the displacement transducers away from the centroid position of the nailgroup.

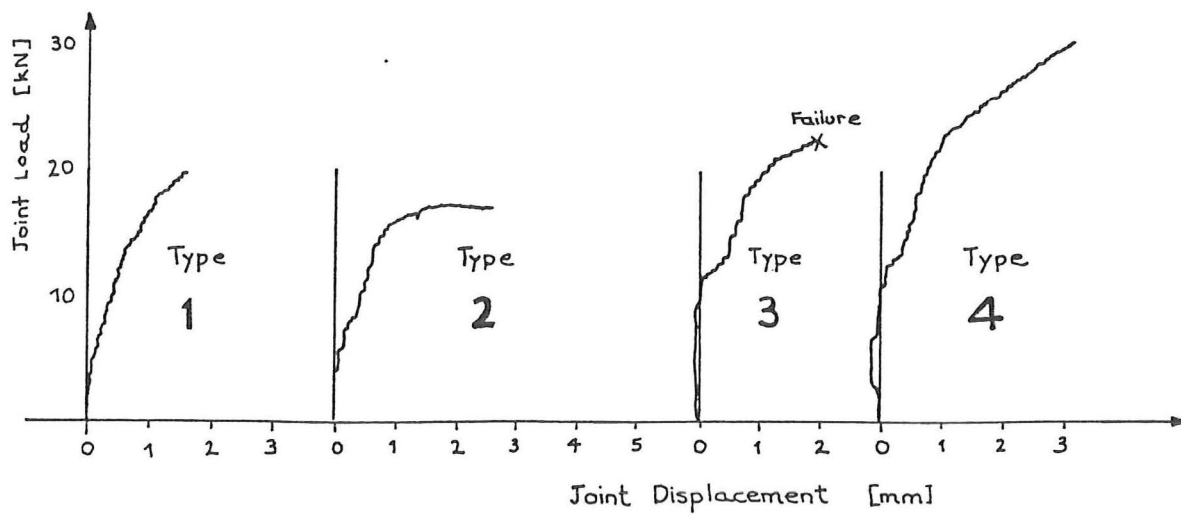
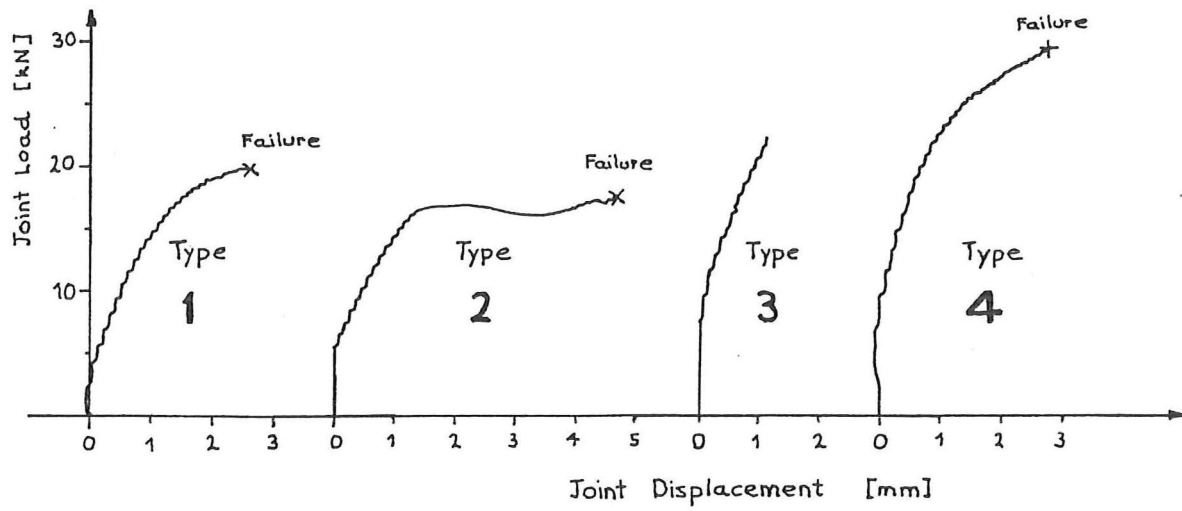


Figure 3.3 Load-deflection curves.

8. DISCUSSION

The joints tested in this series all failed as a result of the timber member failing. The loads at which the joints failed were all higher than computed using the manufacturers wind/seismic load for the nails but the nails did not attain their ultimate loads. Inspection of the members suggests that timber failure resulted from a combination of shear stress and perpendicular-to-grain tension stress in the joint area. Joint type 2 most likely failed as a result of perpendicular-to-grain tension and the failure of joint type 4 indicated the possibility of excessive shear stress contributing to the failure.

Joint 4 was the strongest type of joint tested. This suggests that the combination of distributing the nails across the width of the timber and avoiding a concentration of nails along the grain of the member gives the best nailing pattern. A large number of joints would have to be tested to prove this conclusively.

There is a complex stress distribution within each joint type caused by the proximity of the load point and the positioning of the nails resisting that load. A finite-element analysis of the timber member is required to determine the stresses present in the region of the joint and fracture mechanics would then indicate the likely position of failure initiation, but these aspects are beyond the scope of this project.

The nailing pattern and position of the nails in the joint appears to influence the overall strength of the joint. The strength of the joint is more dependant on the strength of the timber member than on the ultimate nail capacity obtained from perpendicular test results.

CHAPTER IV

BRACED TIMBER FRAMES

1. INTRODUCTION

Ten frames (fig. 4.1) were constructed from ex 100 x 50 mm Pinus Radiata members. These frames were intended to simulate diagonally braced walls in light timber frame construction. Table 4.1 gives a summary of the type of connections used, the average timber moisture content of the timber members, the design loads and the failure load for each of the frames. The letter after the design load indicates the governing conditions from which the design loads were obtained (N = Nail failure, T = Toothplate failure, S = timber shear failure). The blank values in the table indicates moistures content were not recorded, loads not able to be computed or frames which failed because of excessive displacement.

Frame No	Connection type	Moisture content %	Design Wind/Seis Load (kN)	Design Ultimate Load (kN)	Failure Load (kN)
1	Nailstrap		1.1 N	3.2	5.0, 5.4
2	Nailstrap		1.1 N	3.2	--
3	Toothplate	21	8.6	14. T	17
4	Toothplate	27	8.6	14. T	18
5	Toothplate	27	7.8	13. T	--
6	Toothplate	34	9.6	16. T	16
7	Toothplate	25	--	--	--
8	Toothplate	32	6.7	11. T	16
9	Toothpl + Nailon		7.7 S	--	20
10	Toothplate		6.1	10. T	--

Table 4.1 Summary of predicted and failure loads of Frames

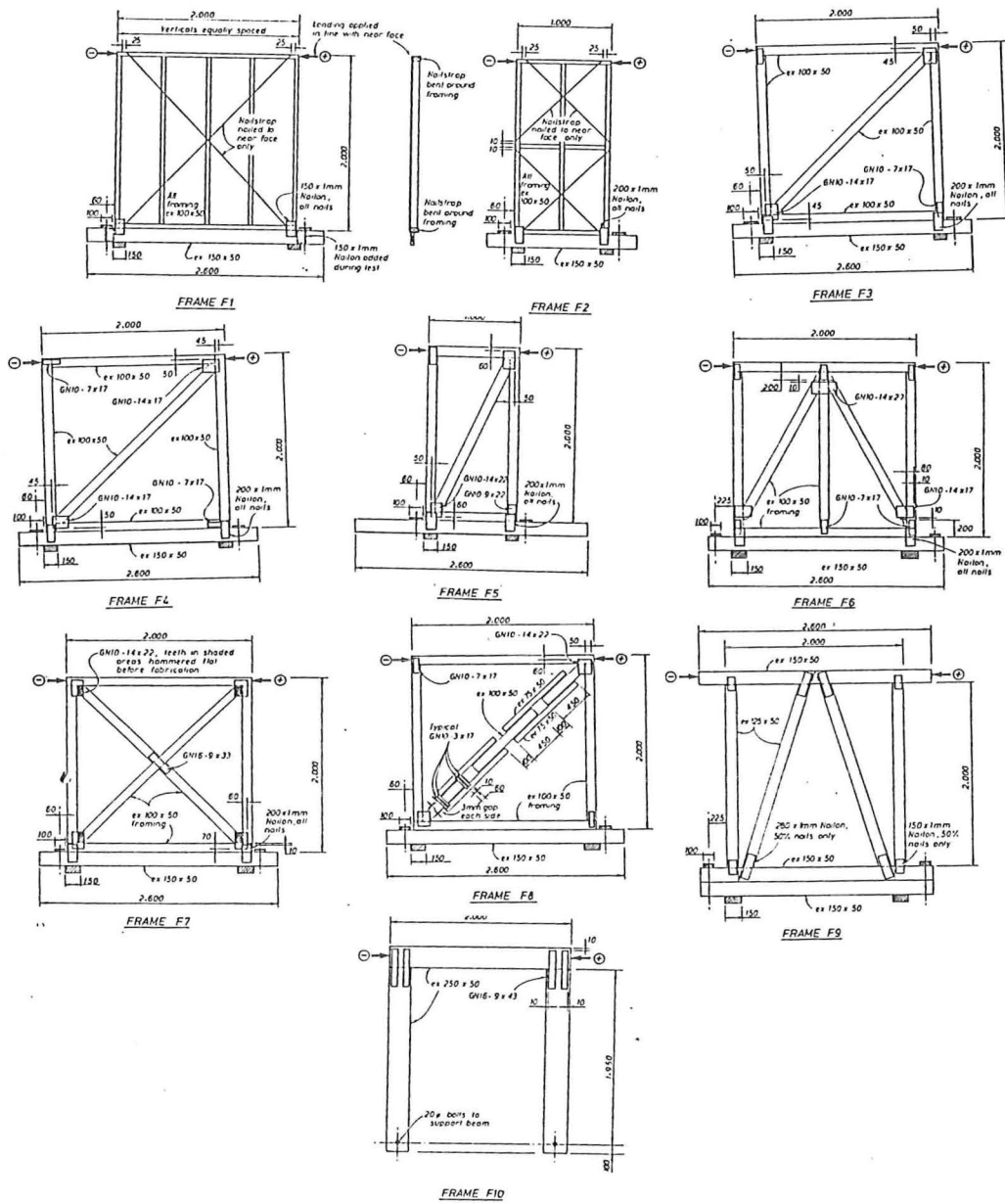


Figure 4.1 Braced timber frames

The Table 4.1 wind/seismic load is the permissible load on the weakest timber member or steel connector calculated in accordance with NZS 3603:1981. This is the basic (i.e. long duration) timber or fastener load multiplied by a load-duration factor of 1.5. The ultimate load is the 5 percentile strength of timber members based on NZS 3603:1981 values or the load at which yield occurs within the steel connectors. For the toothplates yield is defined as basic load divided by a factor of 0.6.

The ultimate load for the shearplate connectors was calculated using using a combined stress failure criterion (Equation 4.1). The distribution of the applied load within the connectors is based on the number of teeth in the timber member. The method of computing this, with an example calculation are included in Appendix C.

Table 4.2 presents the the measured frame sway, the sway arising from rigid body rotation due to hold-down movements, the predicted pin-jointed frame sway and the load at which these sways were measured or computed. The pin-jointed frame sway was computed for a pin-jointed frame with only the axial strain of the members contributing to the sway. Elastic behaviour of the frame was assumed for this calculation.

Frame No	Measured Sway (mm)		Rigid Body Sway (mm)		Pin-jointed Sway (mm)	Load (kN)
	+ve	-ve	+ve	-ve		
1	15	16	--	--	7	4
2	50	30	32	24	8	4
3	13	10	8	9	3	15
4	15	10	7	8	3	15
5	44	39	46	46	7	15
6	9	14	--	--	2	12
7	30	50	--	--	2	13
8	11	10	15	14	3	15
9	16	27	6	7	11	15
10	48	54	10	12	-	8

Table 4.2 Measured and computed sways

All of the frames were connected to ex 150 x 50 bearers with 1 mm Nailon plate (fig. 4.2), and the bearers were clamped to a steel reaction frame. This was intended to simulate a timber flooring assembly at the base of the frame.

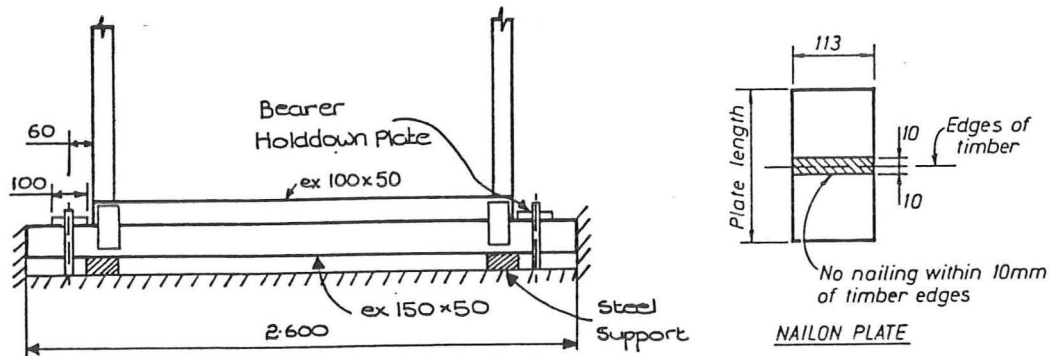


Figure 4.2 Simulated flooring assembly in the reaction frame.

Figure 4.3 shows the joint locations referred to in this chapter and the deflection gauge locations upon the frames.

To test the frames, each frame was loaded in the positive direction, unloaded, loaded in the negative direction to a load of an equal magnitude and unloaded again. This pattern of loading completed one loading cycle. The frame was then cycled to the same or higher loads, with the same magnitude of load in each direction if possible, until failure occurred.

$$\left(\frac{\text{Applied Tension}}{\text{Allowable Tension}} \right)^2 + \left(\frac{\text{Applied Shear}}{\text{Allowable Shear}} \right)^2 \leq 1.0 \quad (4.1)$$

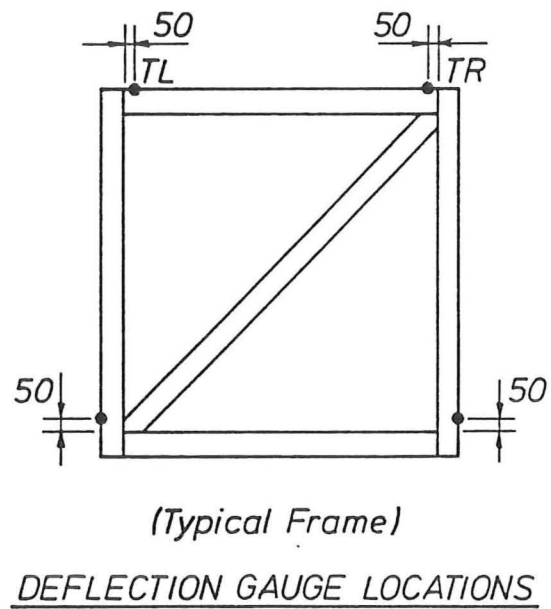
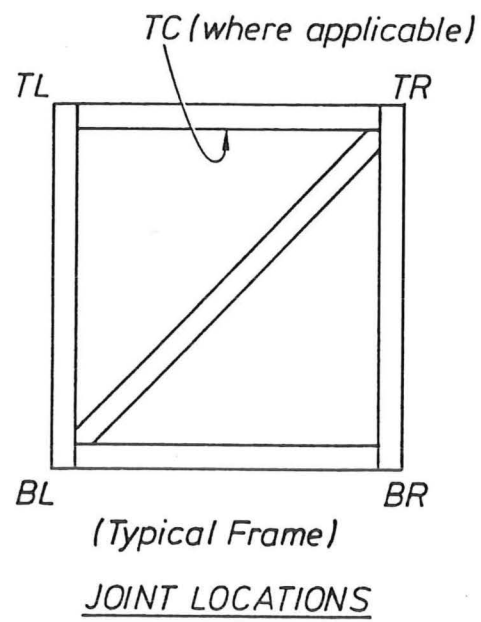


Figure 4.3 Joint and Deflection Gauge Locations.

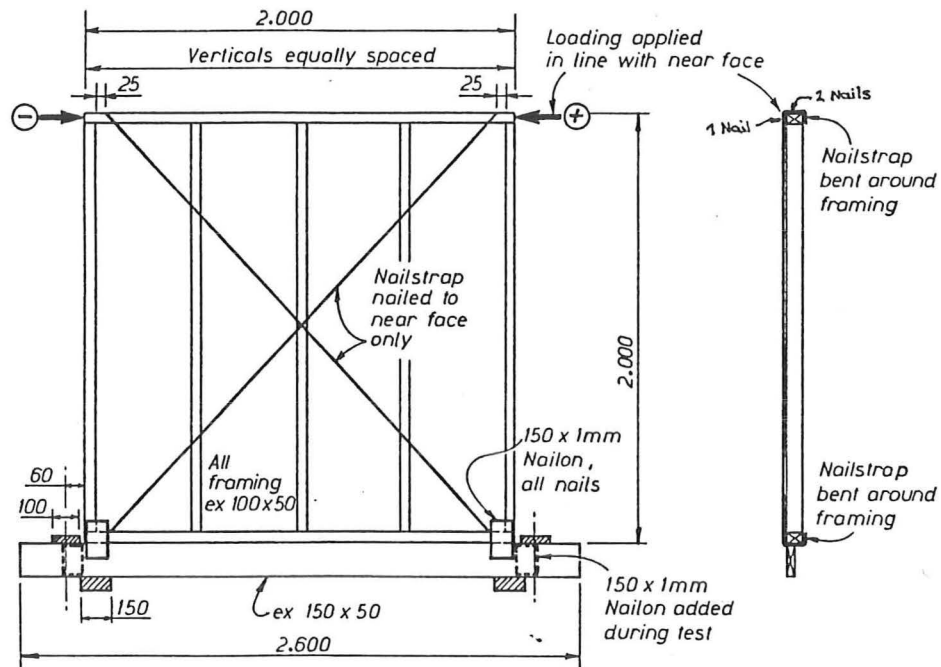
2. FRAME F1

Frame F1 (fig. 4.4 and Plate 4.1) was a lightly strapped frame of the type used in domestic construction. Figure 4.4 also shows the positive and negative loading positions. Lumberlok Stripbrace (27 x 0.6mm cold rolled steel) was used. Each strap was wrapped around the bottom and top framing plates, with three nails at each end (fig. 4.4). One of these nails was driven into the edge of the framing plate, with the other two positioned in the ex 100 face of the framing plate. The ex 150 x 50 bearers were attached to the frame with Nailon plate after the straps were nailed to it.

Slackness increased during the first three cycles, followed by a perpendicular-to-grain failure of the bearer joist under one of the Nailon hold-down plates. Additional plates were attached beside the hold-down Nailons, to prevent further splitting of the bearers. Figure 4.5 is the load-deflection plot for the top of the frame.

Testing was resumed, as Test 2, without retightening of the bracing straps, so the slackness at the end of Test 1 was retained. One nailstrap broke at the position of one of the nails driven into a framing plate edge, at 5 kN applied load. Reverse cycling had caused repeated bending across a transverse crease in the nailstrap at this position and this had evidently caused the failure (Plate 4.2). The strap was replaced with a new one which was tightened as it was nailed. Loads of up to 7 kN were applied during subsequent reverse cycling and the new strap eventually failed at 5.4 kN, again at the first nail position. Figure 4.6 is the load-deflection plot for this second test.

The Table 4.1 design wind/seismic load for this frame is 1.1 kN. The predicted pin-jointed sway at this load is 2 mm. The design ultimate load is 3.2 kN. Both the wind/seismic and ultimate load are based on the design nail loads.



FRAME F1

Figure 4.4 Construction of Frame F1.

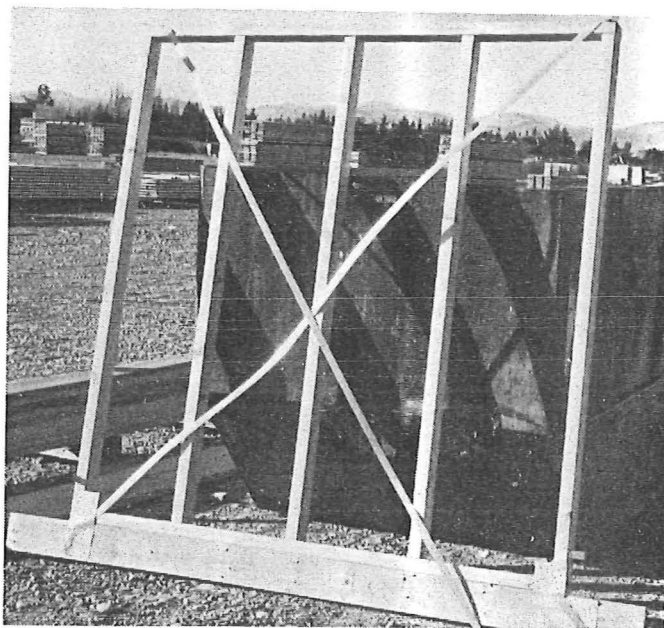


Plate 4.1 Frame F1 after testing.

Figure 4.5 Load-deflection plot for Frame F1.

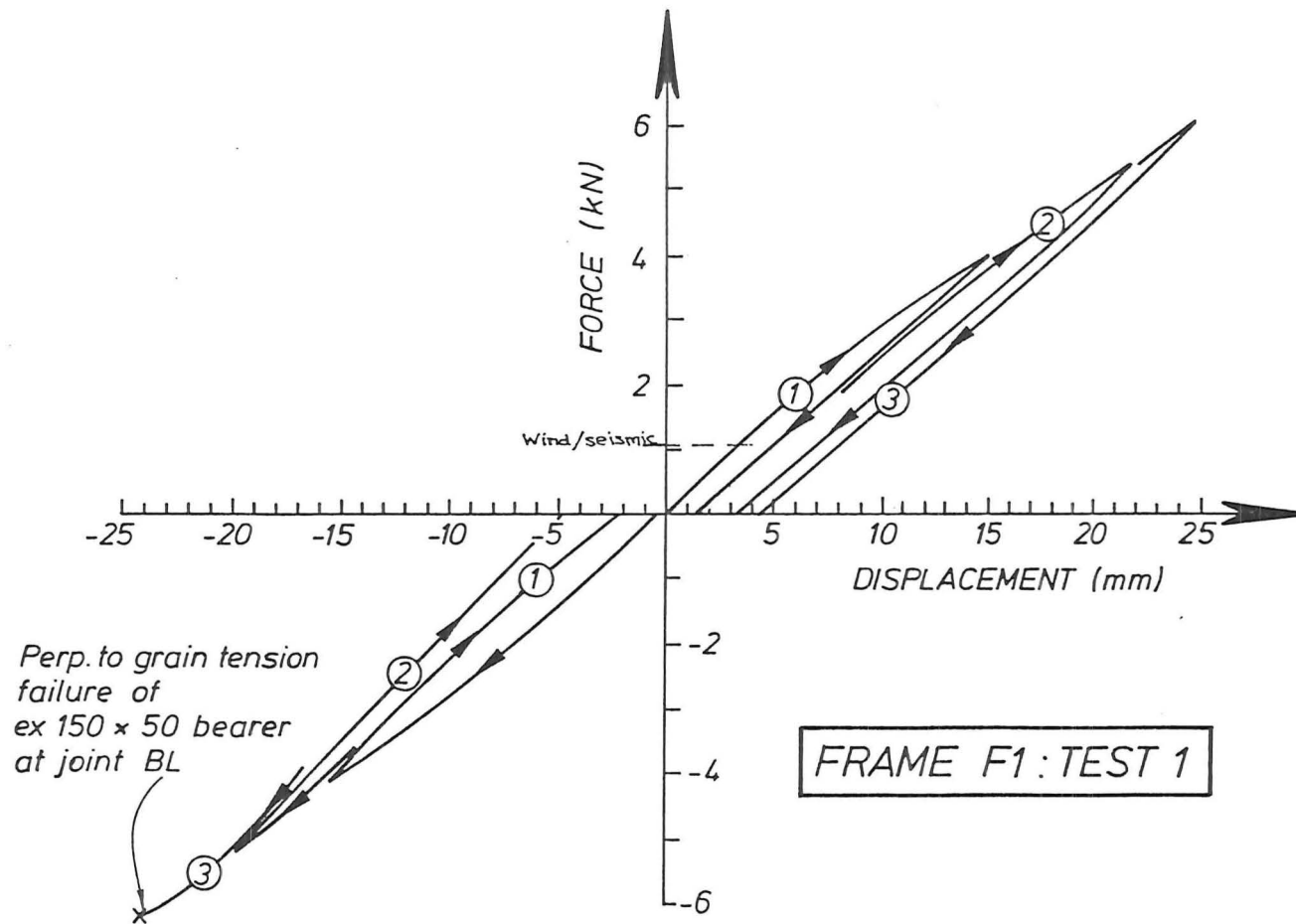
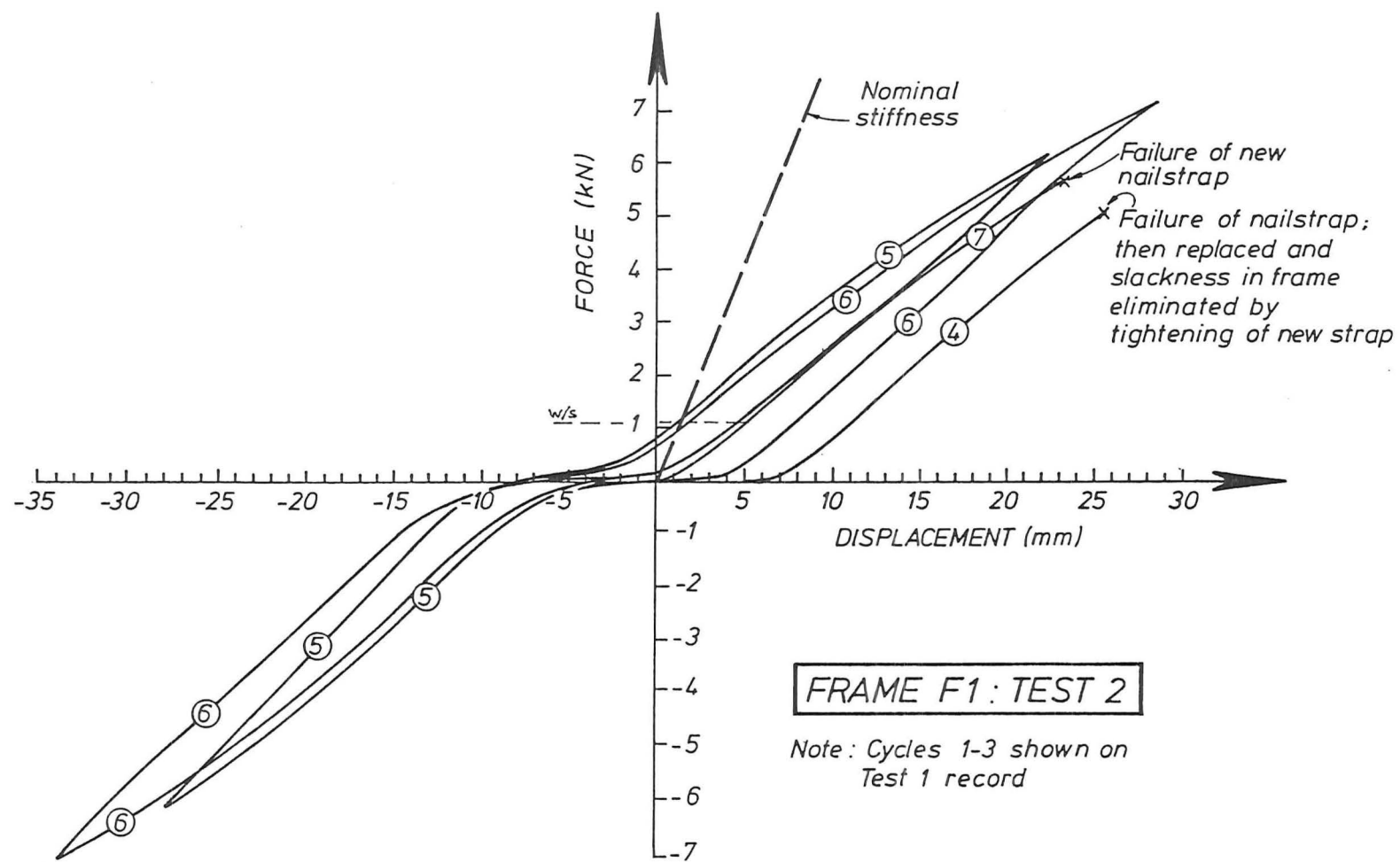


Figure 4.6 Load-deflection plot for Test 2 of Frame F1.



Frame F1 attained a load of 7 times the wind/seismic load in both directions before failure. Failure of the frame was caused by failure of the nailstrap. The nailstrap at the position of the nail had a higher stress than the rest of the nailstrap because of the smaller cross-sectional area. At an applied load of 7 kN the tensile stress in the strap at the nail position was 688 MPa. This stress is higher than the failure stress of 556 MPa from tests by Stewart [10]. When undergoing compression, the nailstrap buckled at the position of the nail because of the dimple that formed when the nail was driven through the nailstrap.

The nail in the edge of the framing member deflected further than the other two nails because the nailstrap dug into the edge of the timber member (fig. 4.7(a)). This resulted in a larger portion of the total load in the nailstrap being carried by the nail in the edge of the framing member.

There were no observed displacements at the lower left or lower right hold-down positions.

The 15 mm sway at 4 kN applied load from Table 4.2 was twice the predicted axial strain deflection of 7 mm. Contributions to the 8 mm extra deflection (connection strain deflection) come from :

- closing of construction gaps in the frame between studs and plates.
- bearing deformations as the top plate rotated because the nailstrap was only on one face of the member (fig. 4.7(b))
- yielding of the nailstrap because the stress was greater than the elastic limit for the steel.

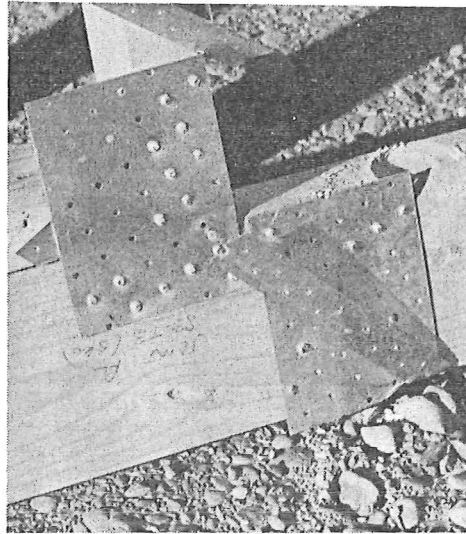


Plate 4.2 Nailstrap after failure.

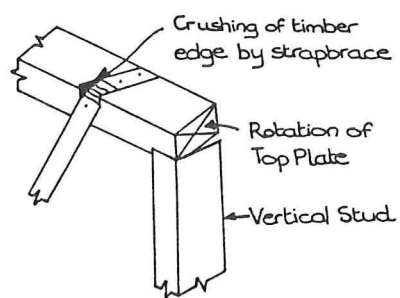


Figure 4.7 a) Nailstrap digging into edge of timber.
b) Rotation of top plate.

3. FRAME F2

Frame F2 (fig. 4.8) was also lightly strapped in a similar manner to Frame F1, but the narrow width required two diagonal strip braces such that the braces were approximately 45 degrees to horizontal. In the first loading cycle, 4 kN was attained and then during the second cycle the Nailon hold-down plates buckled out of plane in the mode A shape (fig. 4.9). With subsequent reverse cycling the plates did not straighten completely even when subject to tensile force. The effect of this permanent buckling of the Nailons was to tighten up the hold-down connection such that the tangent stiffness of the hysteretic loop during cycles 3, 4 and 5 (fig. 4.10) was higher than that during the first cycle. The strap bracing itself did not deteriorate during the cycling.

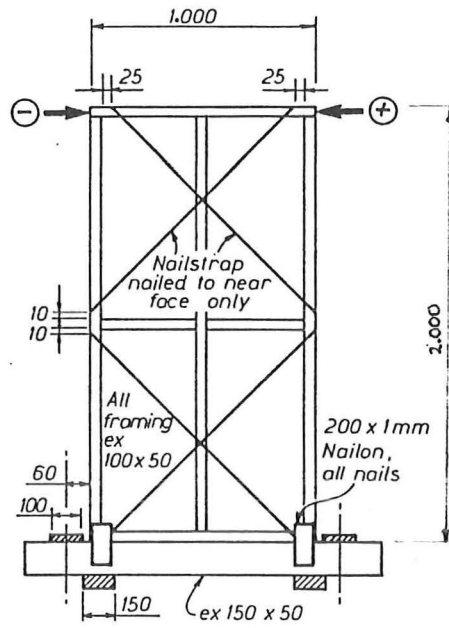
The observed displacements (mm) at the lower left (BL) and lower right (BR) hold-down positions at ± 4 kN applied load were;

	BL	BR	sway
+4 kN	-10	+6	32
-4 kN	+4	-8	24
	(mm)		

where the indicated "sway" = $|BL| + |BR|$ is the sway arising from rigid body rotation due to the hold-down movements.

The Table 4.1 design loads for this frame are the same as Frame F1; a wind/seismic load of 1.1 kN, and an ultimate load of 3.2 kN. The Table 4.2 predicted pin-jointed sway is 2.1 mm at the wind/seismic load.

The sway for this frame was 6 and 4 times the predicted pin-jointed sway of 8 mm at the peak positive and negative loads in the first loading cycle. The BL Nailon plate hold-down buckled at the beginning of cycle 2 when loaded in compression. The BR Nailon also buckled during the negative half of cycle 2. For subsequent cycles the Nailon plates didn't straighten. This caused the frame to stiffen and reduced the deflection at a load of 4 kN to half that of the first loading cycle.



FRAME F2

Figure 4.8 Construction details of Frame F2.

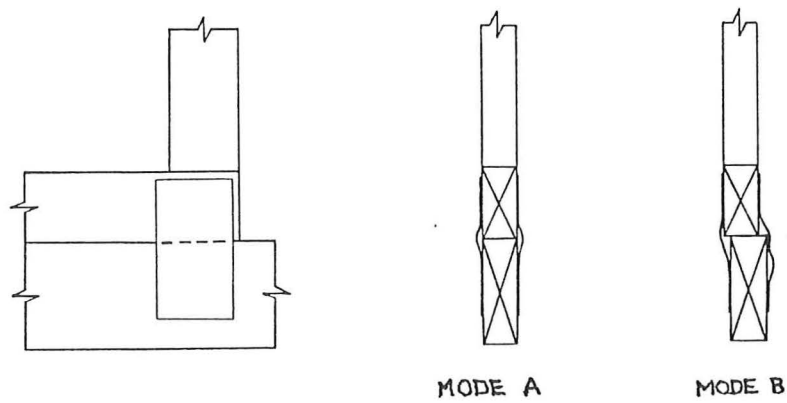
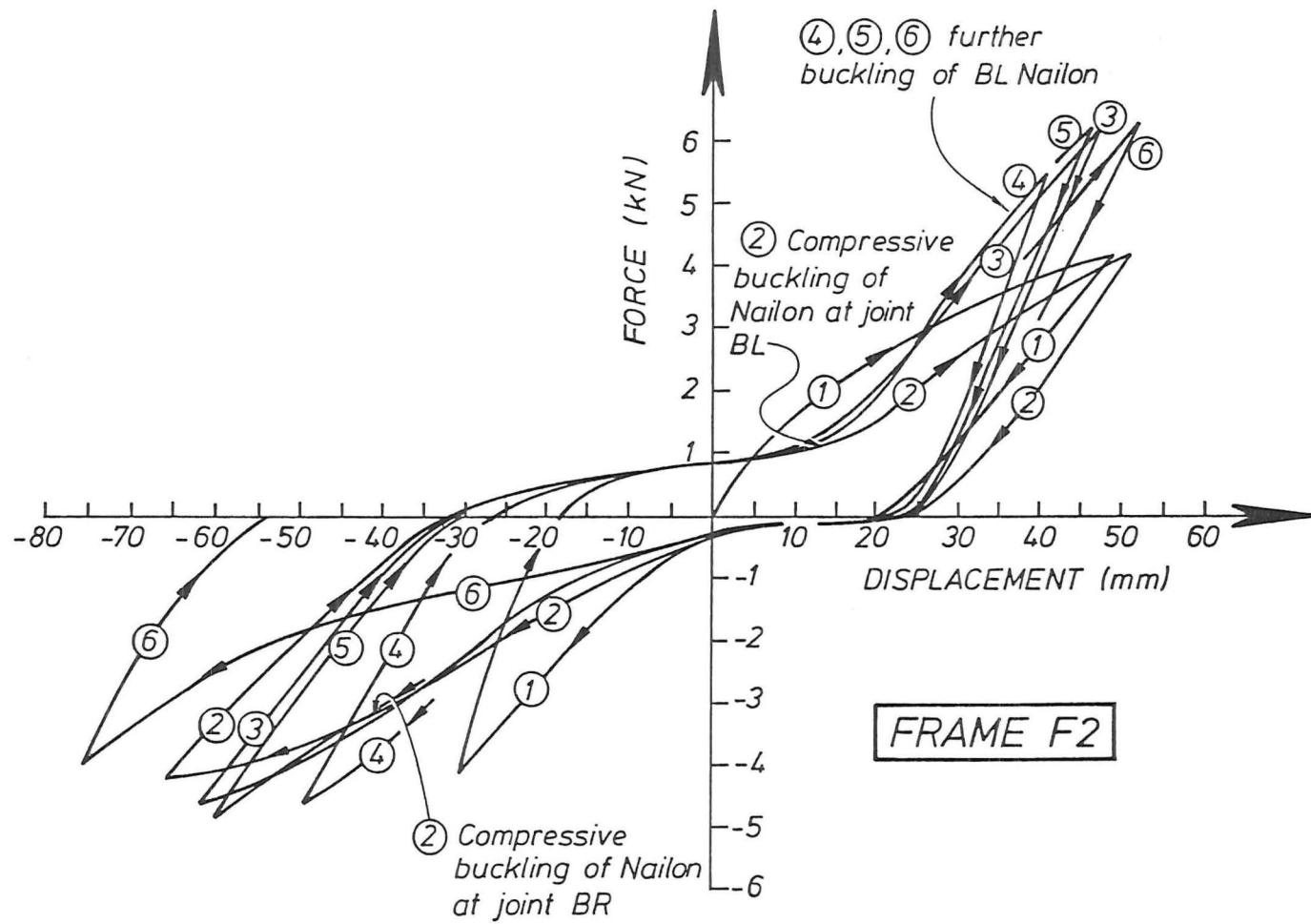


Figure 4.9 Buckling Modes of Nailon plate in compression.

Figure 4.10 Load-displacement plot for Frame F2.



4. FRAME F3

The frame (fig. 4.11 and Plate 4.3) attained 15 kN in the first cycle, but on loading to 16 kN during the second cycle 1 mm shear deformation was observed in the BL and TR plates, and then perpendicular-to-gain failure of the bearer near the BR Nylon hold-down plate occurred. The recorded hold-down displacements and the associated rigid body sway displacements at the first cycle of ± 15 kN were;

	BL	BR	Sway
+15 kN	-5	+3	8
-15 kN	+3	-6	9
	(mm)		

These displacements are a comparatively large proportion of the total sway displacements of +13 and -10 mm (from the load-displacement curve, fig. 4.12). The original Nylon plates were removed and replaced with larger 200 x 1 mm plates, and the test resumed. Approaching -16 kN during the 4th cycle, the BL toothplate sheared (up to 4 mm shear displacement, Plate 4.4) and displacements increased to over 20 mm with load being maintained at approximately 17 kN. It appears that the combined shear and tension forces on the toothplate contributed to the failure.

The Table 4.1 ultimate load for this frame is as 14 kN, limited by tension/shear failure of the BL toothplate. The corresponding wind/seismic load is 8.6 kN, with a pin-jointed sway of 2 mm.

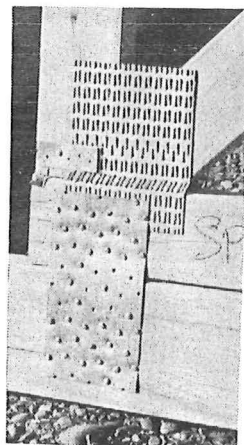


Plate 4.4 Frame F3 BL toothplate joint.

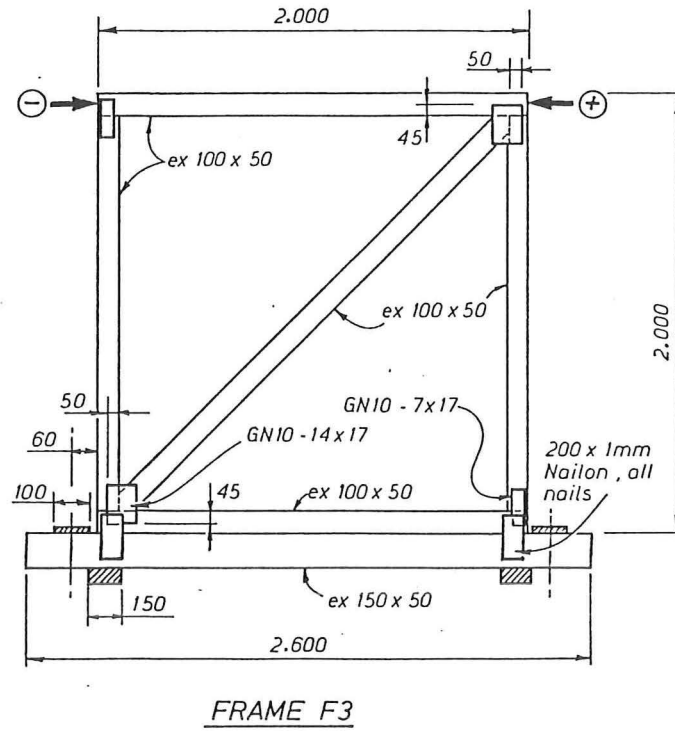


Figure 4.11 Frame F3 construction.

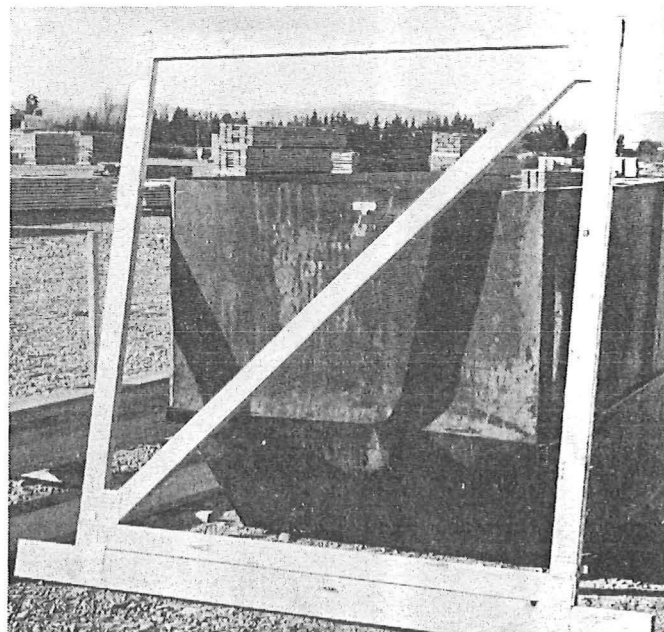
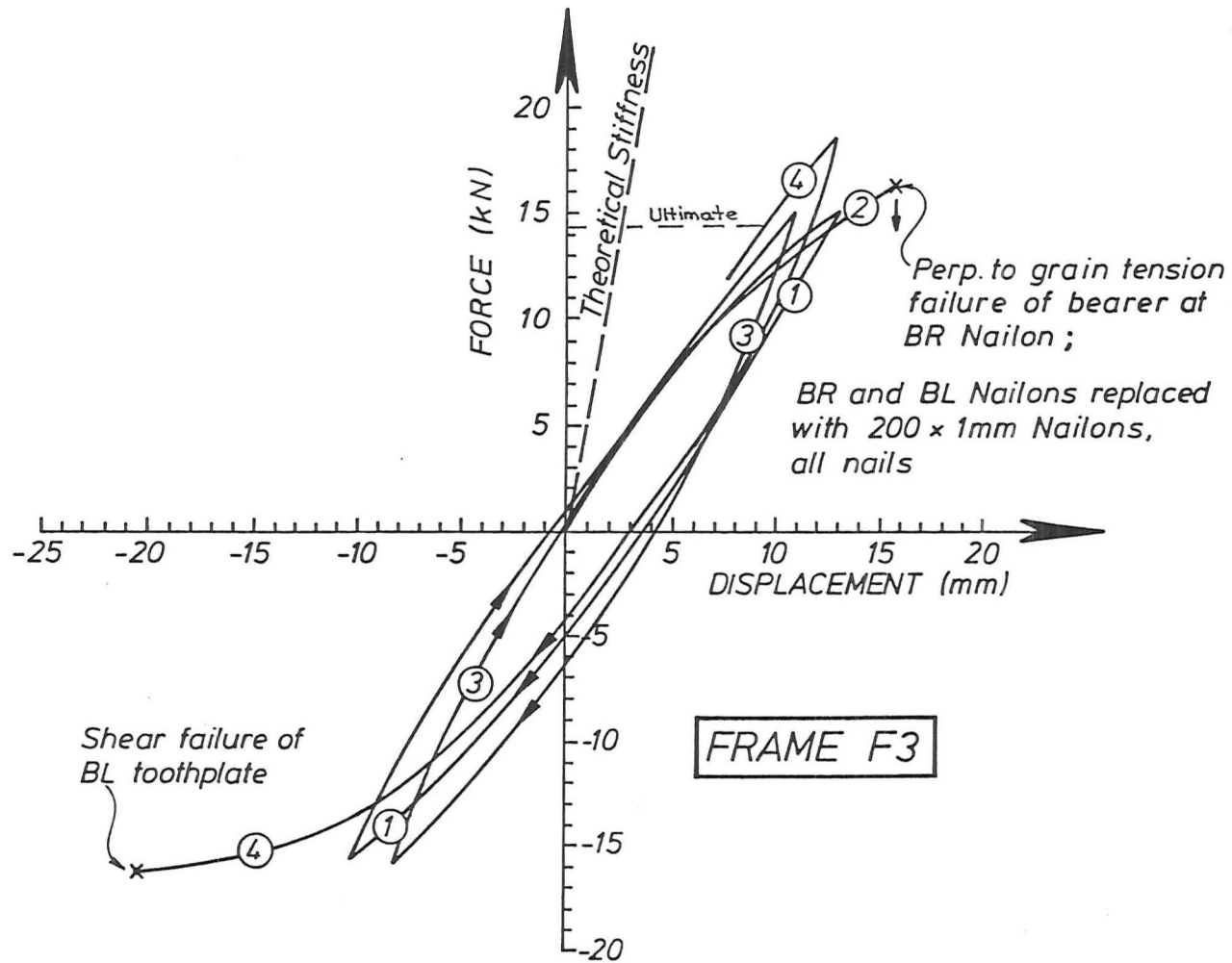


Plate 4.3 Frame F3 after testing.

Figure 4.12 Load-displacement curve for Frame F3.



5. FRAME F4

Frame F4 (fig. 4.13 and Plate 4.5) was similar to Frame F3 but with the toothplates oriented in different directions. Out of plane buckling of the diagonal during the positive load part of the second cycle caused local out-of-plane rotation of the joints at both ends (fig. 4.14), resulting in distress of the toothplates on both sides of the BL joint. Simultaneously, compression across the adjacent Nailon hold-down connection caused local lateral buckling of the joint, as indicated by the asymmetrical mode shape (fig. 4.9(b) and Plate 4.6).

The test was resumed after a stiffener was nailed along the diagonal to prevent buckling. During the reverse loading part of the second cycle, shear displacements increased rapidly in the TR toothplate and this lead to failure at -18 kN at a displacement exceeding 30 mm. The toothplate had sheared 4 mm at failure (Plate 4.7). Figure 4.15 is the load-displacement curve for this frame. The rigid body rotations at 15 kN load as determined from the hold-down displacements were:

	BL	Br	Sway
+15 kN	-3	+4	7
-15 kN	+4	-4	8
	(mm)		

The Table 4.1 ultimate design load for this frame is 14.3 kN limited by a tension/shear failure of the BL toothplate, similar to Frame 3. The wind/seismic design load is 8.6 kN. The pin-jointed sway at this load is 3 mm.

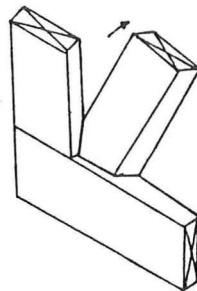


Figure 4.14 Out-of-plane rotation of diagonal at joint.

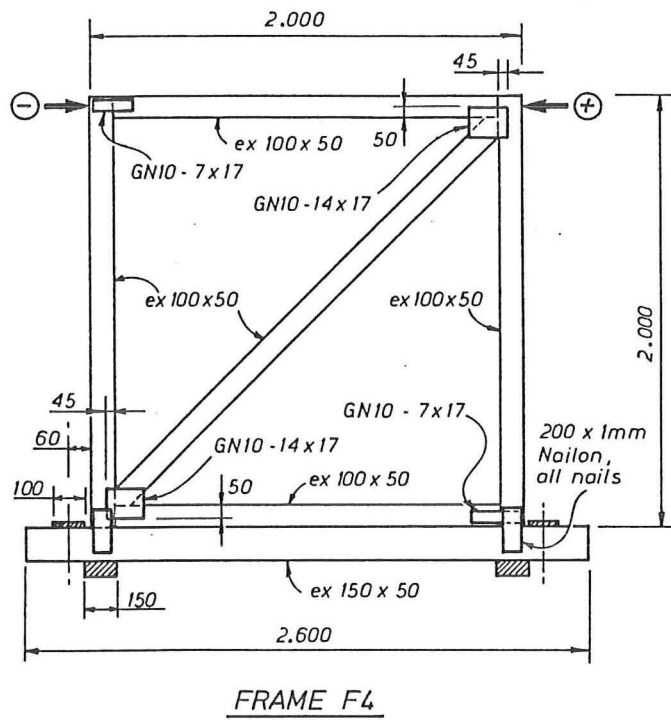


Figure 4.13 Frame F4 construction.

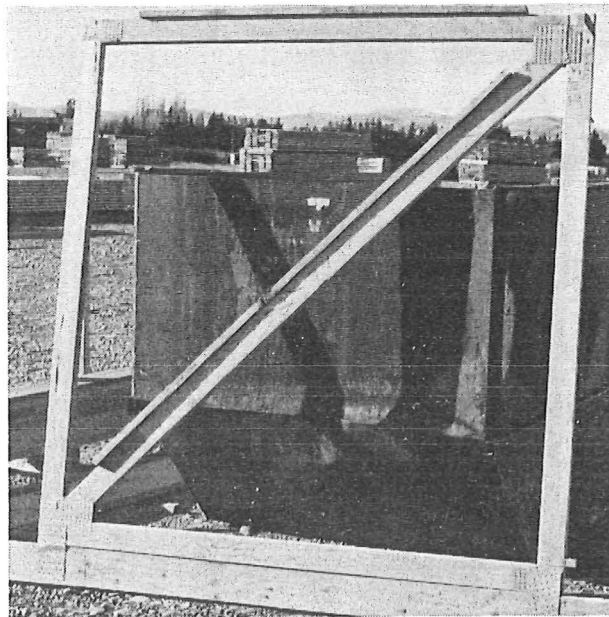
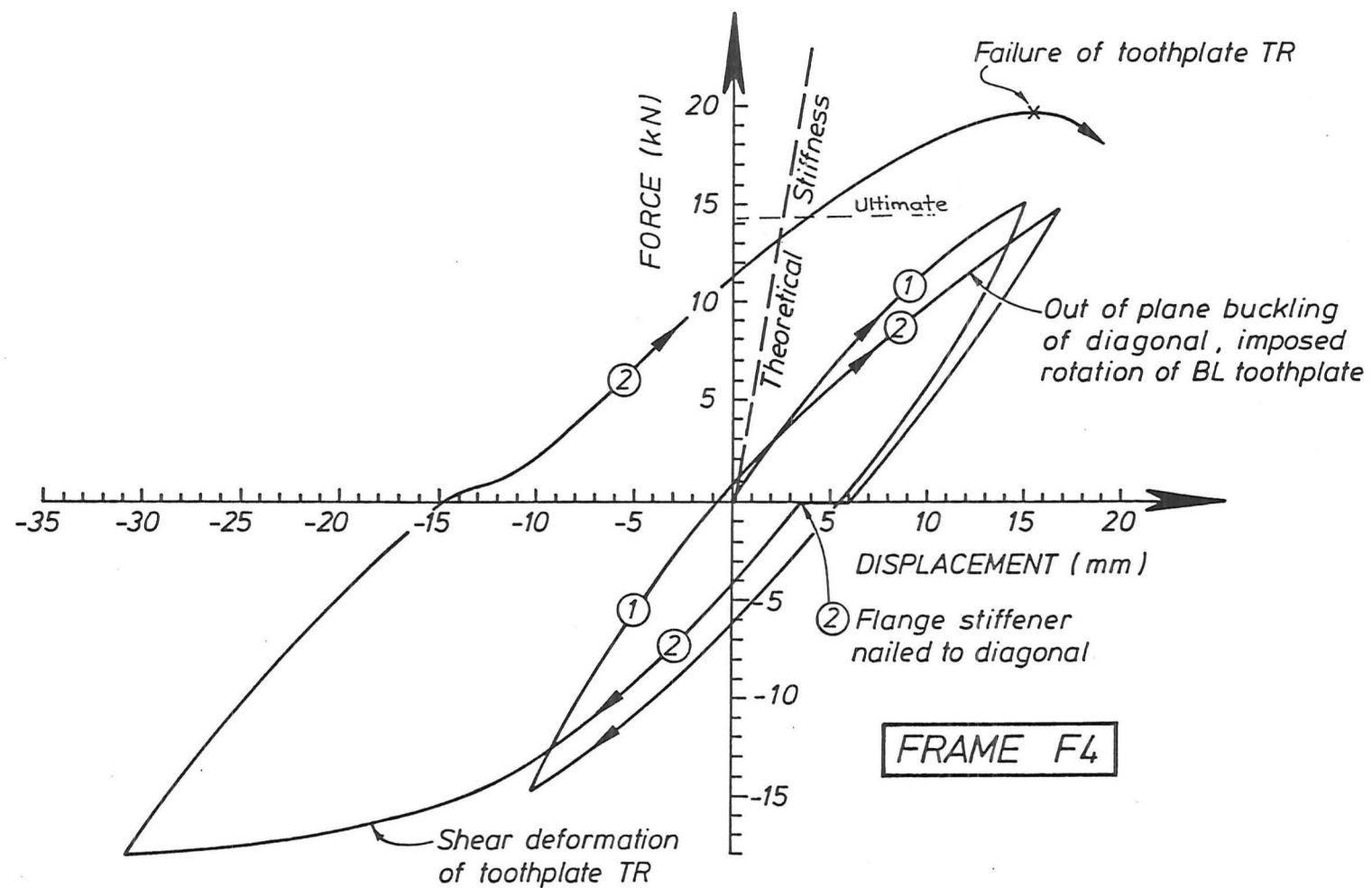


Plate 4.5 Frame F4 after testing.

Figure 4.15 Load-displacement curve for Frame F4.



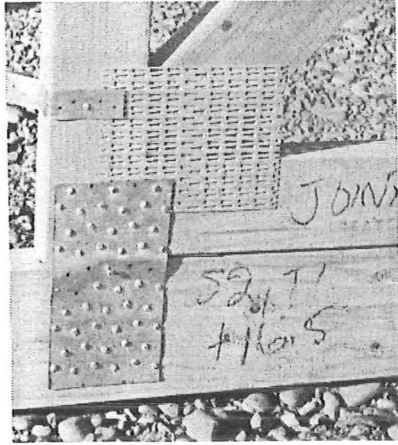


Plate 4.6 Buckling of BL Nailon plate - Mode 'B'.

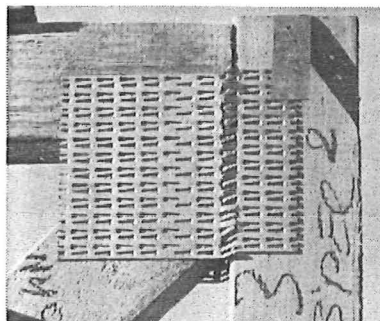


Plate 4.7 Toothplate failure at TR joint.

6. FRAME F5

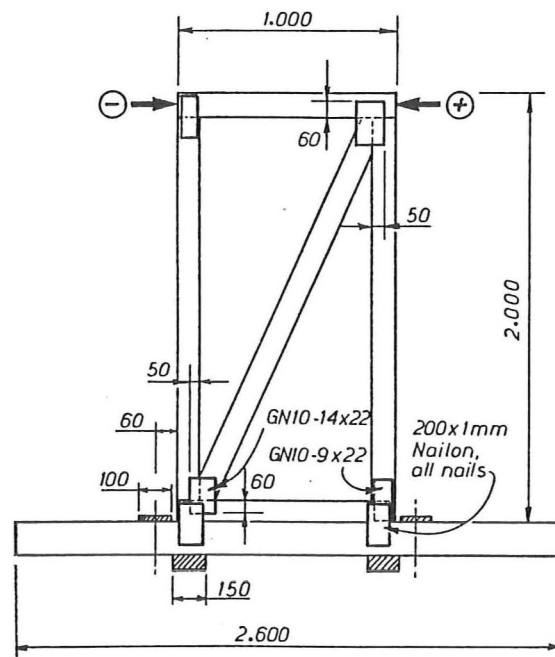
This frame (fig. 4.16 and Plate 4.8) was similar to Frame 3, but only half the width. At first loading to 12 kN the diagonal buckled out of plane, and the frame was unloaded and the diagonal stiffened before reloading. Figure 4.17 is the load-displacement curve for this test. Large compressive and tensile displacements were measured at the hold-down positions;

	BL	BR	Sway
+15 kN	-11	+12	46
-15 kN	+10	-13	46
	(mm)		

The compressive buckling of the Nailon hold-down plates (Plate 4.9) conformed with Mode A (fig. 4.9). Further rigid body rotation sway over and above that tabulated above arose because of crushing of the bearer under the hold-down washer plate and also due to shear deformation within the bearer between the hold-down washer and the Nailon plate.

Minimal shear or tensile displacements developed within the toothplates themselves, and the frame appeared to be capable of sustaining cyclic loading without toothplate damage. The frame failed after jacking to -80 mm displacement and 13 kN applied load when longitudinal cracks formed within the bearer at the BL position which then failed in shear.

The Table 4.1 ultimate design load of this frame is 12.9 kN. This corresponds to a shear/tension failure of the BL toothplate. The wind/seismic design load is 7.7 kN. The predicted pin-jointed sway at 15 kN is 7 mm.



FRAME F5

Figure 4.16 Frame F5 construction.

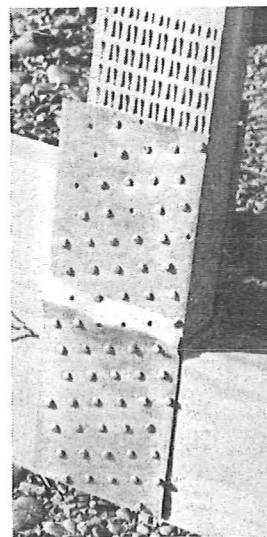
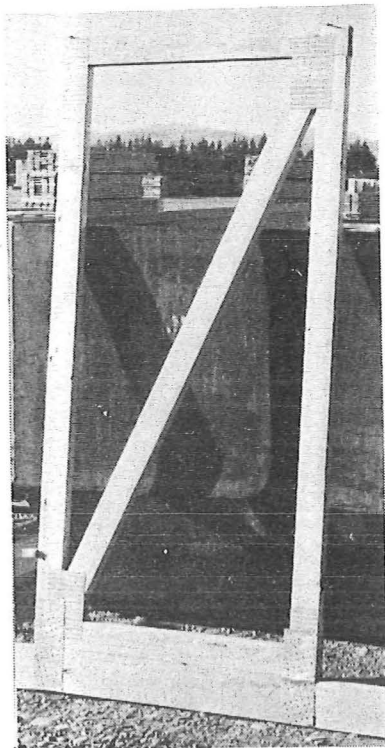


Plate 4.8 Frame F5 after testing.

Plate 4.9 BR Nailon plate after testing.

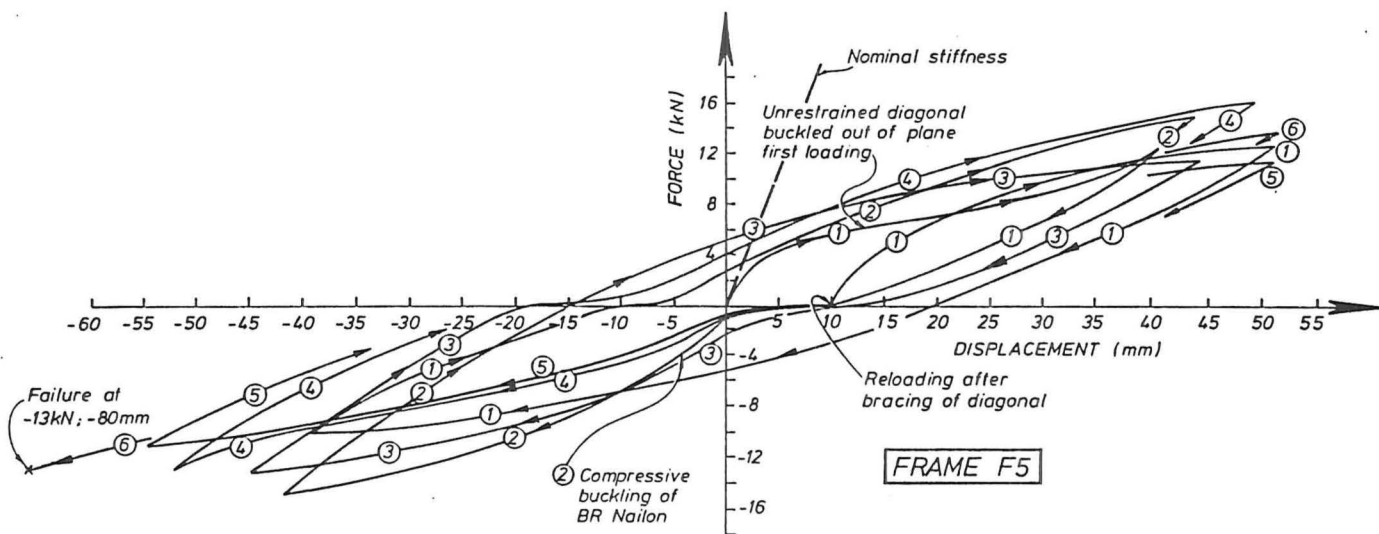


Figure 4.17 Load-displacement curve for Frame F5

7. FRAME F6

This frame (fig. 4.18 and Plate 4.11) was designed to maximize lateral displacement ductility capacity arising from shear displacements in the toothplate joints. On first loading, the top central joint was found to be inadequate to transfer the shear from the top horizontal to the central vertical member. A Nailon plate over the toothplate then allowed further loading up to a load of 16 kN in the third cycle (fig. 4.19), when shearing occurred in the BL and BR toothplates. These joints were then reinforced with Nailon plates nailed over the toothplates.

Testing was resumed as Test 2 (fig. 4.20). Reverse cycling to about 15 kN caused degradation of the top of the central vertical member both in flexure and shear (Plate 4.10). The top Nailon plate simultaneously bent out of plane. At -30 mm sway splitting at the top of the vertical member increased. The frame was loaded until a sway of -45 mm was attained. Although load was maintained with increasing displacement, further reverse loading could not be sustained.

The Table 4.1 ultimate load for this frame was 16 kN, with a shear/tension failure of the diagonal member toothplates. The TC toothplate had an ultimate design load of 8 kN, the BL and BR toothplates had an ultimate design load of 14 kN. The wind/seismic load for this frame is 9.6 kN based on failure of the diagonal member toothplates. The predicted pin-jointed sway at 12 kN load is 2 mm. Most of the frame deformation occurred within the TC, BL and BR toothplates.

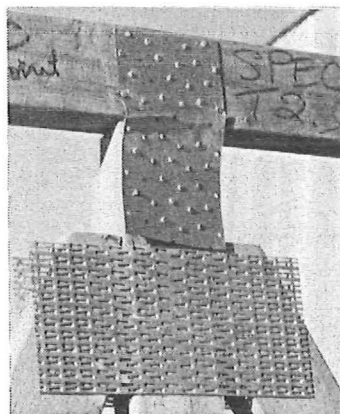


Plate 4.10 TC joint after testing.

A black and white photograph showing a large, dark, rectangular object, possibly a piece of machinery or a container, mounted on a wooden frame. The frame features a prominent A-frame structure in the center. The background shows a landscape with hills and some buildings.

Plate 4.11 Frame F6 after testing.

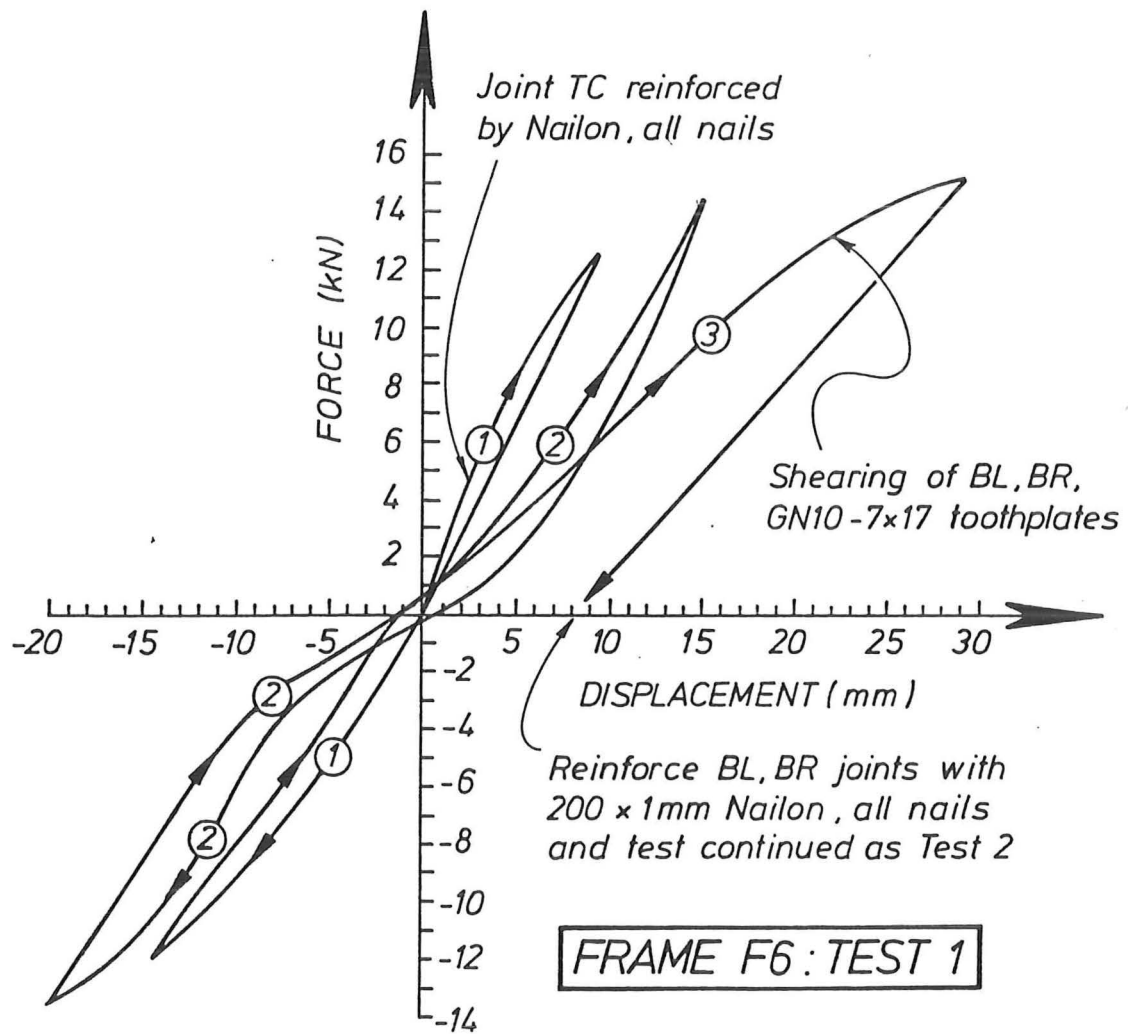
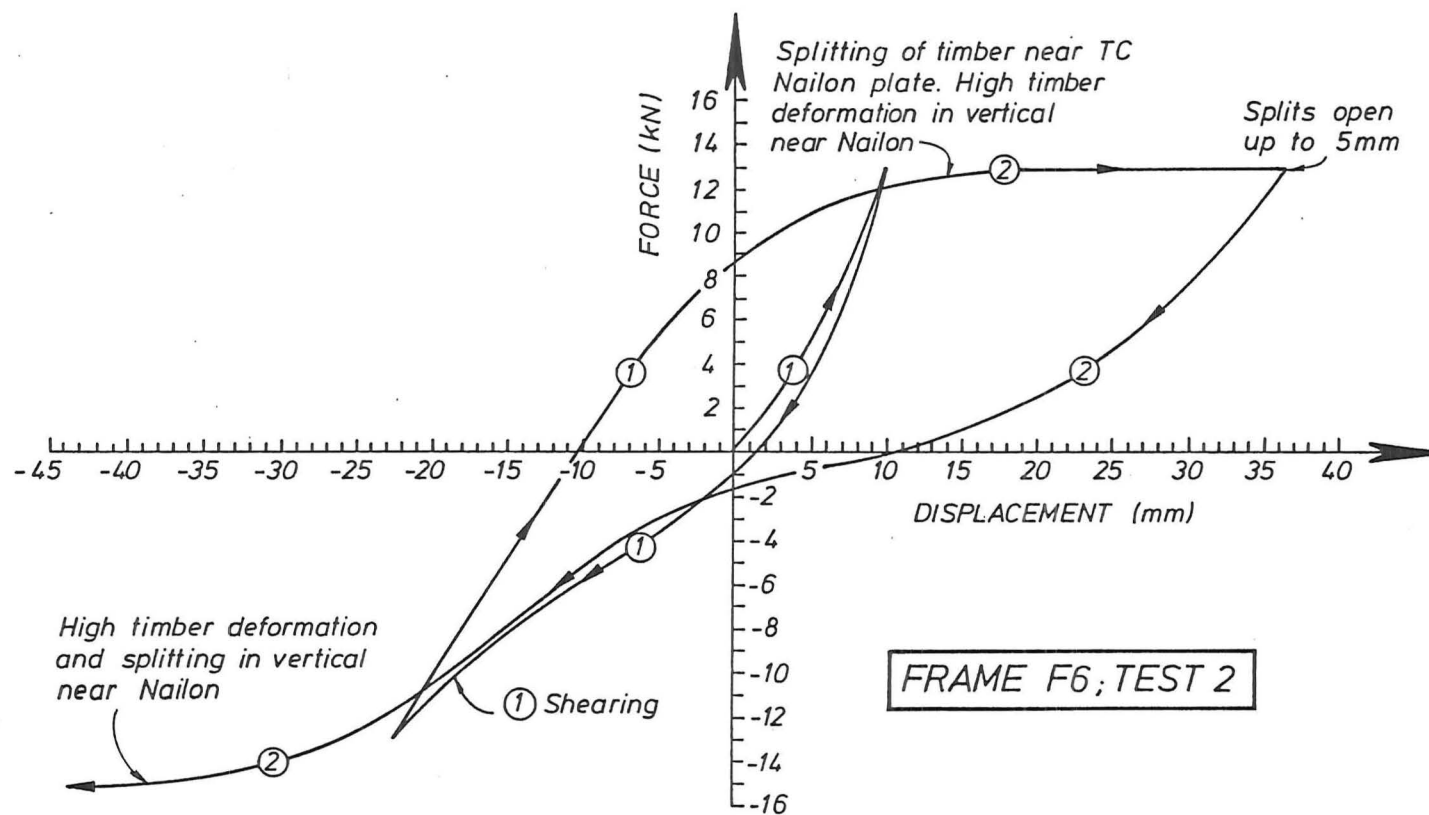


Figure 4.19 Load-displacement curve for Frame F6:Test 1.

Figure 4.20 Load-displacement curve for Frame F6: Test 2.



8. FRAME F7

This frame (fig. 4.21 and Plate 4.12) was designed to achieve large displacement ductilities in a frame incorporating conventional toothplate joints. It was not intended to be representative of frames in general use. Figure 4.21 shows areas of the teeth within the corner plates which were hammered flat on the plate before the frame was assembled, so that the diagonals were simply trapped within the plates rather than positively engaged by the plates. The plate connection over the intersection between the diagonals was a conventional joint. The ends of the diagonals themselves were cut square, so that the two corners of each diagonal end just made contact with the vertical and horizontal frame members. Subsequent loading caused the corners to penetrate these members as perpendicular to grain deformation occurred. The diagonals were restrained from out of plane buckling by a central external restraint. The design of the frame resulted in horizontal load being entirely resisted by compression action in the timber bracing. As crushing occurred at the ends of the diagonals (fig. 4.22), the overall slackness of the assembly increased (fig. 4.23).

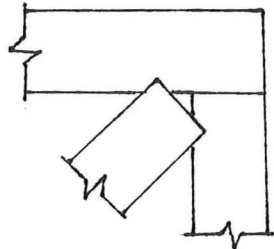


Figure 4.22 Deformation of timber members at corners.

At displacements above 50 mm (fig. 4.23) the rotation between the horizontal and vertical members at the corner joints caused local buckling at the outstanding corners of the plates but without apparently weakening them. The assembly sustained five reverse cycles and appeared capable of further cycling. At displacements greater than 80 mm there was some risk of the diagonals dropping out of the slot between the plates.

Plate 4.12 Frame F7 after testing.

Figure 4.23 Load-displacement curve for Frame F7

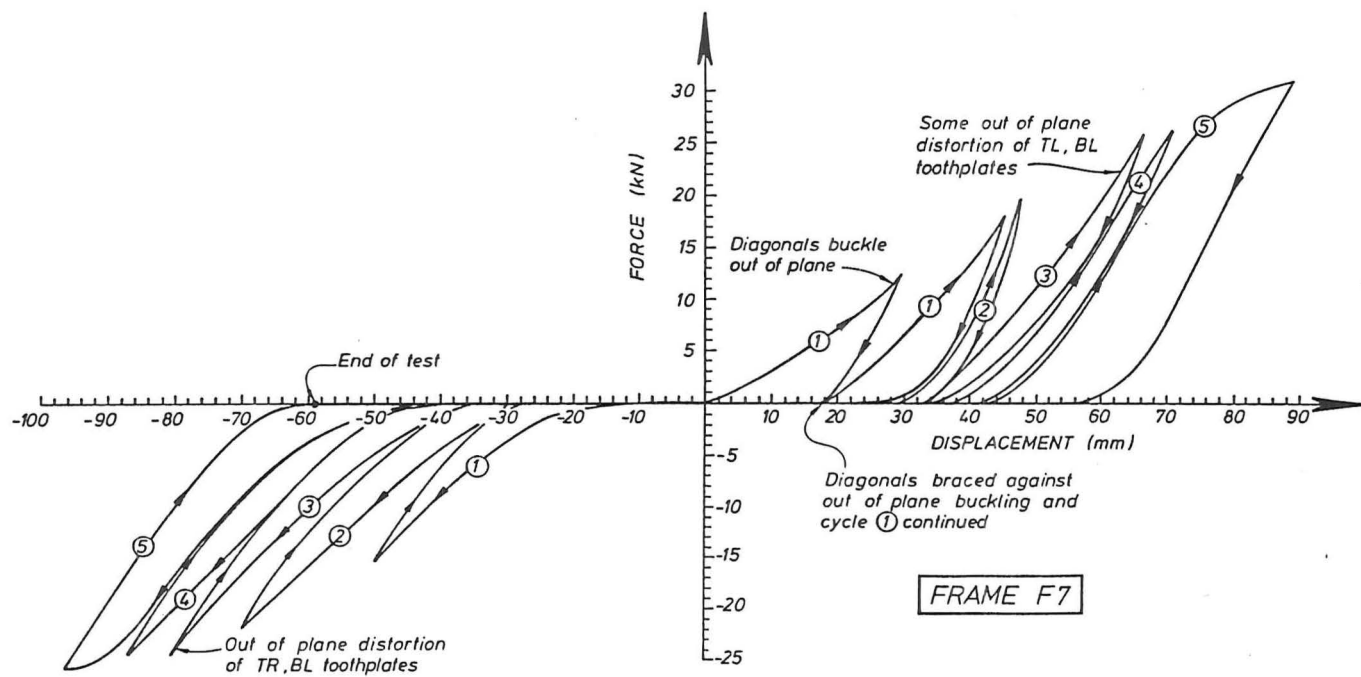


Table 4.1 design loads were not computed for this frame because of the uncertainty of determining the distribution of load in the toothplate connectors. The test load attained suggests that there was a considerable portion of the shear transferred by bearing between the diagonal and top members (fig. 4.22), loading the toothplates mostly in tension.

9. FRAME F8

Frame F8 (fig. 4.24 and Plate 4.13) was also designed to develop large overall displacements from the shear displacement of individual toothplates. In this case the diagonal was a composite member made up of members allowed to slide over each other and connected by toothplates acting in shear.

At the first cycle loading to 15 kN there was some distress in the corner plates, which developed a tooth slip of about 1 mm. These were reinforced with Nailon plate at the completion of the first cycle. On loading to 20 kN in the second cycle, one pair of plates developed 2mm slip, with the other pair remaining rigid. On reverse loading to -19 kN, large reverse deformations occurred within the same pair of toothplates. It appeared that the one pair of plates was accommodating all the diagonal deformation with the other pair remaining rigid throughout the test. Clearly the additional shear developed as these plates deformed plasticly was insufficient to mobilise large displacements within the other pair. At a total assembly displacement of -40 mm the pair of toothplates had deformed 8 mm in shear (Plate 4.14).

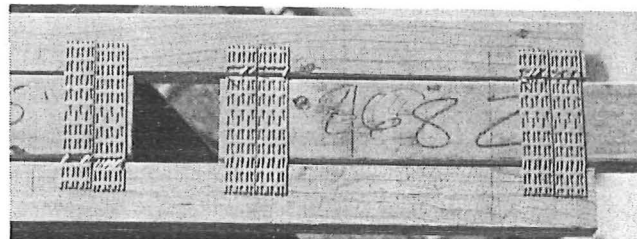


Plate 4.14 Diagonal member after failure.

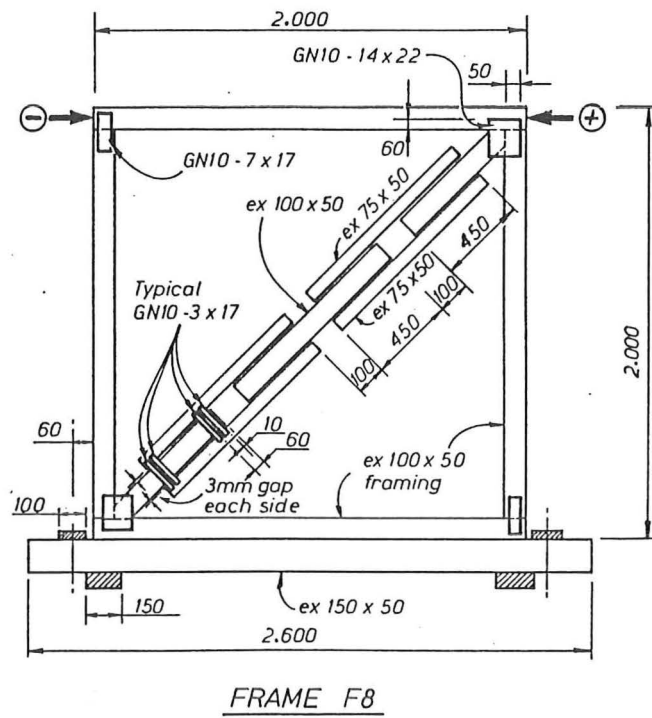


Figure 4.24 Frame F8 construction.

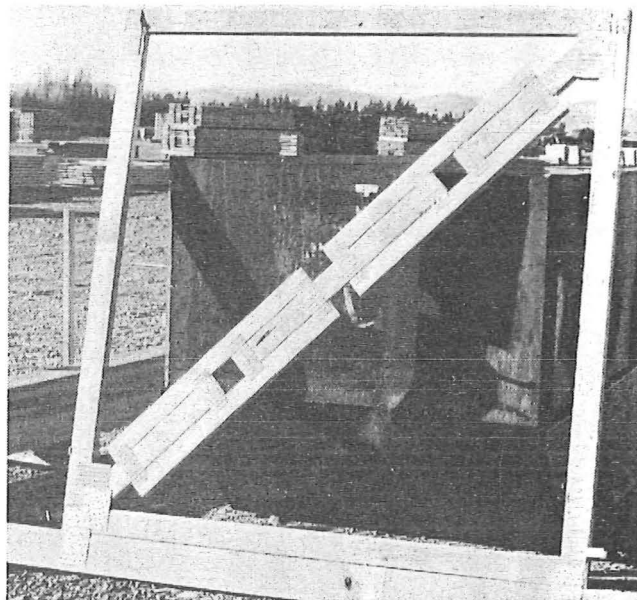


Plate 4.13 Frame F8 after testing.

Figure 4.25 Load-displacement curve for Frame F8.

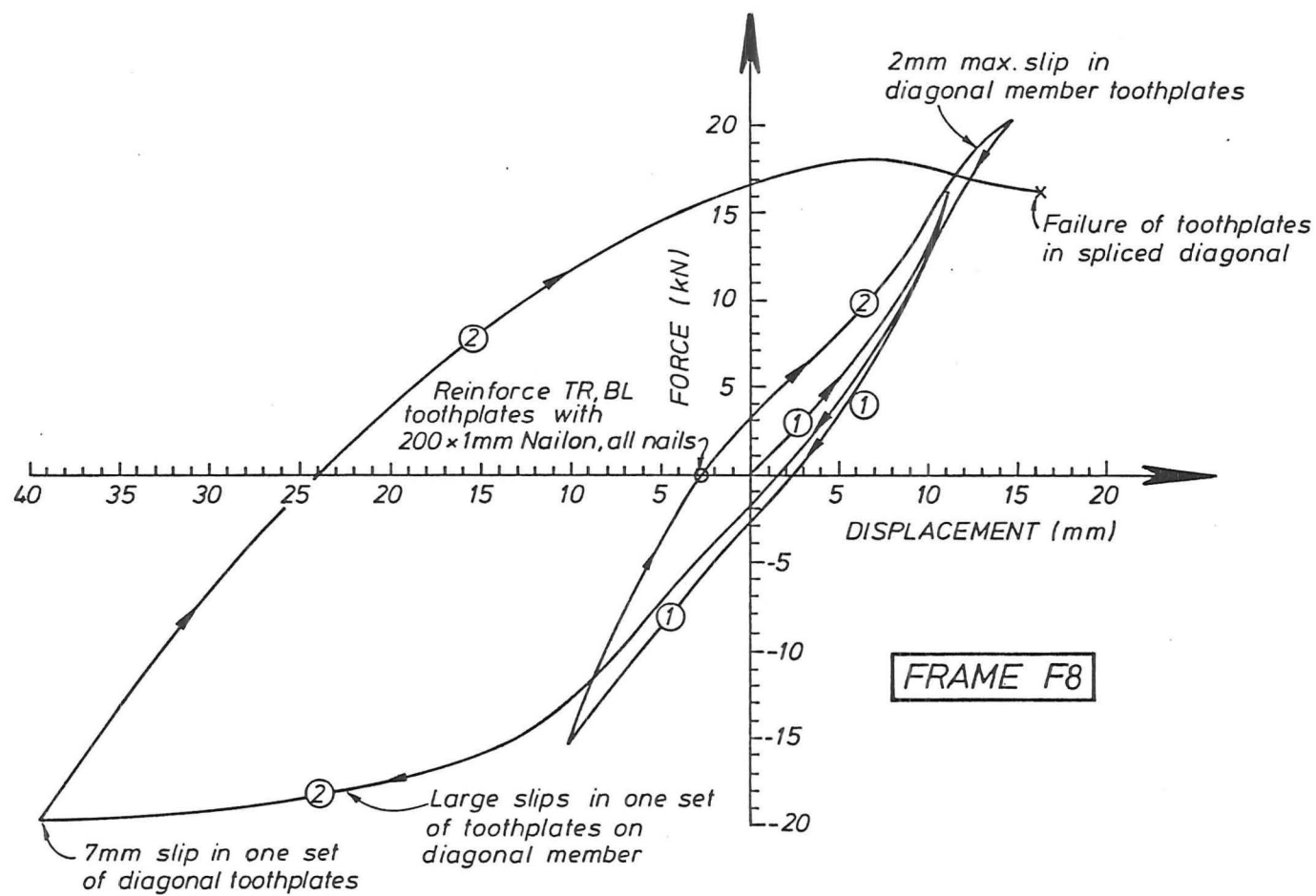


Figure 4.25 is the load-displacement plot for this frame. The measured hold down displacements and associated rigid body rotations were;

	BL	BR	Sway
+15 kN	-8	+7	15
-15 kN	+7	-7	14
	(mm)		

The Table 4.1 ultimate design load for this frame is 11 kN, limited by shearing of the diagonal member toothplates. The predicted pin-jointed sway at 15 kN is 3 mm.

10. FRAME F9

Frame F9 (fig. 4.26) was designed to achieve a ductile Nailon plated frame having a comparatively large displacement capacity. Accordingly the diagonal members were inclined at a steep angle so that moderate axial deformations of the members and their end connections, led to large sway displacements.

First loading to 11 kN caused longitudinal cracking along the grain of the upper horizontal member between the two central Nailon plates. The central region was then reinforced by an additional Nailon plate and the test resumed into the negative part of the first cycle. Reverse loading of -11 kN caused compressive buckling of the BR diagonal member Nailon, and subsequent cycling of 15 and 20 kN caused shear degradation of the centre of the upper horizontal member (Plate 4.15). Cycling caused progressive buckling of the diagonal BL and BR Nailons and consequently a "tightening up" of these joints in both the compression and tension mode. Figure 4.27 is the load-displacement plot for this frame. Measured displacements at these joints were;

	BL	BR	Sway
+15 kN	-4	+2	6
-15 kN	+3	-3	7
	(mm)		

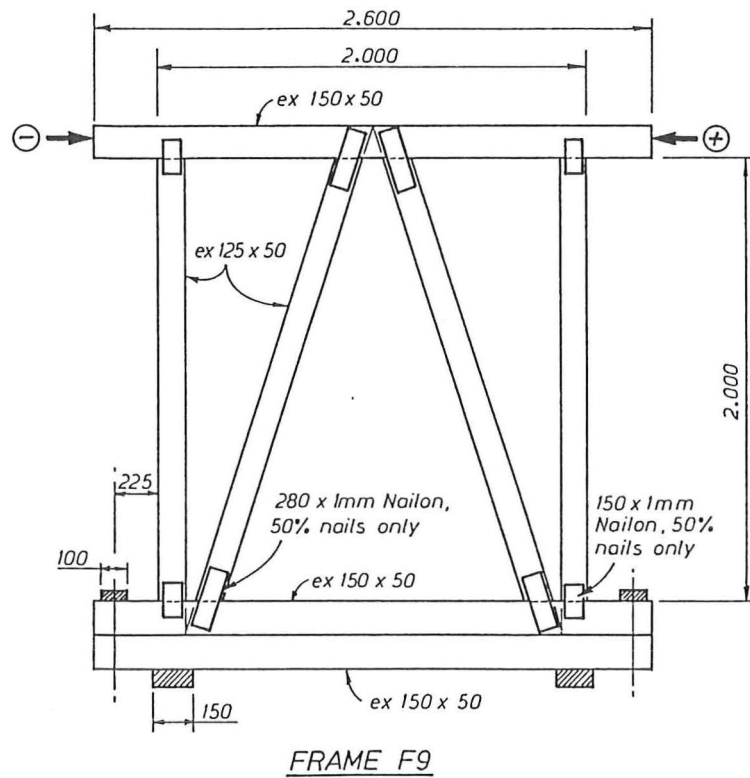


Figure 4.26 Frame F9 construction.

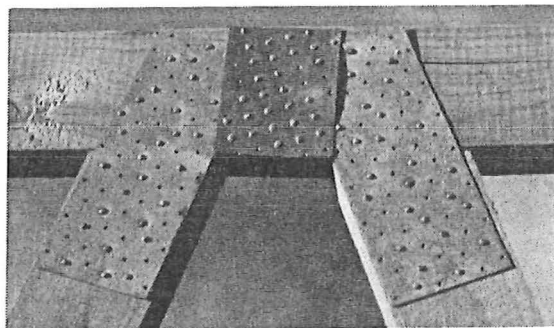
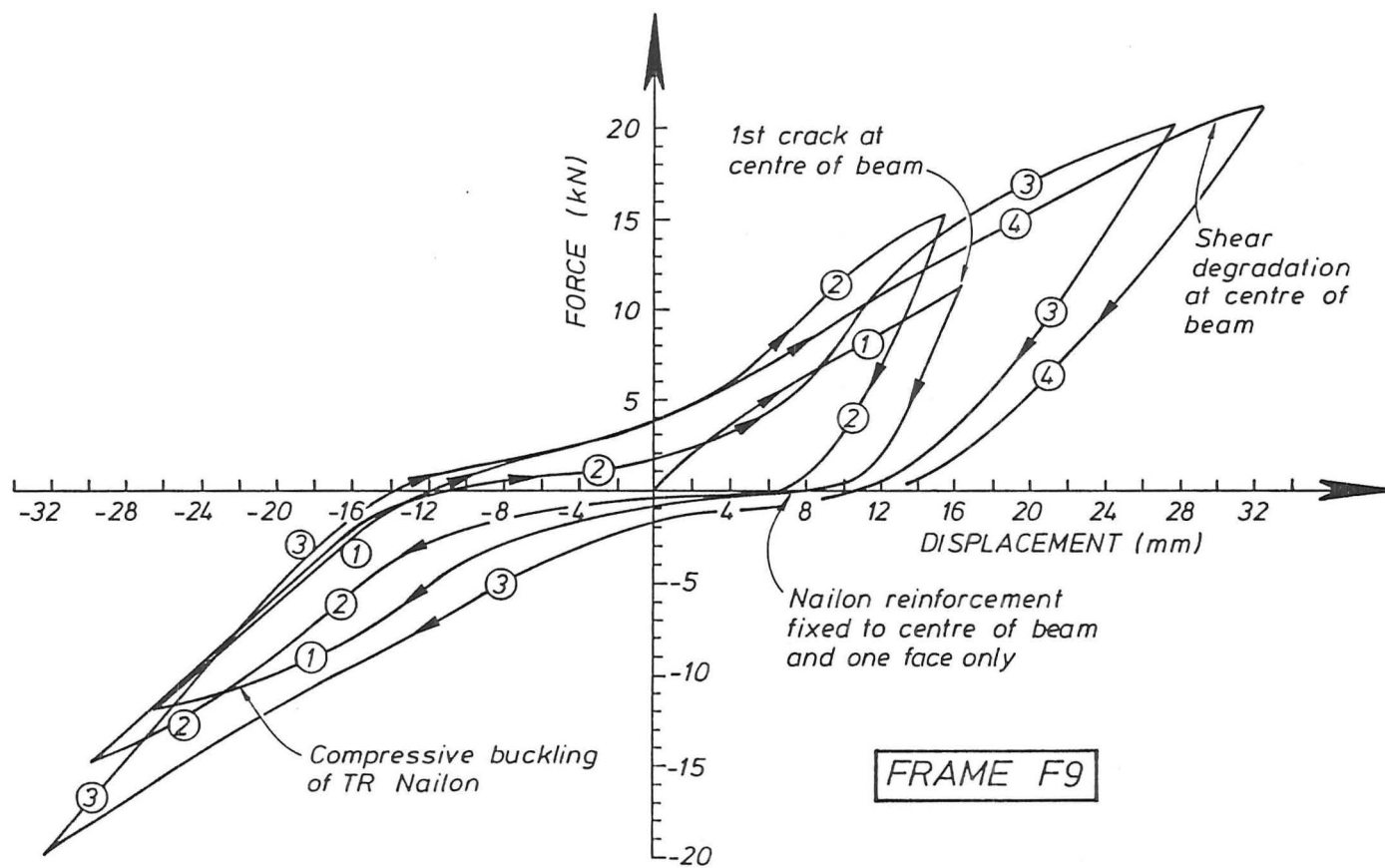


Plate 4.15 TC joints after testing.

Figure 4.27 Load-displacement plot for Frame F9



Cycling was stopped at 4 cycles when longitudinal cracking of the central part of the upper bearer had become worse.

The Table 4.1 wind/seismic design load is 7.7 kN. This is limited by shear in the central region of the top member. The Table 4.2 pin-jointed sway for this frame at 15 kN is 11 mm.

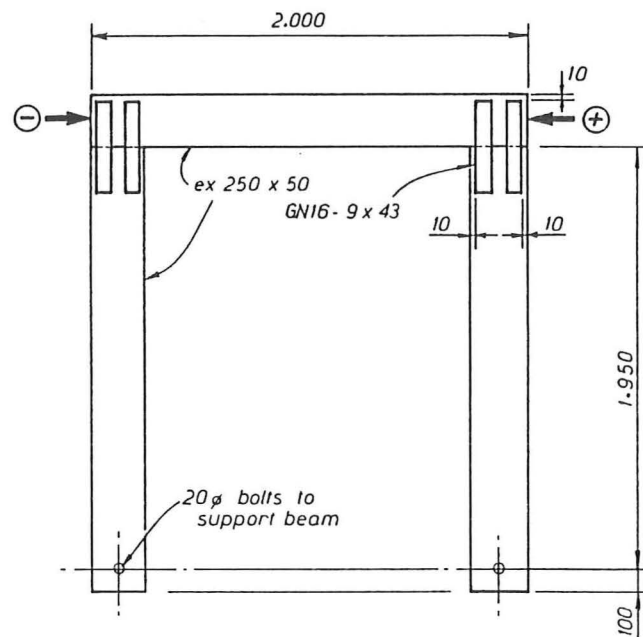
11. FRAME F10

Frame F10 (fig. 4.28 and Plate 4.16) was designed to simulate a toothplated portal frame knee joint assembly, and in particular to determine the rotational capacity of the moment resisting joints. The arrangement is one commonly used for small span plated frames. First cycle loading to 6 kN was followed by second cycle loading to 8 kN, and subsequent cycles were within the displacement limits of the second cycle. The increase in measured load within the third cycle probably arose from tightening up of the joints arising from buckling of the toothplates (Plate 4.17). As in some of the previous tests, buckling of the toothplates was not removed during the tensile part of the loading cycle. Progressively less load was attained during the 4th, 5th and 6th loading cycles as the displacement increased out to 80 mm. Buckling of the toothplates increased throughout the cycling. Figure 4.29 is the load-displacement plot for this frame. Displacements at the bolt supports were;

	BL	BR	Sway
+8 kN	-2	+8	10
-8 kN	+9	-3	12
	(mm)		

The joint rotations can be estimated from the horizontal displacements less the calculated flexural displacement of the members themselves.

The Table 4.1 ultimate load for this frame is 10 kN. This assumes that the compression load is carried by the toothplates only, with no contribution from the timber.



FRAME F10

Figure 4.28 Frame F10 construction.

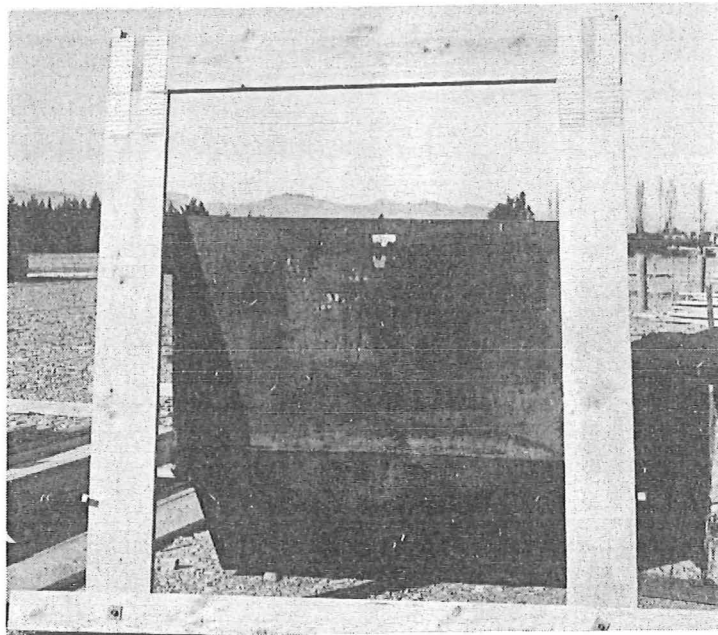
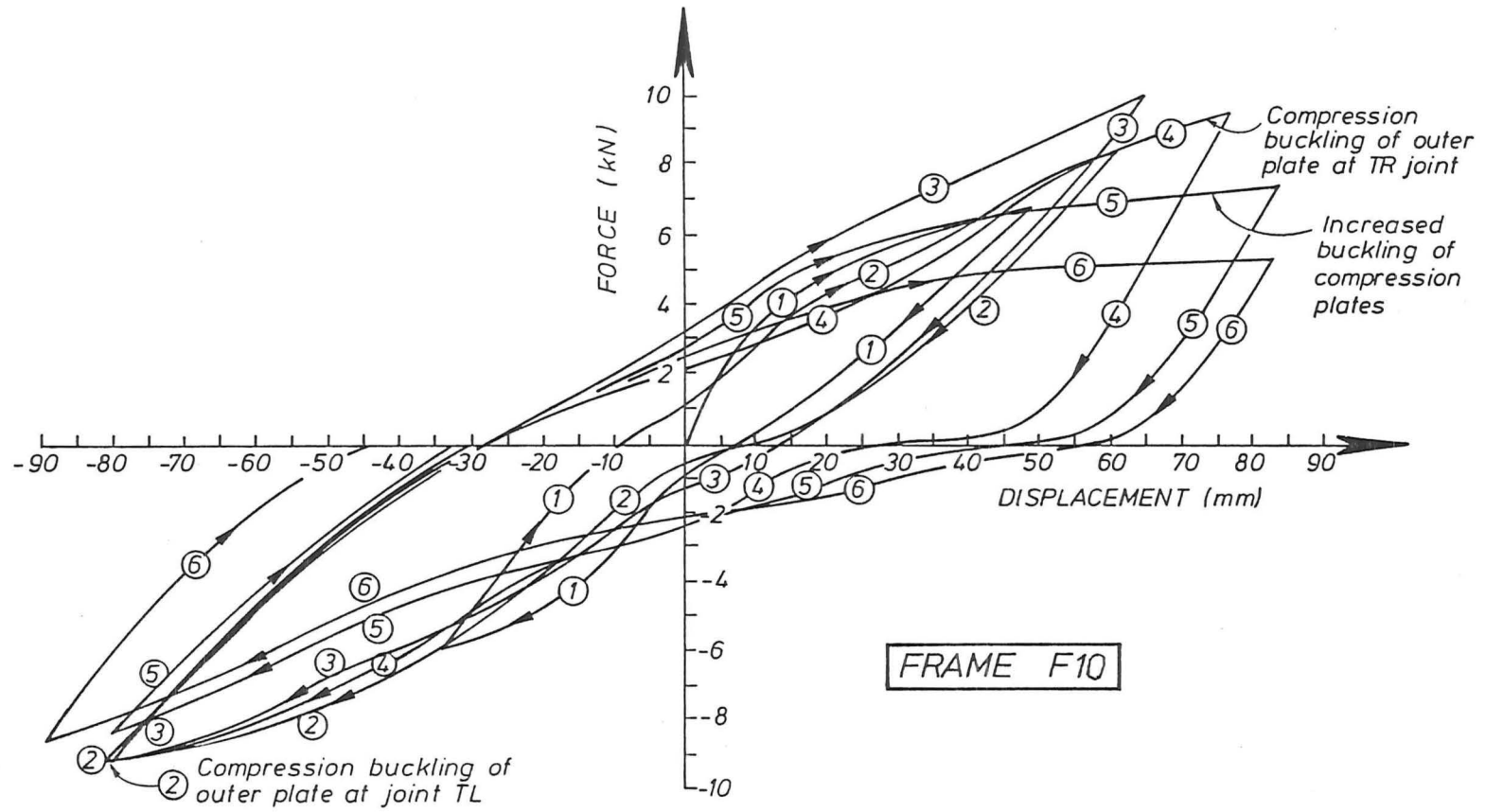


Plate 4.16 Frame 10 after testing.

Figure 4.29 Load-displacement plot for Frame F10.



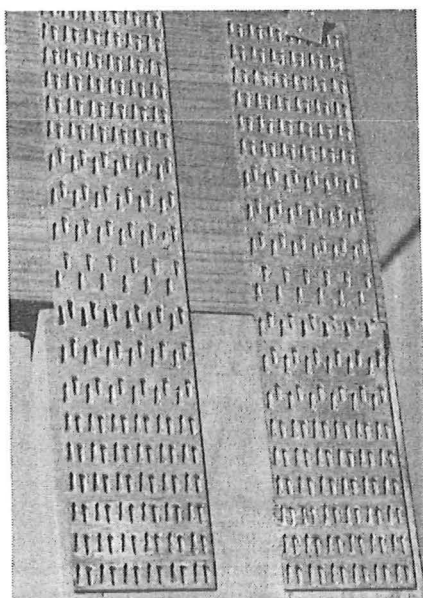


Plate 4.17 Buckling of toothplate with compressive load.

12. DISCUSSION

The failure load was greater than the design ultimate for all of the frames tested.

The frames were not as stiff as expected. The square diagonally braced (2 m x 2 m) frames ranged between $1/2$ and $1/4$ of the calculated stiffness and the narrower (2 m x 1 m) frames were about $1/6$ of the expected stiffness.

Lozenging of the frames accounted for less than $1/2$ of the total sway for all of the frames.

Except for Frame F9, all of the frames failed in the metal connections and most of these were sudden failures.

CHAPTER V

NAILON PLATE FRAMES

1. INTRODUCTION

These were diagonally braced timber frames suitable for resisting lateral forces in timber structures. These Frames (fig. 5.1) were designed using an ultimate strength approach. The joints were proportioned to have approximately 75 % of the ultimate (lower 5 %ile) strength of the timber members, based on the Lumberlok ultimate load of 1.5 kN/ nail and timber stresses derived from the NZS 3603:1981 values. Shear stress in the horizontal members in the region of the diagonal (i.e. the connection between the horizontal and diagonal members, fig. 5.1) and frame (i.e. the connection between the horizontal and vertical members) joints was greater than the allowable but was neglected as allowed by NZS 3603:1981 because of the small distance between the two Nailon plates (fig. 5.1).

To simulate the positioning of a frame between two gravity load bearing members, such as portal frame columns, each frame was restrained in the vertical direction by two ex 150 x 50 members on edge (restraining columns) connected to the frame by folded angle shearplates (Detail A,fig. 5.2). The shearplates had a large number of nails to ensure failure would occur in the joints of the frame. Each restraining column was restrained by a pinned support under its base (Detail C,fig. 5.2) and full height tension rods over the top (Detail B,fig.5.2).

Table 5.1 gives a summary of the design and test loads of the four frames. In the table '+' indicates that the frame was loaded first to the specified load in the positive direction (fig.5.1) and then a load of equal magnitude in the negative direction. The frame was loaded in the indicated direction and released where a '+' or '-' only is specified for the load.

Frame No	w/s load	ultimate load	Test load at cycle No. (rounded values)											
			1	2	3	4	5	6	7	8	9	10	11	12
1	13	39	±13	±13	±19	±19	±26	±26	+35	±39	±39	+45		
2	13	39	±13	±13	±27	±28	±38	+38	-42	-39				
3	13	39	±13	±13	±26	±26	+39	-34	+39	-31	+40			
4	10	30	±10	±10	±20	±20	+30	-26	+40	-34	+40	+43	+53	-32

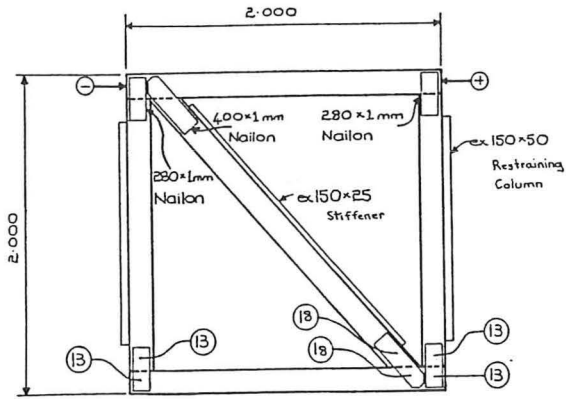
Table 5.1 Frame design and test loads.

2. FRAME 1

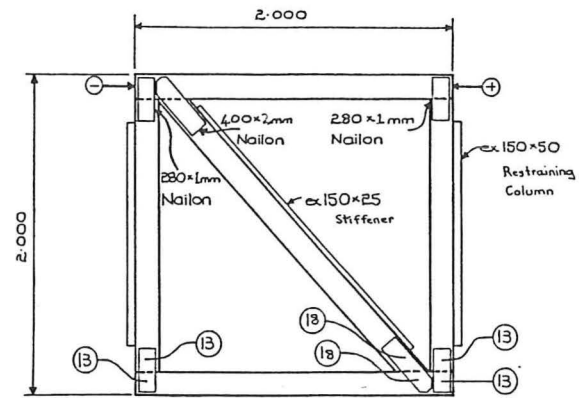
This frame (fig. 5.3 and Plate 5.1) had a wind/seismic design load of 13 kN and an ultimate design load of 39 kN from Lumberlok data. There were 13 nails in each nailgroup in the frame joints and 18 nails in each nailgroup in the diagonal joints. All of the joints were constructed with 1 x 110 mm Nailon plate.

The frame was loaded to the wind/seismic load of 13 kN in the +ve direction (fig. 5.3), such that the diagonal member was in tension. The load was removed, the frame loaded to 13 kN from the other direction and the load released again to complete the first cycle of the loading sequence. During the first -ve loading cycle, it was observed that the diagonal member buckled 20 mm out of the plane of the frame, and a 150 x 25 stiffener was nailed to the diagonal member to prevent this occurring again. The stiffener was only lightly nailed so it did not contribute to the area of the diagonal in compression. Buckling occurred in the diagonal plates (Plate 5.2) during the -ve loading cycle.

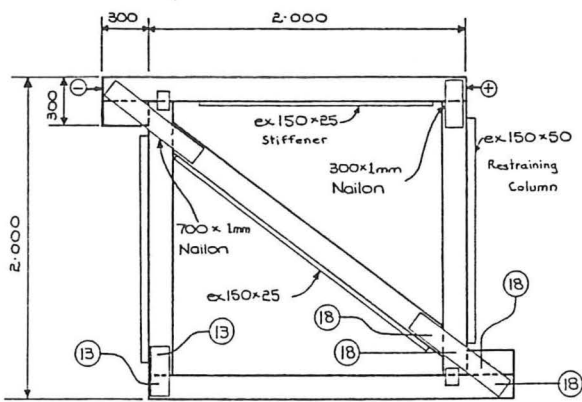
This 13 kN loading cycle was repeated followed by two cycles each with target loads of 19.5 and 26 kN. The frame behaved in a similar manner for all of the loading cycles, with deformations and buckling of the Nailon plate becoming more significant at the higher loads. The next load cycle to 35 kN caused the frame to buckle significantly out of plane (fig. 5.4) and the testing was stopped to rectify this. Figure 5.5 is the load-displacement plot for this first part of the test.



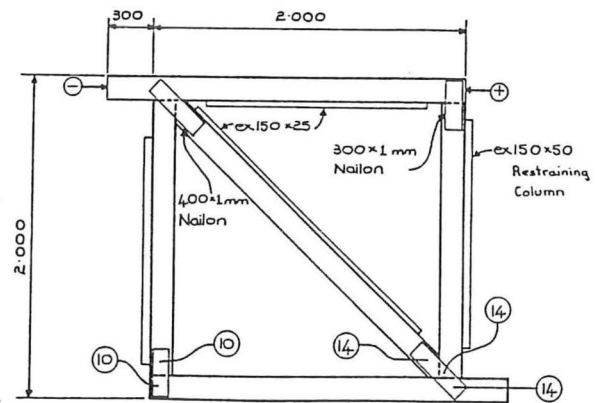
FRAME 1



FRAME 2



FRAME 3



FRAME 4

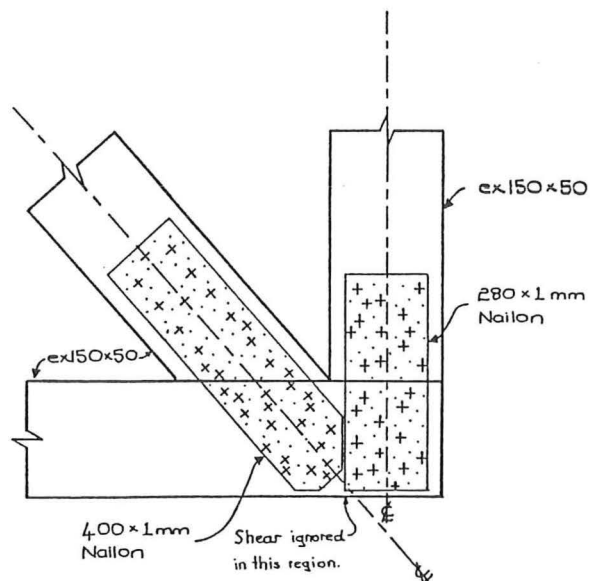


Figure 5.1 Nailon plate frames.

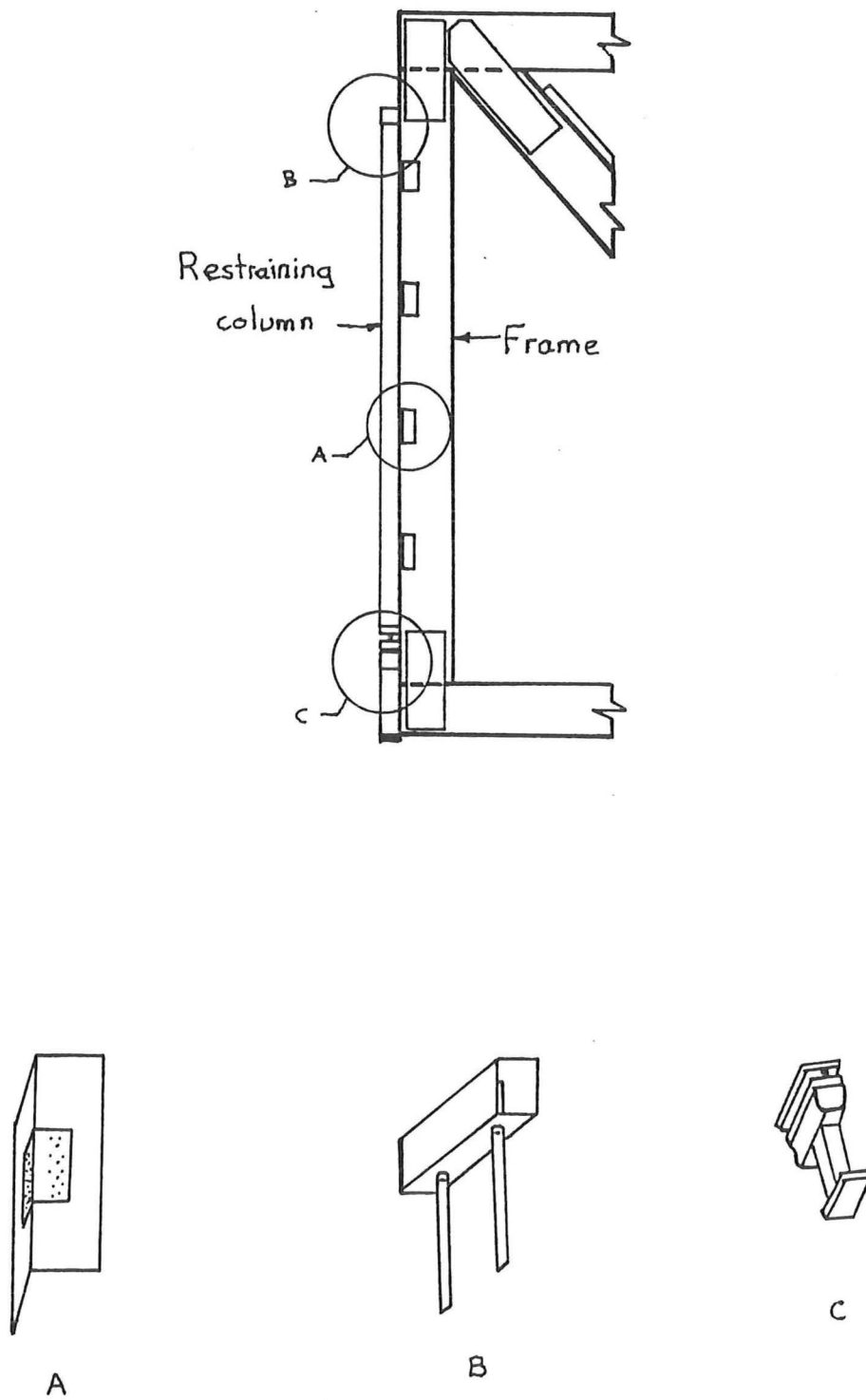


Figure 5.2 Restraining column details.

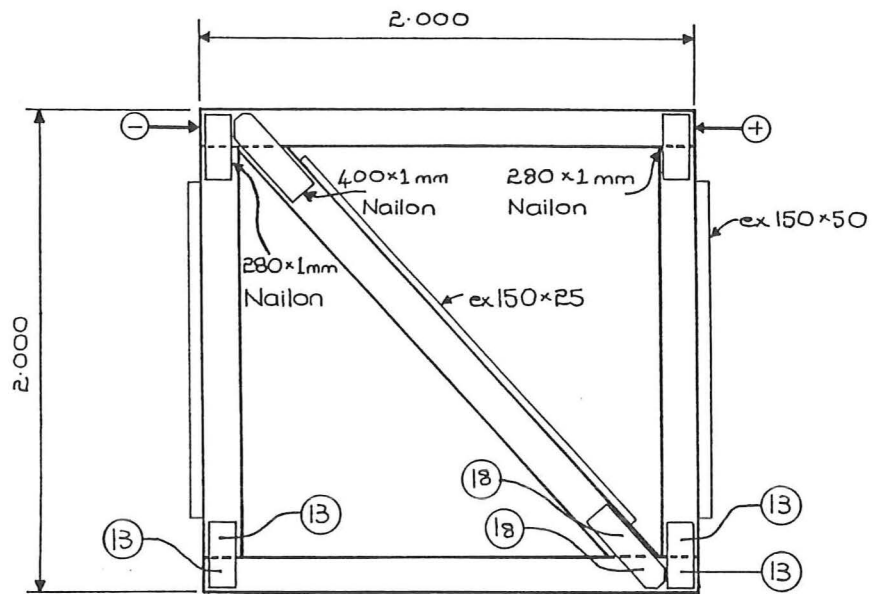


Figure 5.3 Construction details of Frame 1.

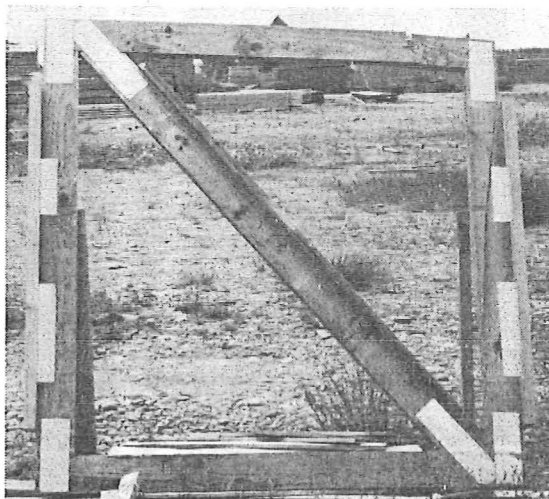


Plate 5.1 Frame 1 after testing.

Testing was resumed with extra restraining timber members positioned to prevent out-of-plane movement of the top of the frame. The top member failed at a knot position (Plate 5.2) when loaded to 45 kN. Prior to failure the top member had a high curvature out of the plane of the frame at the knot position. Figure 5.6 is the load-displacement plot for this second test.

Two deformation modes of the Nailon plate were observed in this test. The first resulted from rotation of the timber members as the frame displaced horizontally. The Nailon plate buckled out-of-plane on the compression side of the joint while remaining flat on the tension side (fig. 5.7). The buckling was more prominent in joints which had a compressive load applied across the joint i.e. the TL frame joint when loaded in the +ve direction.

The second deformation mode occurred when the plate was loaded in compression and shear simultaneously. Two variants of this deformation mode were observed (fig. 5.8 and Plate 5.3), depending on the pattern of nailing close to the edges of the two timber members.

The buckling which occurred in the Nailon plates was insufficient to create a permanent deformation of the plates and all plates straightened completely when the load was reversed.

The diagonal member joints translated out of the plane of the frame when loaded in compression, but returned to their previous position when reloaded in tension. This is the Mode B compressive buckling described in Chapter 4 (fig. 4.9).

Neither the plate buckling nor the translation of the timber members was observed in the joints tested in the laboratory (Chapter 2). These two mechanisms are not likely to cause a significant departure from the joint load-displacement relationships obtained from the laboratory tests.

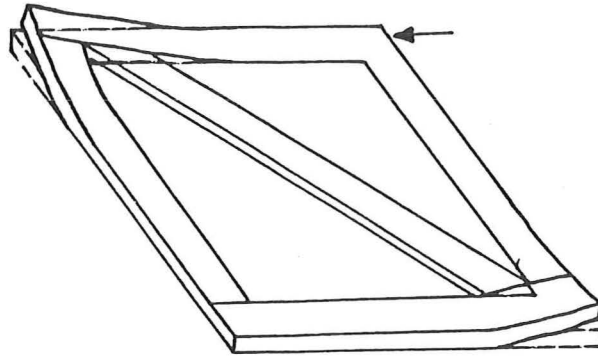


Figure 5.4 Cut-of-plane buckling of TL and BR corners.

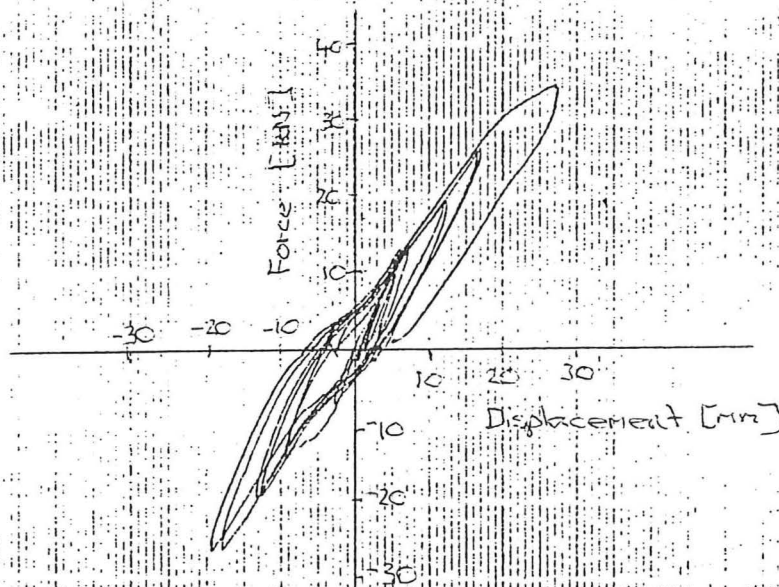


Figure 5.5 Load-displacement plot for top of frame.

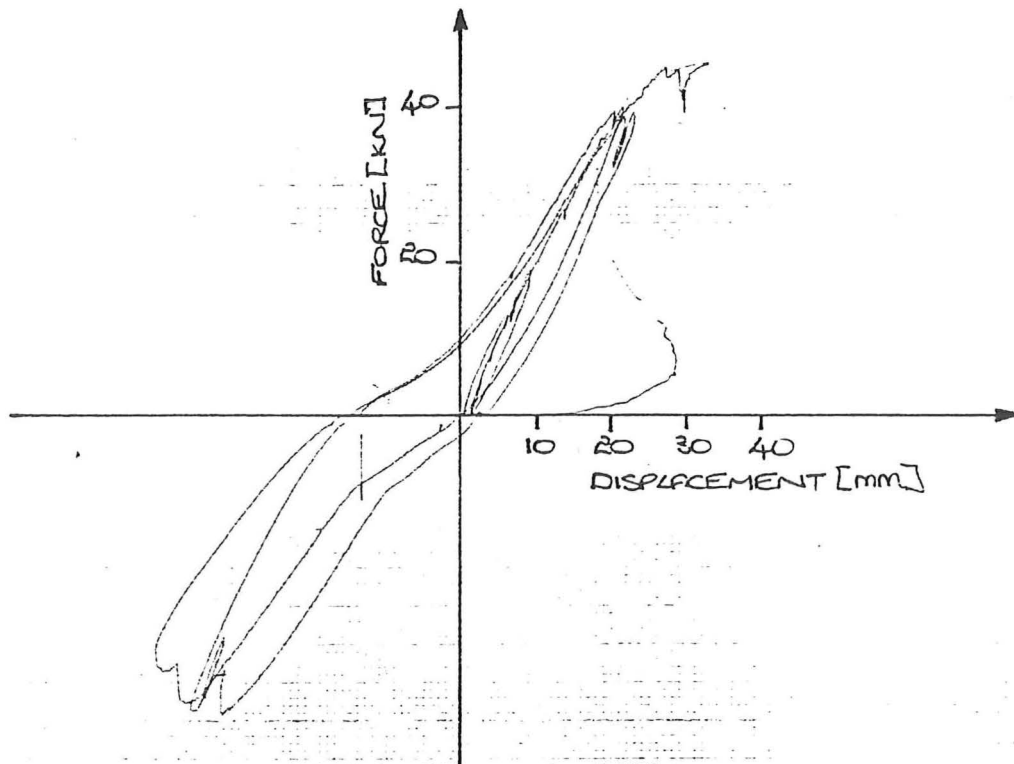


Figure 5.6 Load-displacement plot for Frame 1 Test 2

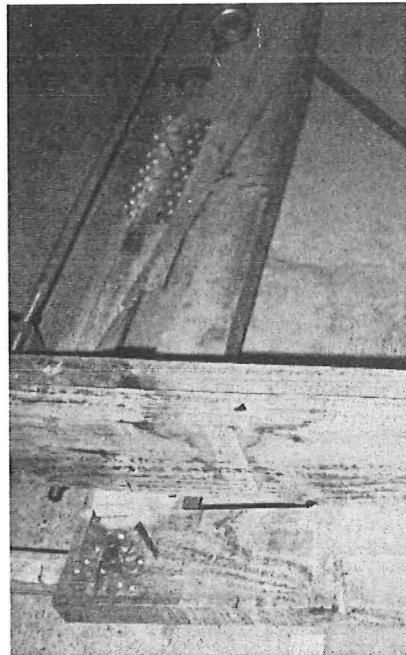


Plate 5.2 Failure of timber at TR corner.

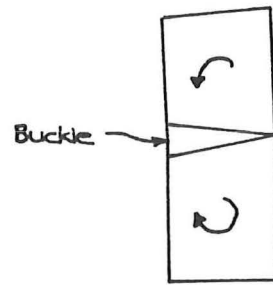


Figure 5.7 Buckling from applied moment.

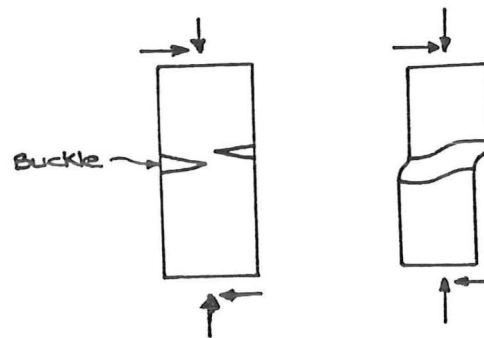


Figure 5.8 Buckling from compression and shear.

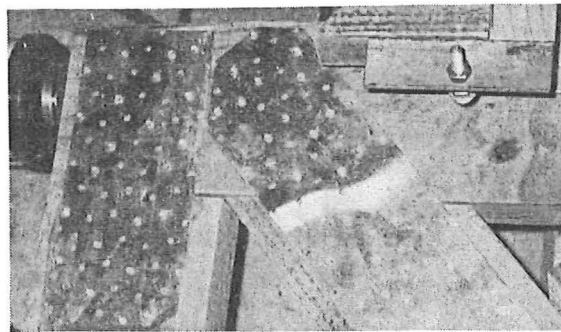


Plate 5.3 Buckling of diagonal Nylon plate.

3. FRAME 2

The dimensions of this frame (fig. 5.9 and Plate 5.4) were the same as those of Frame 1, but 2 mm Nailon plate was used for the diagonal joints and 1 mm Nailon plate for the frame joints. The design loads for this frame were the same as for Frame 1. To construct this frame, the diagonal and top members of Frame 1 were removed, the frame turned over (i.e. TL became TR etc.) and the diagonal and top were replaced with new timber members.

The method of testing was the same as that for Frame 1, with two loading cycles each with target loads of +13 and +26 kN followed by one cycle of +39 kN. The frame was then loaded to +39 kN and -42 kN at which it failed. Figure 5.10 is the load-deflection plot obtained from this frame.

Failure was sudden as the top member split longitudinally in the region of the TL joints (fig. 5.11(a) and Plate 5.5), the timber on either side of the split displacing longitudinally to give a step in the end of the member, suggesting that high shear stresses may have been present. This failure is similar to the failure observed in one of the joint pairs described in Chapter 3. The calculated shear stress in the timber at this load was 8.4 MPa (i.e. $4.3 \times \text{NZS 3603 allowable wind/seismic}$).

More nails were placed in the nailgroups in the two TL joints and the frame reloaded in the negative direction. No increase in load capacity of the frame was obtained. The top member failed again but in a different manner (fig. 5.11(b) and Plate 5.6).

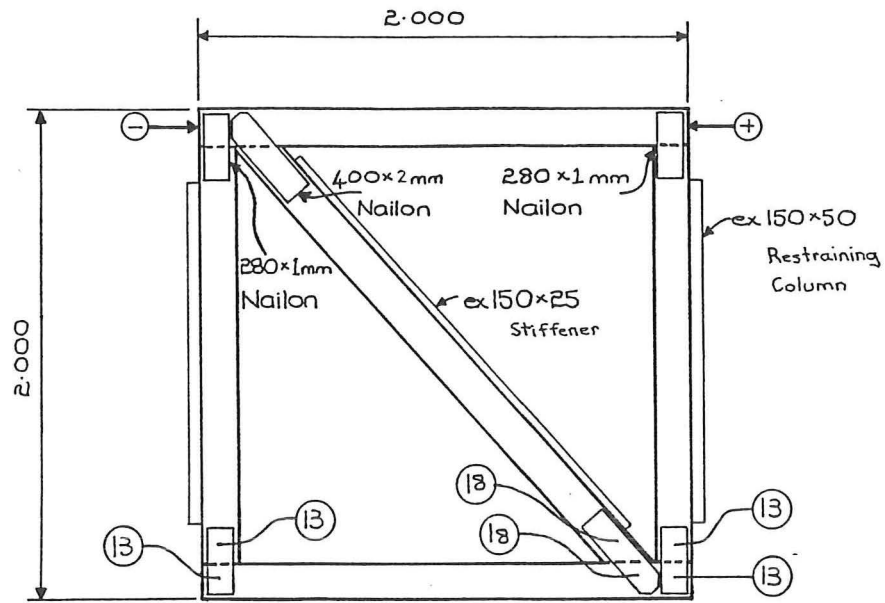


Figure 5.9 Construction details of Frame 2.

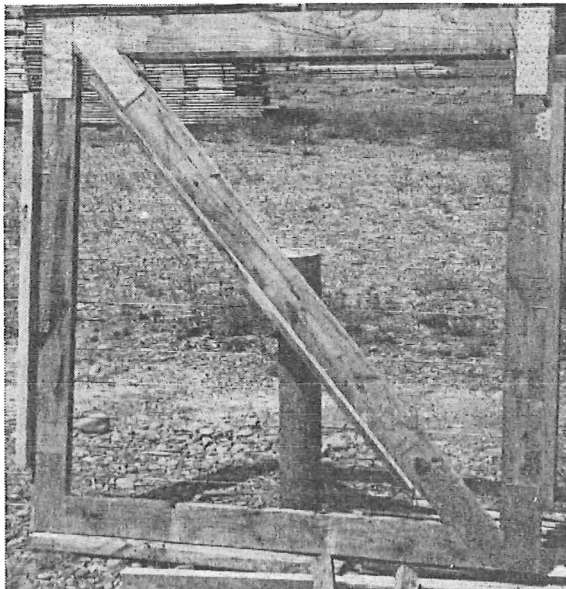


Plate 5.4 Frame 2 after testing.

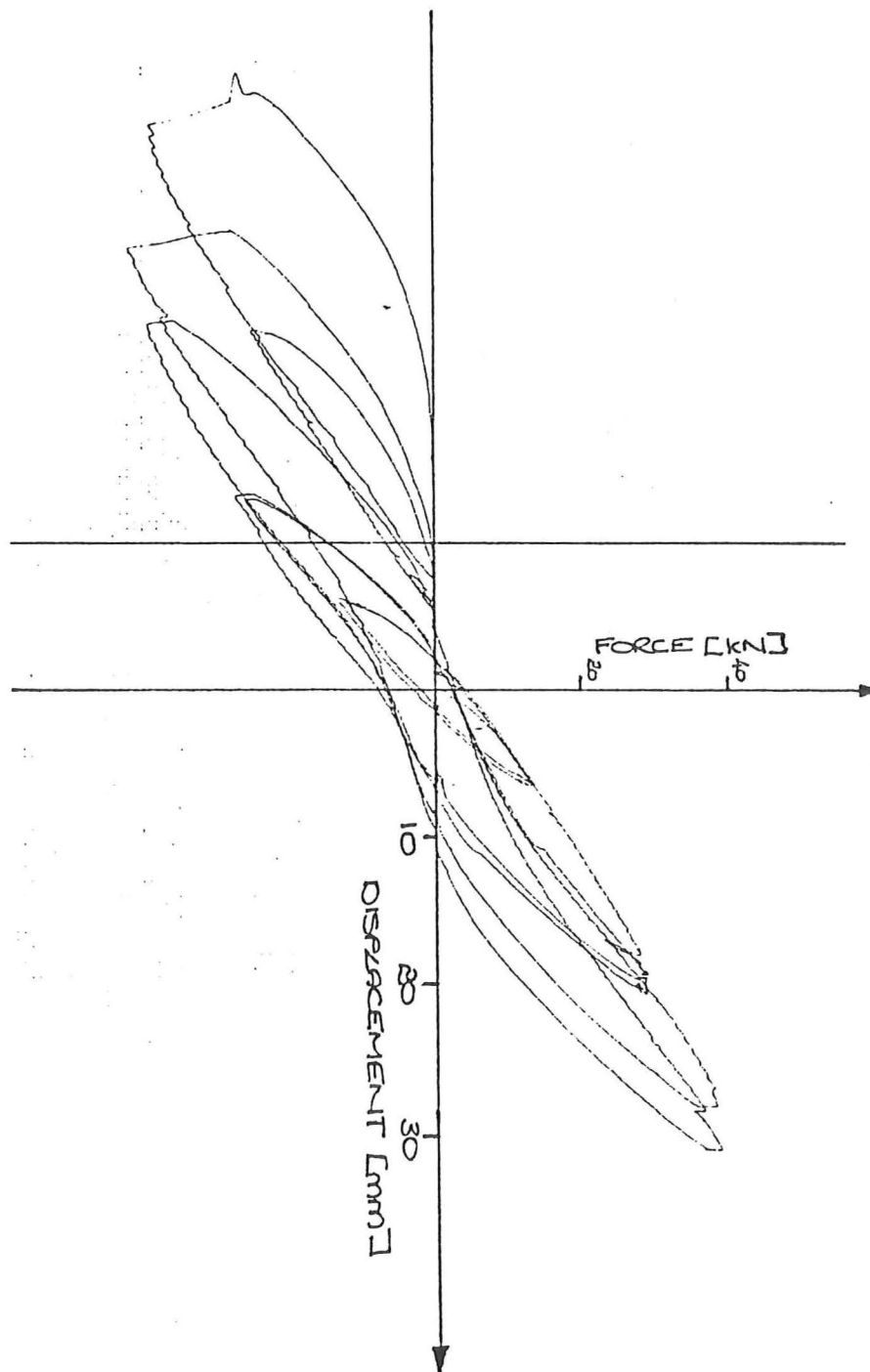


Figure 5.10 Load-deflection plot for Frame 2.

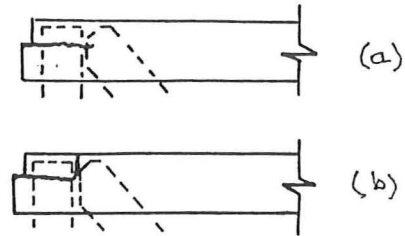


Figure 5.11 a) First failure of Frame 2.
b) Second failure.

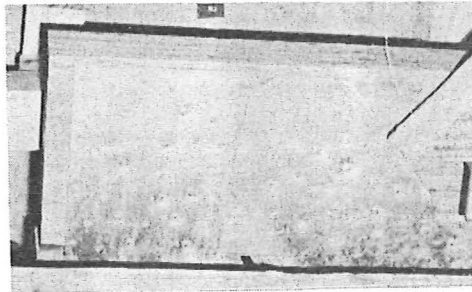


Plate 5.5 First failure at TL corner.

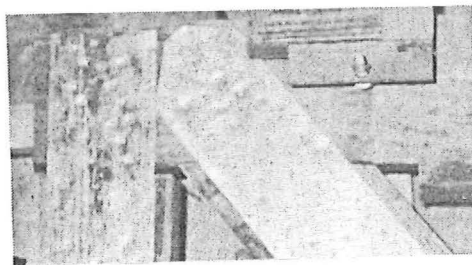


Plate 5.6 Second failure at TL corner

The frame characteristics were similar to those of Frame 1, having approximately the same stiffness and having a similar hysteretic curve. This is because the joints do not contribute significantly to the total deflection of the frame. The only difference between the behaviour of this frame and that of Frame 1 occurred because of the diagonal Nailon plate connection. The thicker plate did not buckle in compression or allow significant out-of-plane translation of the diagonal member when loaded in compression.

4. FRAME 3

Frame 3 (fig. 5.12 and Plate 5.7) had a wind/seismic design load of 13 kN and an ultimate load of 39 kN. It was designed with a single pair of Nailon plates covering the diagonal, vertical and horizontal members. The block of timber parallel to the horizontal members is required to prevent the Nailon plate buckling. This method of construction eliminates the high shear stresses in the horizontal members of Frames 1 and 2.

No deformations were observed in the joints at a load of +13 kN. The load of -13 kN caused shear/compression mode buckling of the Nailon plate between the diagonal and vertical members similar to that observed in Frame 1 (Plate 5.8). The buckle did not straighten completely upon loading to +13 kN.

A large curvature was observed in the horizontal members (Plate 5.9) at +26 kN due to the joint geometry. Plate 5.8 shows the buckling of the diagonal to vertical connection at a load of -26 kN. The shear/compression mode buckle between the diagonal and vertical members was more prominent than at -13 kN. There was also a rotational mode buckle on the other side of the vertical member.

The frame failed by splitting the top member (fig. 5.13 and Plate 5.9b) at a load of -34 kN. Figure 5.14 is the load-deflection plot for this test.

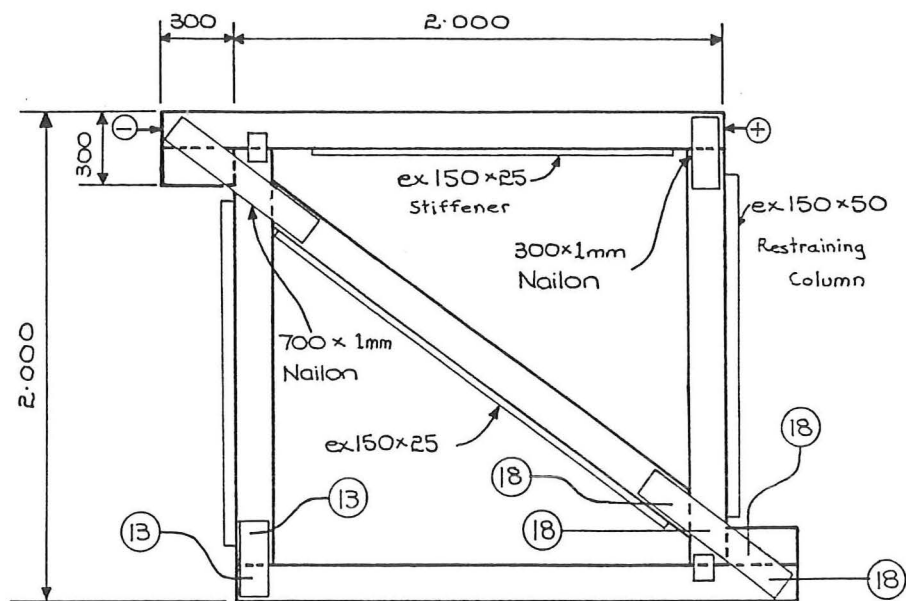


Figure 5.12 Construction details of Frame 3.

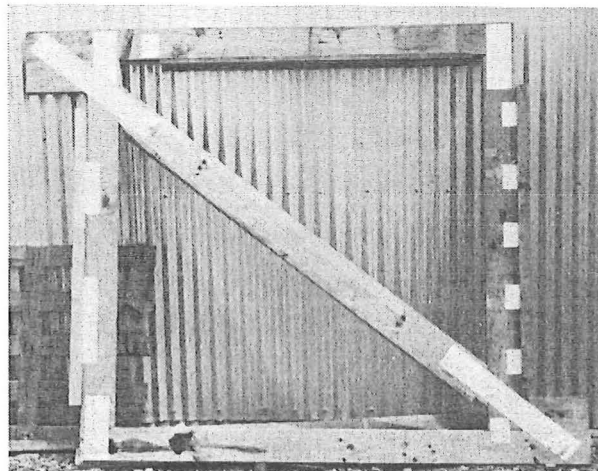


Plate 5.7 Frame 3 after testing.

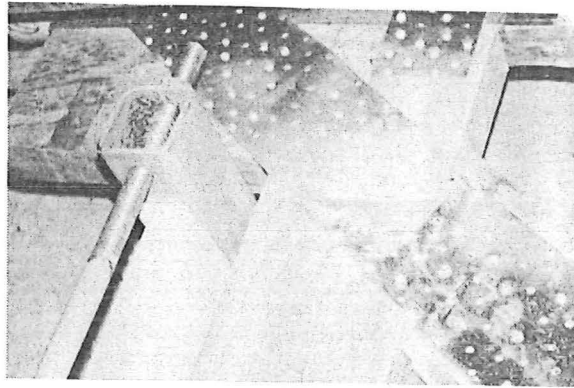


Plate 5.8 Buckling at TL diagonal Nailon plate.

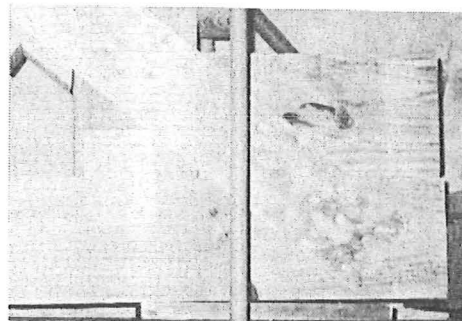


Plate 5.9 Curvature of frame at BR corner.

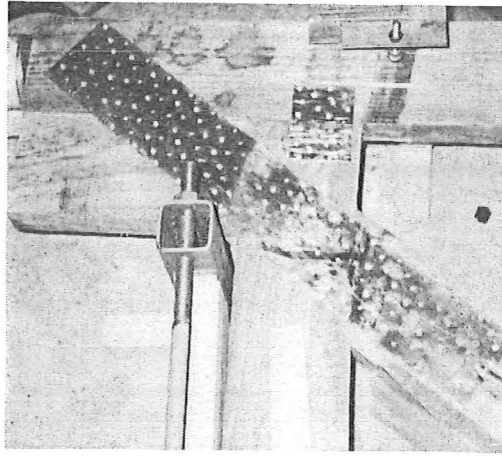


Plate 5.9b Failure after testing.

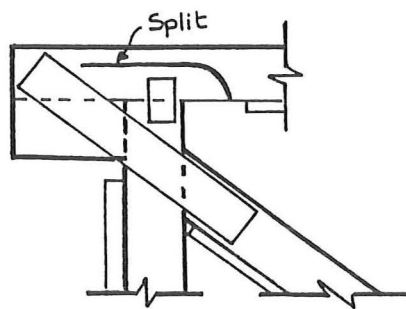


Figure 5.13 Failure by splitting in top member.

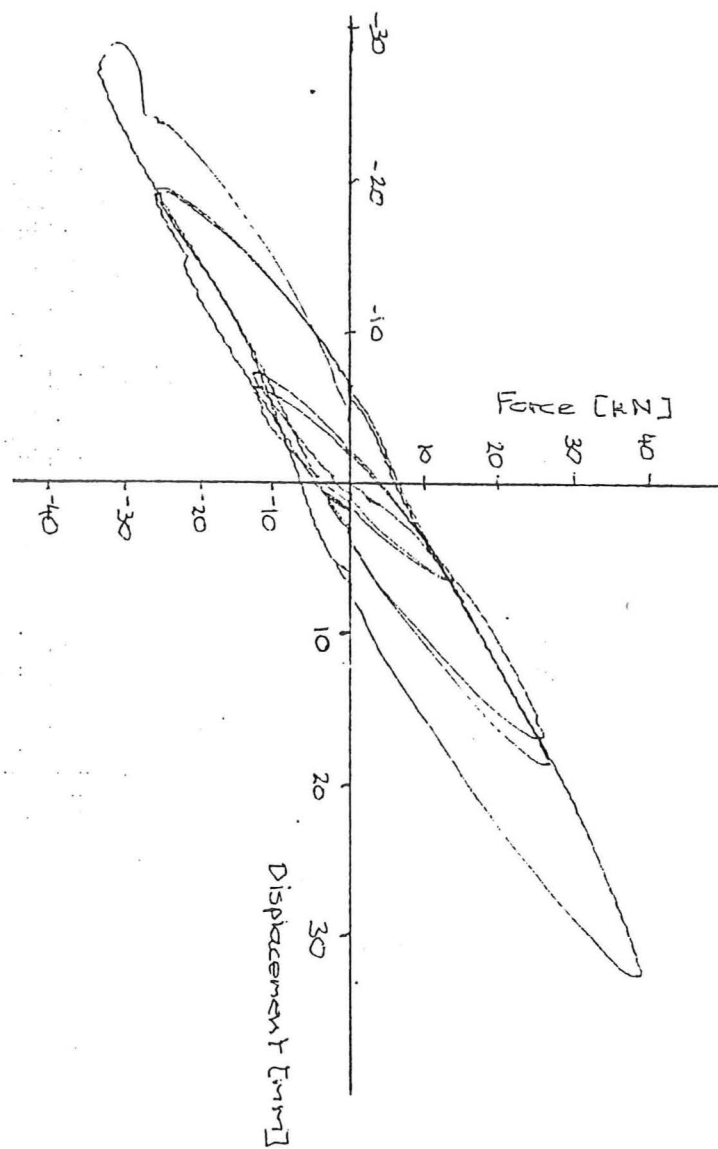


Figure 5.14 Load-deflection plot for Frame 3 Test 1.

The small Nailon plate between the vertical and horizontal members was then replaced with a larger plate which covered the split (Plate 5.10) and the frame reloaded to +39 kN, -31 kN and then +40 kN. The frame failed in the same position again so testing was stopped. The load-deflection plot for this test is Figure 5.15.

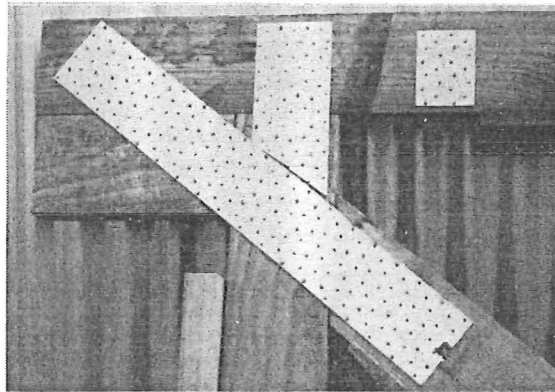


Plate 5.10 Construction of TL corner for Test 2.

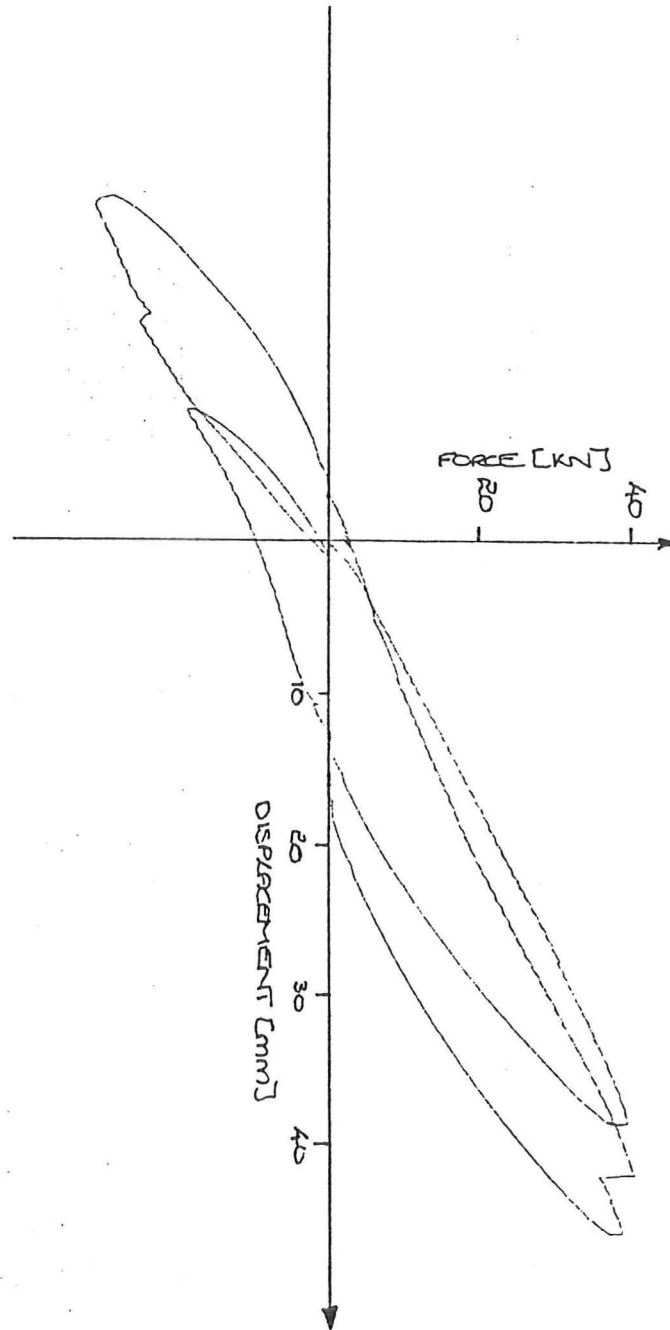


Figure 5.15 Load-deflection plot for Frame 3 Test 2.

5. FRAME 4

This frame (fig. 5.16 and Plate 5.11) was also constructed with a single pair of plates over the intersection of the three members at the corner. The top member, the diagonal member and part of the left vertical member of Frame 3 were replaced to construct this frame. The number of nails in the joint nailgroups was decreased to reduce the possibility of failure of the timber members. The diagonal member was repositioned, from the position for Frame 3, to reduce the bending moment Frame 3 had in its horizontal members.

Cycles of +10 kN load produced deformations similar to Frame 3 at a load of 13 kN. The horizontal member displaced 4 mm horizontally relative to the diagonal member at a load of -20 kN, recovering the displacement upon reloading in the positive direction during two cycles of +20 kN. A cycle of +30 kN was attempted but the Nailon plate began to buckle between the nail positions at the join between the horizontal and vertical members (Plate 5.12) as the load increased beyond -20 kN.

The Nailon plate was straightened, by applying a load of +40 kN to the frame, and extra nails were placed along the edges of the plate to reduce the buckling. The frame was then reloaded to +43 kN but the whole frame buckled out of plane so the load was released. The frame was reloaded, with extra restraining members in place, to +54 kN but the BL corner began to fail (Plate 5.13) so the load was released and the frame loaded to -32 kN before the load reduced as the Nailon plate again buckled (Plate 5.14). Figure 5.17 is the load-displacement curve for this frame.

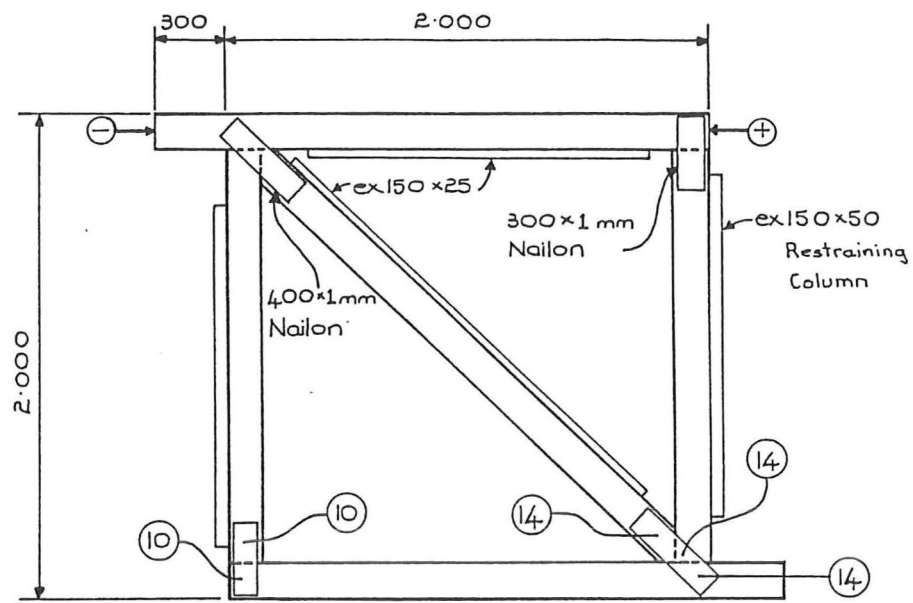


Figure 5.16 Construction details of Frame 4.

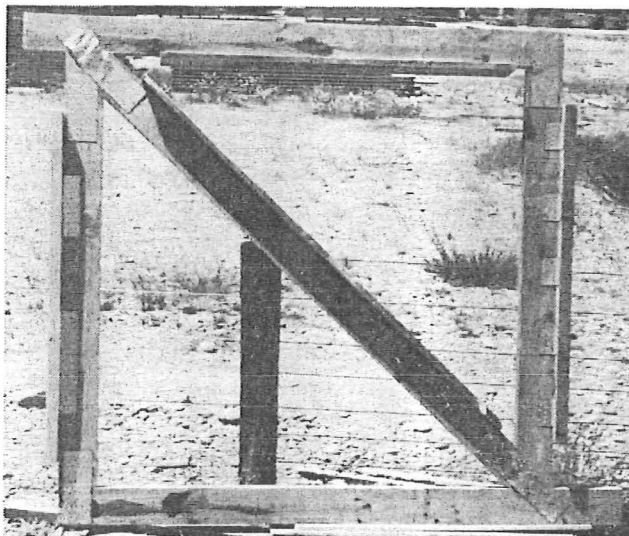


Plate 5.11 Frame 4 after testing.

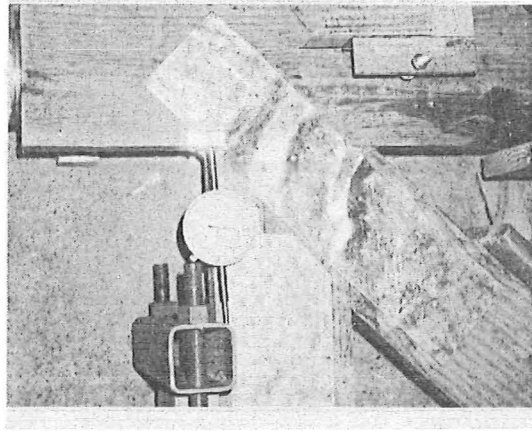


Plate 5.12 Buckling of TL Nailon plate.

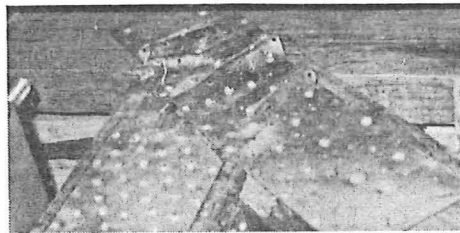


Plate 5.13 Buckling of TL Nailon plate after renailing.

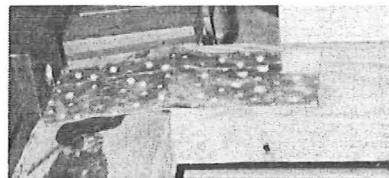


Plate 5.14 Failure of BL corner under positive loading.

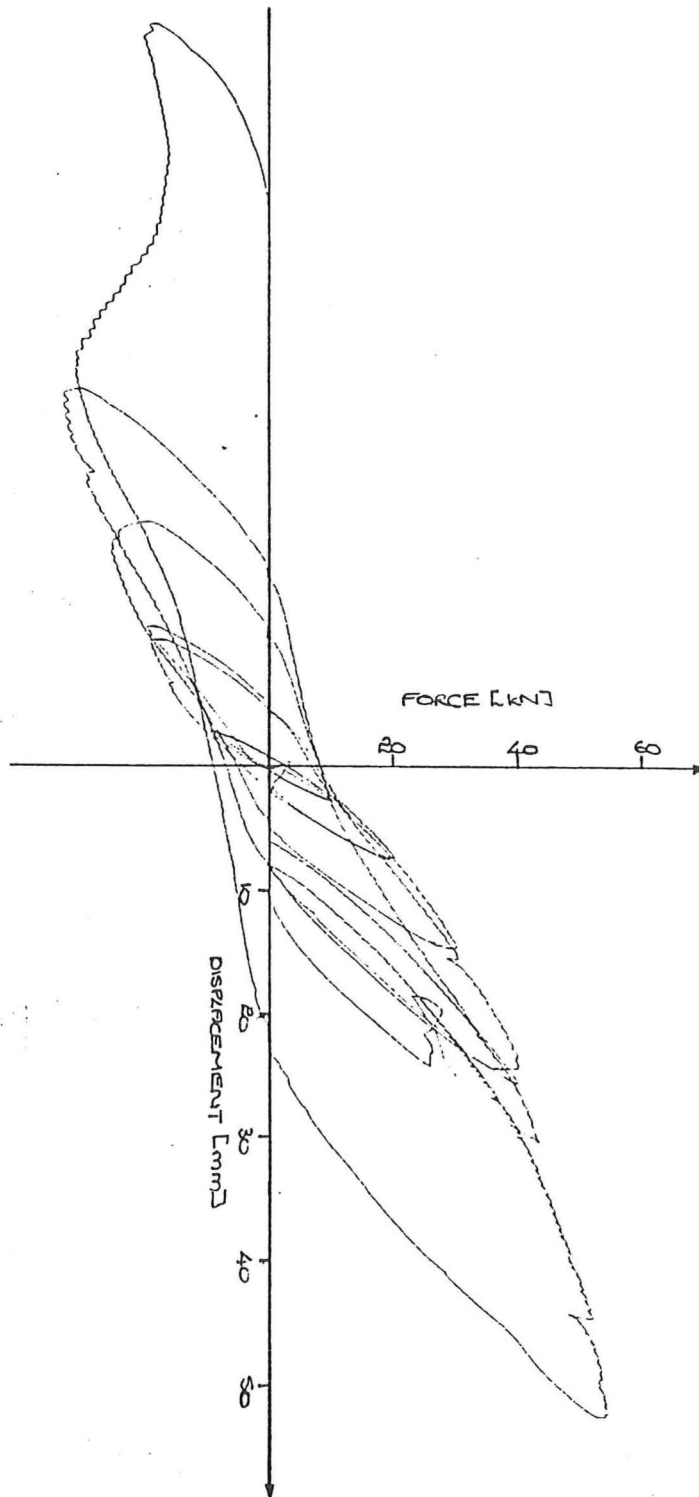


Figure 5.17 Load-displacement curve for Frame 4.

6. DISCUSSION

There was no difference in the load deflection behaviour of Frames 1 and 2, so there appeared to be no advantage in using the 2 mm Nailon plate for the diagonal joints.

Frames 1, 2 and 3 failed because the timber members were overstressed. These failures were sudden and significantly reduced the load carrying capacity of the frames. Frame 4 failed because of buckling of the Nailon plate when loaded in one direction and the frame buckled out of plane when loaded in the opposite direction.

All of the frames tested achieved loads of at least 3 times wind/seismic, based on Lumberlok data, before failing.

Buckling of the Nailon plate contributed to the ductility of the frame. This is unlike the nailstrap described in Chapter 4 where buckling lead to failure of the steel.

Compressive buckling of the Nailon plate generally occurred when the load on a pair of plates was greater than 10 kN. This buckling is difficult to prevent with the 1 mm Nailon plate. The buckling does not appear to be detrimental to the behaviour of the frame.

CHAPTER VI

HOLD-DOWN TESTS

1. INTRODUCTION

The connection between the timber frame and the supports is termed "hold-down" connection in this report. This connection resists vertical loads at the tension end of the frame (fig. 6.1). The shear load is transferred to the supports by another connection, usually in the centre of the frame.

This chapter presents the results of tests of two types of hold-down (fig. 6.1) and an angle shearplate. Three specimens with Lumberlok concrete fixing cleats, type CF1 [6], and two specimens with Lumberlok prototype shearwall holddowns were constructed and tested in the laboratory. In addition an angle shearplate used on the frames described in Chapter 5 was tested.

2. CONCRETE FIXING CLEATS

Three tests were carried out on Lumberlok type CF1 (fig. 6.2) concrete fixing cleats to determine their characteristics when used as hold-down connectors for a frame. Stewart [10] has tested a similar cleat made of 2 mm Nailon plate and fixed with a large number of nails, but only reported the failure load. The cleats were tested with different supports (fig. 6.3) and washers between the head of the bolt and the cleat.

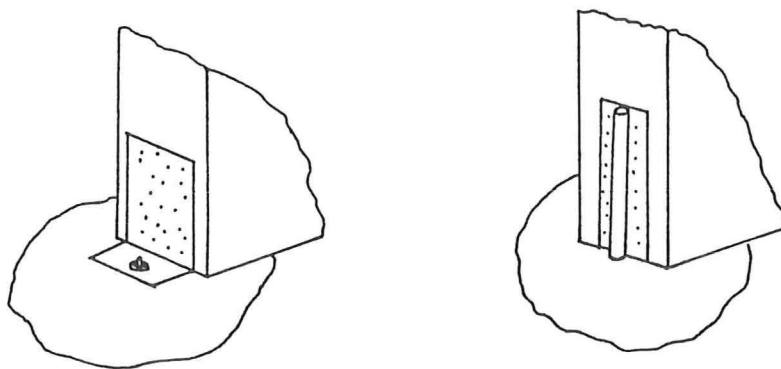
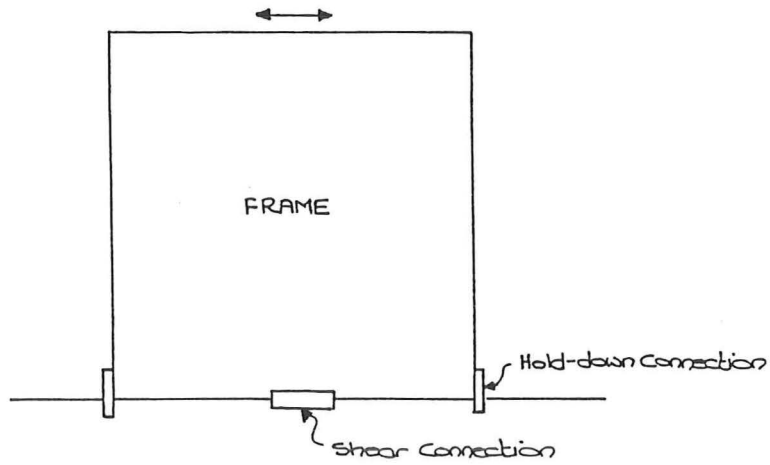


Figure 6.1 Lumberlok CF1 and prototype shearwall hold-downs.

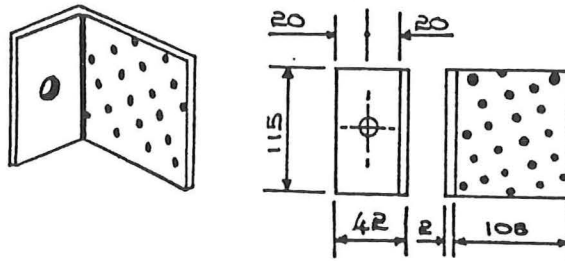


Figure 6.2 Lumberlok concrete fixing cleat CF1.

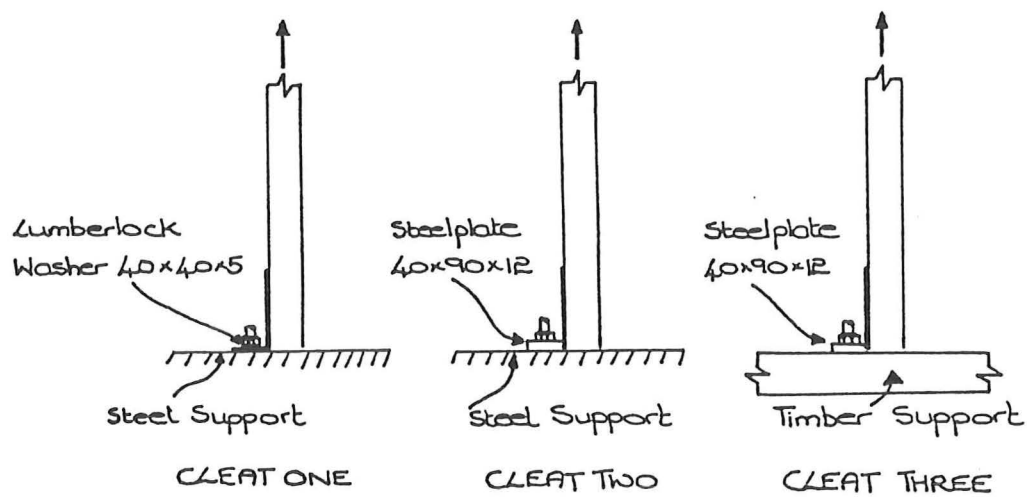


Figure 6.3 Support materials and washers for tests.

Table 6.1 gives the details of the three cleats. The wind/seismic (w/s) and ultimate loads are based on the loads for the 12 nails in the timber member. The washer for Cleat 1 is the standard Lumberlok product, the other two washers were fabricated in the laboratory. The support type is the material beneath the cleat to which the cleat was clamped with the bolt. A concrete support behaves in a manner intermediate between that of timber and steel. The force at 4 mm slip enables a comparison of forces at a small but reasonable displacement. The displacement at the maximum load shows how much slip is required to develop the full load on the connection.

Cleat No	w/s kN	Ultimate kN	Washer size	Support type	4mm slip Force	Max Load slip
1	6.1	18	40x40x5 *	Steel	9 kN	---
2	6.1	18	40x90x12	Steel	20 kN	10 mm
3	6.1	18	40x90x12	Timber	13 kN	17 mm

* Lumberlok washer

Table 6.1 CF1 Test Details

Plate 6.1 shows the test setup used for Cleat 3, the other two tests were similar to this. Figure 6.3 shows the force-displacement curves for the three tests. The displacement is that of the timber member relative to the support. The displacement of the Nailon plate relative to the timber is plotted on the same graph for comparison with the total displacement (the Nailon plate displacement was not recorded for Cleat 3).

The total stiffness of Cleat 2 was similar to that of the Nailon plate stiffness, especially after the maximum load was attained during loading. Cleat 1 with the Lumberlok washer had the lowest total stiffness, but this remained reasonably constant above 10 kN load. Cleat 3 with the timber support had a total stiffness which lay between the other two cleats. Plate 6.2 shows the three cleats after testing with their respective supports and washers.

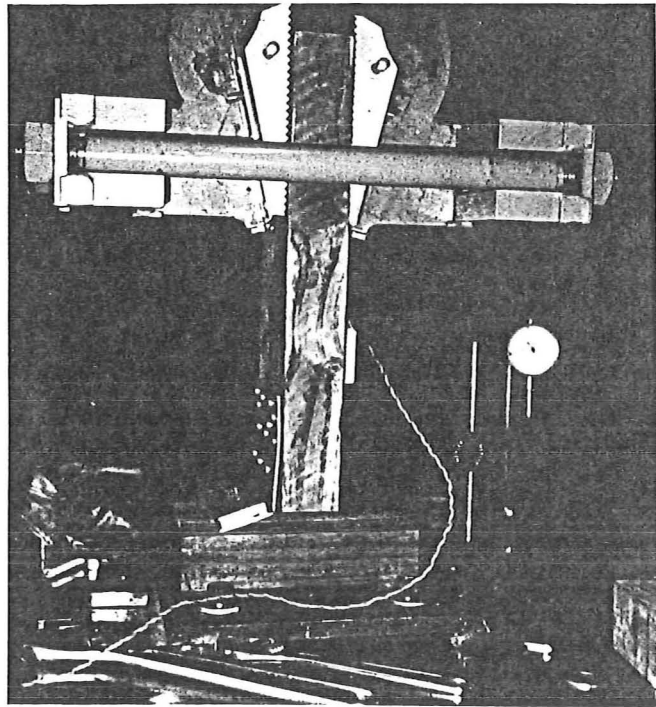


Plate 6.1 Testing of Cleat 3.

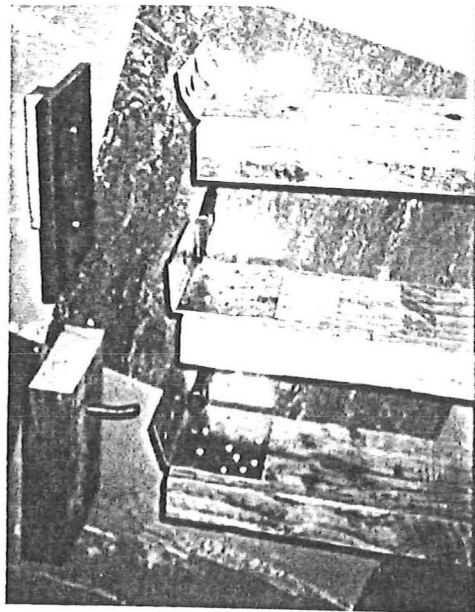


Plate 6.2 Comparison of 3 cleat tests.

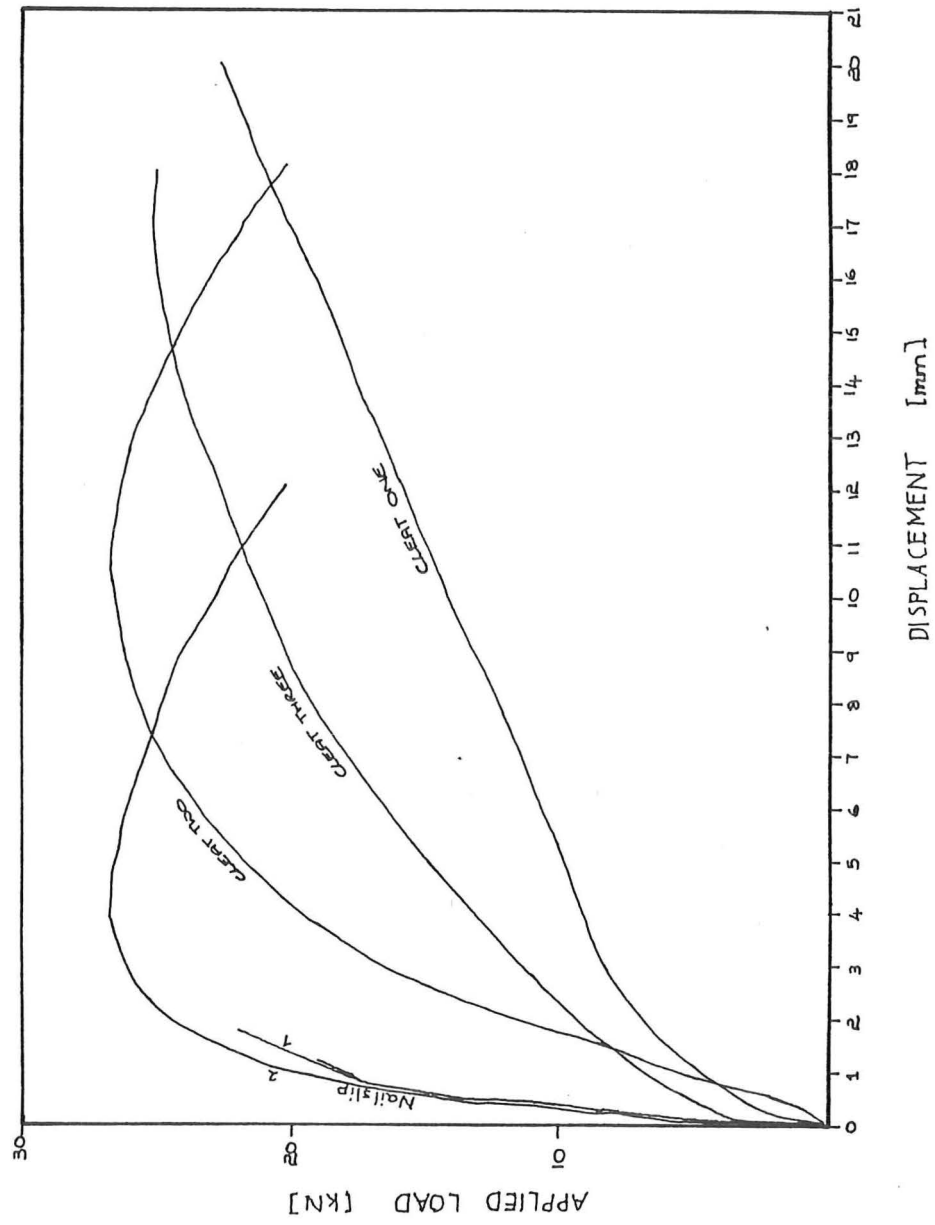


Figure 6.3 Load-displacement plots for the 3 cleats.

3. PROTOTYPE SHEARWALL HOLDDOWN

Two prototype hold-downs (fig. 6.4 and Plate 6.3) were tested. Table 6.2 summarizes the design and test details for the two prototype hold-downs. The nail load is the design load on the hold-down the nails allow and the tierod load is the load that the tierod will sustain. Prototype hold-down 1 was designed to fail in the nails, and Prototype hold-down 2 in the steel tierod.

Quantity	Units	1	2
Plate Length	mm	200	300
Number of nails		18	42
Nail wind/seismic Load	kN	9	21
Nail Ultimate Load	kN	27	63
Tierod Design (0.6 Fy, Grade 250)	kN	12.6	12.6
Tierod Yield (Fy Grade 250)	kN	21	21
Load at 4 mm slip	mm	26	26
Maximum load on hold-down	kN	33	35
Displacement at Maximum	mm	9.5	14
Failure mechanism		Nails	Tierod

Table 6.2 Shearwall hold-down Details

Figure 6.5 is the load-displacement plot for the two Prototype hold-downs. Prototype 1 gave a load-deflection plot which is similar to Cleat 2, except for a fall and subsequent rise in stiffness at 4 mm displacement. This distortion in the curve is caused by yielding of the steel tierod. Thus Prototype 1 had almost enough nails to cause a tension failure of the tierod. The effect of tierod yield is more pronounced in the plot for Prototype 2.

Plate 6.4 shows Prototype 1 with a load of 20 kN, where the hold-down is beginning to pull away from the timber at the top. This is a result of the eccentricity of the centreline of the tierod. This feature was not noticed in Prototype 2.

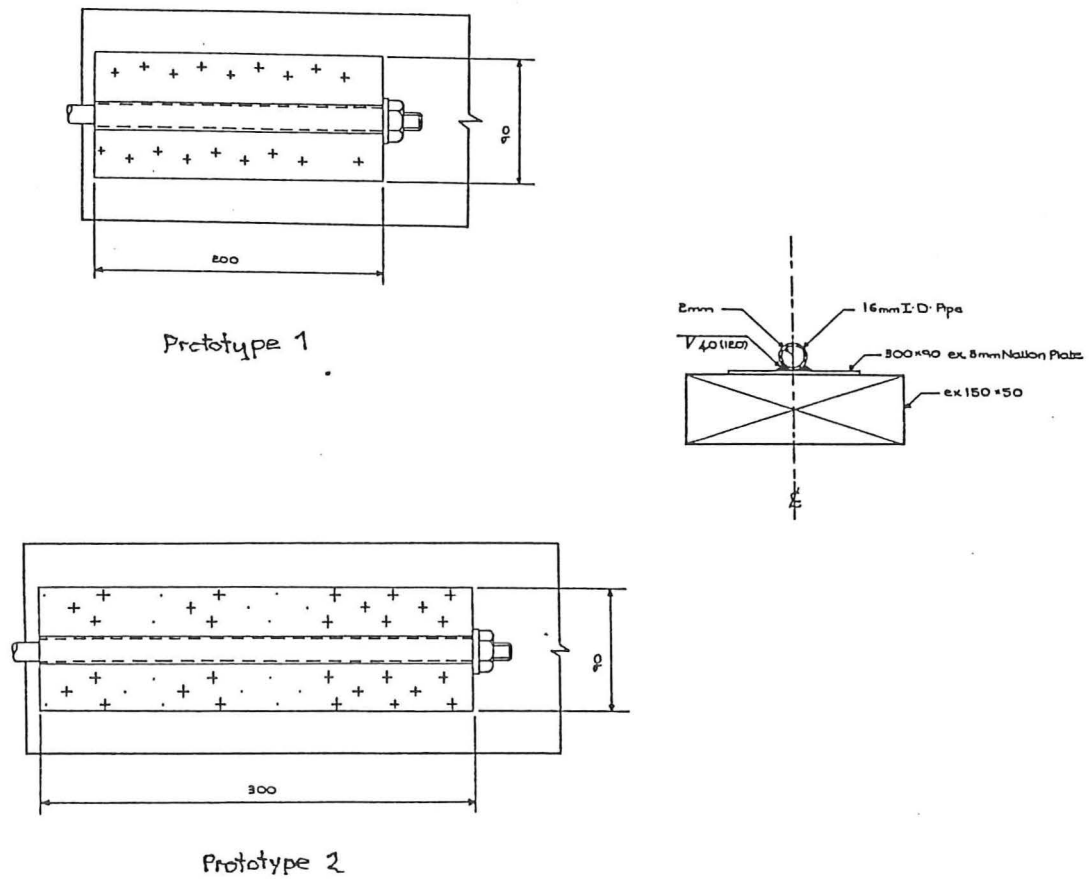


Figure 6.4 Prototype hold-down construction details.

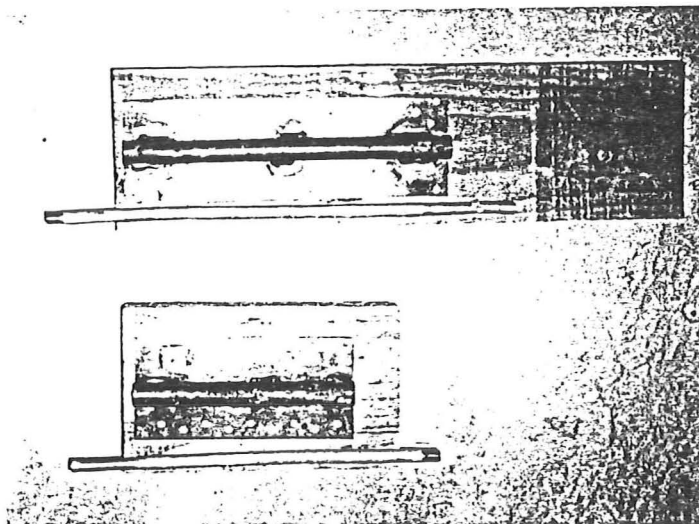


Plate 6.3 The Prototypes after testing.

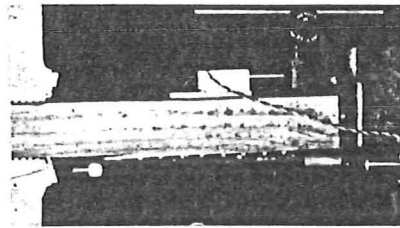


Plate 6.4 Prototype 2 being tested.

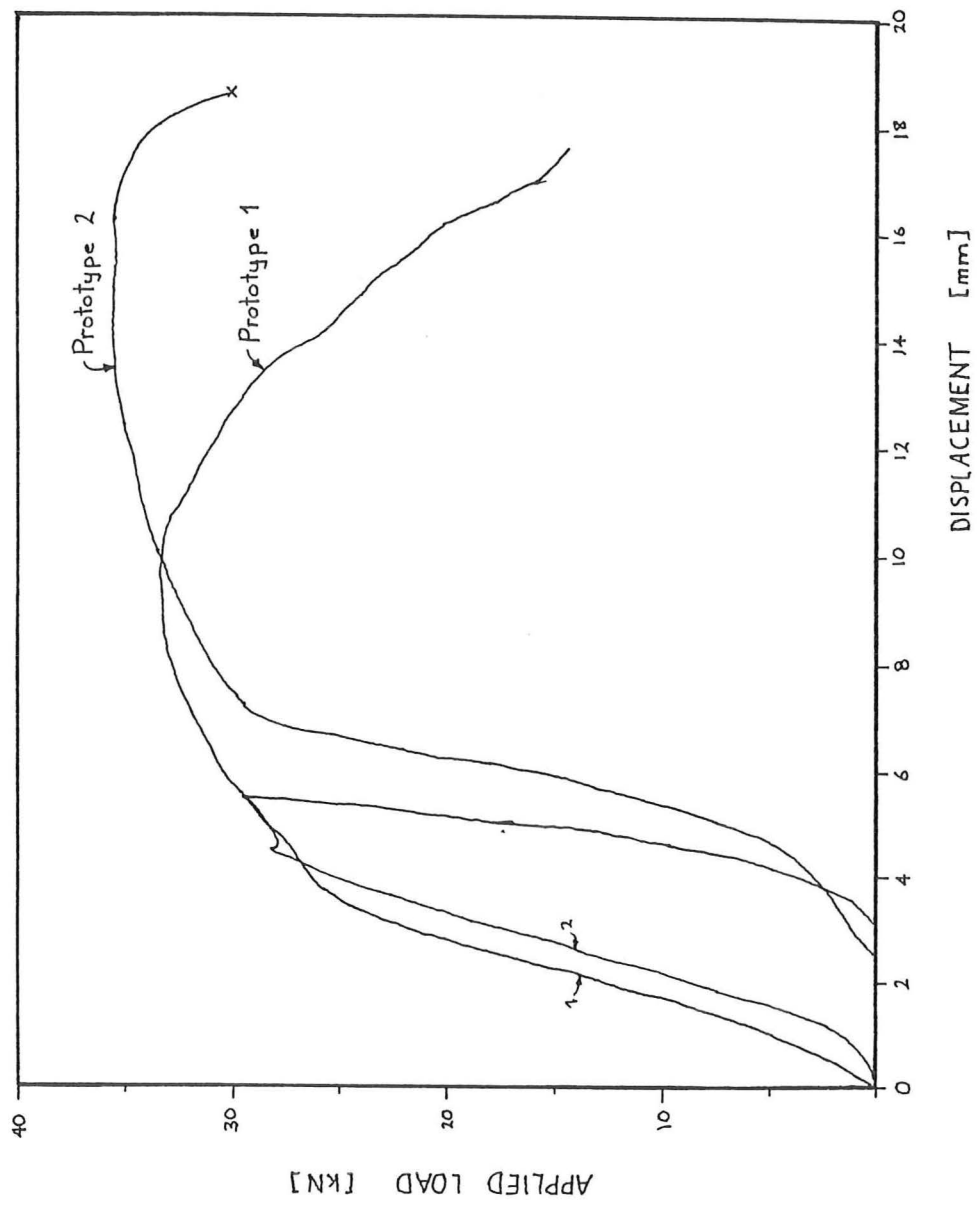


Figure 6.5 Load-displacement curves for Prototype hold-downs.

4. ANGLE SHEARPLATE

An angle shearplate (fig.6.6 and Plate 6.5) used on the frames described in Chapter 5 was tested. Dial gauges were used to record the displacements of the angle shearplate at peak loads in the loading history.

Table 6.3 gives the force on the frame (Column 1) and the resulting displacements. Column 2 gives the displacement of the top of the frame. Columns 3 and 4 give the vertical displacements of the frame relative to the restraining column on each side of the frame. The left hand side of the frame was free (fig. 6.7(a)), but the right hand side had a steel plate under the base (fig. 6.7(b)) to simulate a concrete floor. The last three columns of Table 6.3 give the rotation and displacements of the angle shearplate relative to the frame member.

Load kN	Frame mm	Right mm	Left mm	Rot rad	X mm	Y mm
0	0.0	0.0	0.0	0.0	0.0	0.0
17	9.5	.40	.43	.0009	0.0	-.01
0	1.7	.23	.27	.0007	0.0	-.02
-17	-7.0	.15	-.60	-.0013	0.0	-.03
0	-1.5	.17	-.39	-.0010	0.0	-.01
17	9.5	.38	.38	.0010	0.0	.00
0	1.7	.24	.24	.0010	0.0	-.01
-17	-7.0	.15	-.62	-.0016	0.0	-.02
0	-1.5	.17	-.42	-.0014	0.0	-.01
32	21.5	1.87	1.85	.0086	.21	.01
0	6.0	1.22	1.24	.0088	.11	.03
-25	-16.2	.48	-1.40	-.0099	-.30	.10
0	-4.0	.57	-.77	-.0056	-.24	.08
25	18.5	1.53	1.70	.0112	.05	.06
0	5.0	1.16	1.13	.0080	.05	.06
-34	-24.5	.23	-2.92	-.0232	-.92	.23
0	-7.5	.37	-2.08	-.0256	.32	.70
34	27.0	1.93	1.96	.0161	.04	.11
0	6.0	1.66	1.40	-.0031	.04	-.56
-42	-33.0	.12	-5.04	-.0380	1.60	.40
0	-10.0	.31	-3.98	-.0262	1.25	.34

Table 6.3 Data from angle shearplate test.

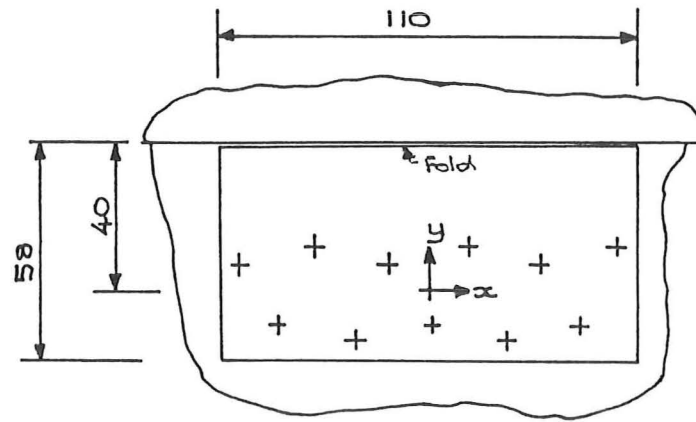


Figure 6.6 Dimensions of angle shearplate.

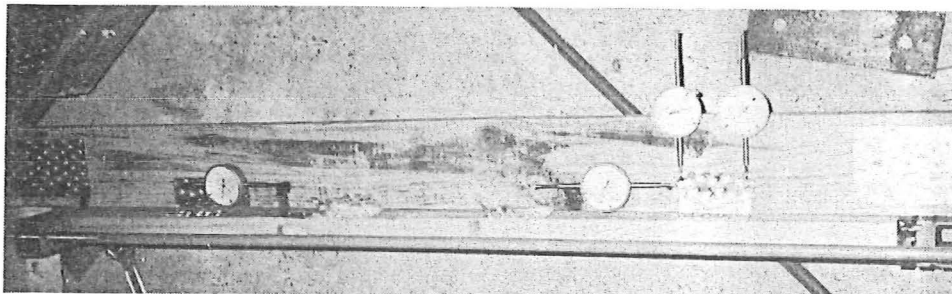


Plate 6.5 Testing of the angle shearplate.

Columns 2 and 3 of Table 6.3 show similar magnitudes of displacement between the frame and retaining column on both sides of the frame when loaded in the positive direction. When loaded in the negative direction the free side (left) displaced but the right side was prevented from displacing to a negative value by the steel plate under the base.

Figure 6.8 is the load-deflection plot for the top of the frame. It shows that the behaviour of the frame was reasonably symmetric when loaded in both directions, but when loaded in the negative direction the frame was stronger. This is most likely due to the presence of the steel plate under the base of the frame.

5. DISCUSSION

The concrete fixing cleats all had a large displacement before the load reached the maximum. To minimise the displacement of the hold-down connection the washer has to be larger than the standard Lumberlok washer and the supporting material should be stiff.

The displacements of the prototype hold-downs at the maximum load were similar to those for the cleats but the load at 4 mm displacement were higher.

There appears to be no advantage in the extra plate length or the greater number of nails in Prototype hold-down 2.

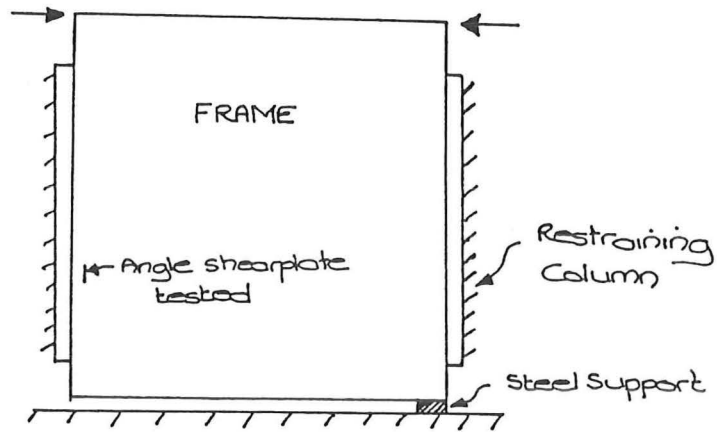


Figure 6.7 Supports for test frame.

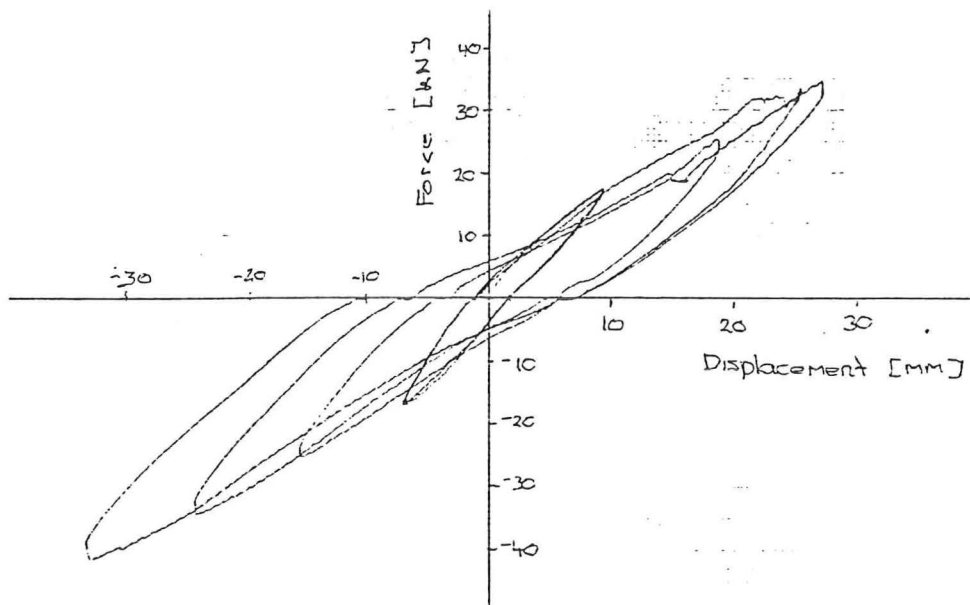


Figure 6.8 Load-deflection plot for frame.

CHAPTER VII

NAILON PLATE JOINT MODEL

1. INTRODUCTION

The numerical model presented in this chapter represents the behaviour of a Nailon plate to timber connection subjected to monotonic loading, the load being applied at a position which is not concentric with the centroid of the nailgroup.

Yap[12] and Edwards[3] have both used numerical models to compute the moment applied to a nailgroup for given a joint rotation. Their models are for large moment-resisting joints with hundreds of nails as would be found in a portal frame joint. Because of the large magnitude of the moment in those joints and the large number of nails sharing the applied load, their models did not include the effects of translation of the plate.

2. THEORY

The model presented here assumes that the Nailon plate itself rotates and translates as a rigid body (fig. 7.1). This is based on the assumption that the plate is unable to buckle between the nails because of their close spacing.

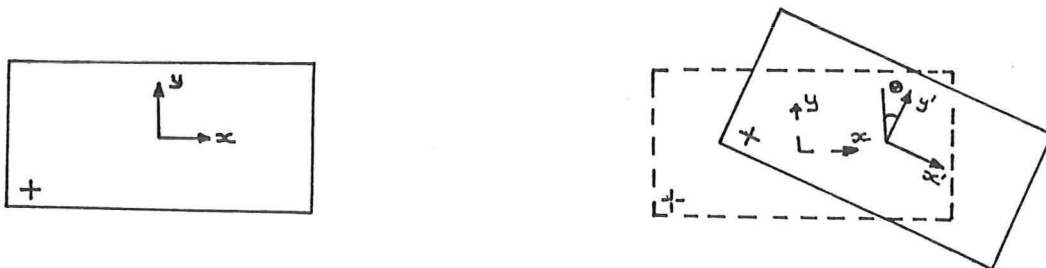


Figure 7.1 Rigid body rotation of the Nailon plate.

Because the Nailon plate is assumed to rotate and translate as a rigid body, computation of the total applied force in a given direction is a simple summation of the forces resisted by the individual nails in that direction. The components of the displacements in the two axis directions are summed vectorially to obtain the total displacement (fig. 7.2) of each nail. The resulting force on the nail is computed using the force-displacement relationship derived in Chapter 2. The components of the nail force in the axis directions are assumed to be proportional to the displacement in those directions. These forces are then summed to obtain the total force in each direction and also the total moment about the centroid.

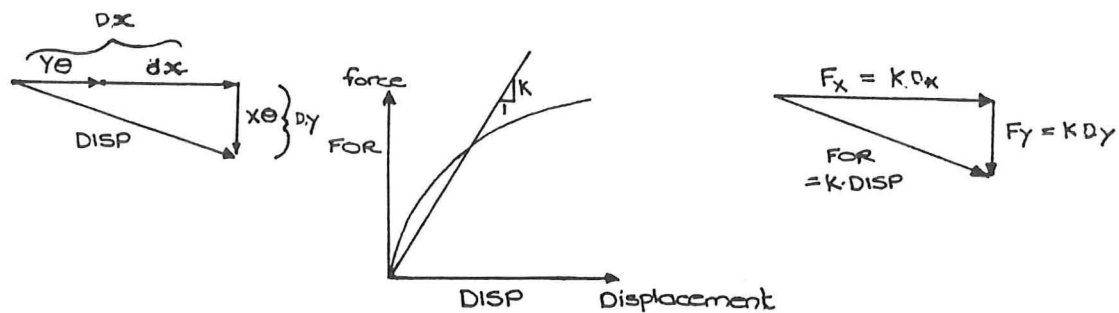


Figure 7.2 Individual nail force contribution.

- Let X = the x-coordinate of the nail relative to the nailgroup centroid.
- Y = the y-coordinate of the nail relative to the nailgroup centroid.
- dx = the displacement of the nailgroup centroid along the x axis.
- θ = the angle through which the plate rotates.
- DX = the nail displacement in the x direction.
- dy = the nail displacement in the y direction.

From Figure 7.2, assuming that the angle θ is small, DX and DY are related to the nailgroup displacements dX and θ by equations 7.1. The total displacement ($DISP$) of the nail is the vector sum of the components DX and DY , given by equation 7.2.

$$DX = Y.\theta + dX \qquad DY = X.\theta \qquad (7.1)$$

$$DISP = \sqrt{DX^2 + DY^2} \qquad (7.2)$$

The tangent stiffness is then computed with the displacement equation obtained in Chapter 2 modified to give the stiffness (K) instead of the force (eq. 7.3). This equation is independent of the orientation of the grain as is Equation 2.2 from which it is obtained. The direction of the force is the same as the direction of the displacement as $DISP$ and K are both positive.

$$K = \begin{matrix} 1 (1.357 DISP^{0.54} & 0 < DISP < 1.0 \text{ mm} \\ DISP (0.933 + 0.5 \ln (2.DISP)) & 0.5 < DISP < 5.5 \text{ mm} \end{matrix} \qquad (7.3)$$

The total force on the plate is then computed, using equations 7.4, as the sum of the contribution of the individual nail forces.

$$\begin{aligned} X \text{ Force} &= K.DX \\ Y \text{ Force} &= K.DY \end{aligned} \qquad (7.4)$$

$$\text{Moment} = K (Y.DX + X.DY)$$

These equations give the total force and moment applied to the plate by the nails. The magnitudes of these forces are a function of the magnitudes of the translation and rotation of the plate. The plate must satisfy the equations of equilibrium of the applied forces, so one of the displacements (translation or rotation) must be iteratively changed until equilibrium is satisfied.

For the angle shearplate model described in the next section, equations 7.5 are the equilibrium equations which govern. Equations 7.6 are obtained from equations 7.4 and 7.5, and these must be satisfied for values of translation and rotation applied to the plate. The first equation is assumed be true for all values of dX and θ . To satisfy the second equation the value of dX is changed, using the secant method of approximation, until the values computed for the two sides of the equation differ by a sufficiently small amount.

$$\begin{aligned} X \text{ Force} &= FX \\ Y \text{ Force} &= \text{zero} \\ \text{Moment} &= FX * ARM \end{aligned} \tag{7.5}$$

Where ARM is the distance between FX and the nailgroup centroid.

$$\begin{aligned} K.DY &= 0 \\ K (Y.DX + X.DY) &= ARM * K.DX \end{aligned} \tag{7.6}$$

This model is not expected to provide data which exactly matches that of a real plate because of the variation in nail data as observed in Chapter 2, but it will provide a model which will have the overall characteristics of the connection being modelled.

3. CALIBRATION OF THE MODEL

This section gives a comparison between the results obtained from the numerical model and that of a real connection.

The connection is that of the angle shearplate described in Chapter 6. The dimensions of the connection are shown in Figure 7.3. For the model, the force is assumed to act through the fold in the plate giving a value of ARM of 40 mm.

The computer program for this numerical model is presented in Appendix B. The subroutine second subroutine NAILIN was for this model. The data file used for this angle shearplate is on same page as the code for the subroutine NAILIN.

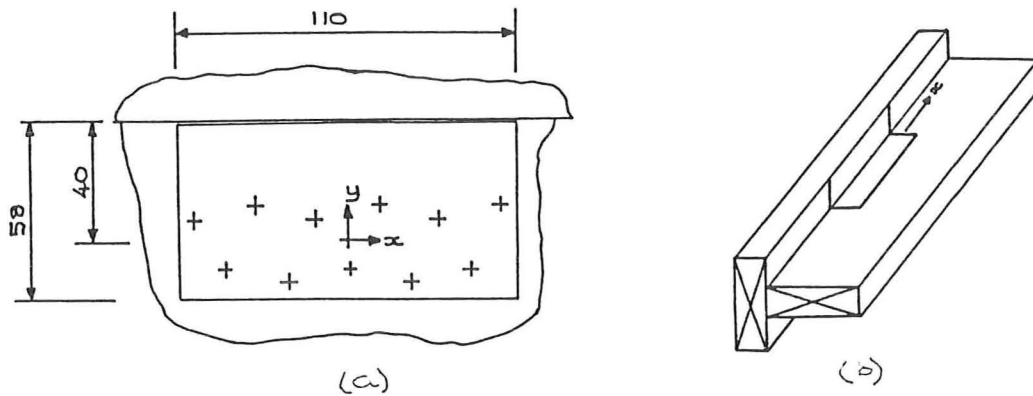


Figure 7.3 Dimensions of the angle shearplate tested and numerically modelled.

Plots of force vs centroid displacement and of force vs plate rotation have been generated (fig. 7.4). On top of these, the measured displacement and rotation have been plotted for comparison. There is a difference between the magnitudes of the results from the model and those of the tested joint, but the model does have the same characteristics. There are two reasons which may attribute to this difference in numerical value. The first reason is that there were three similar joints resisting the total load and it was assumed that each joint resists a third of the applied load. This joint may have a smaller portion of the total load than the other two because of its position in the structure (fig 7.5).

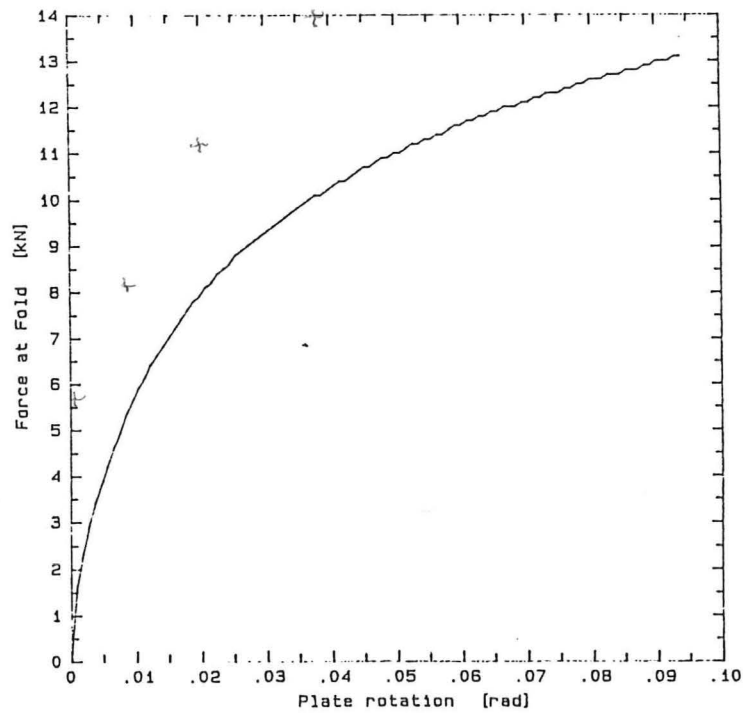
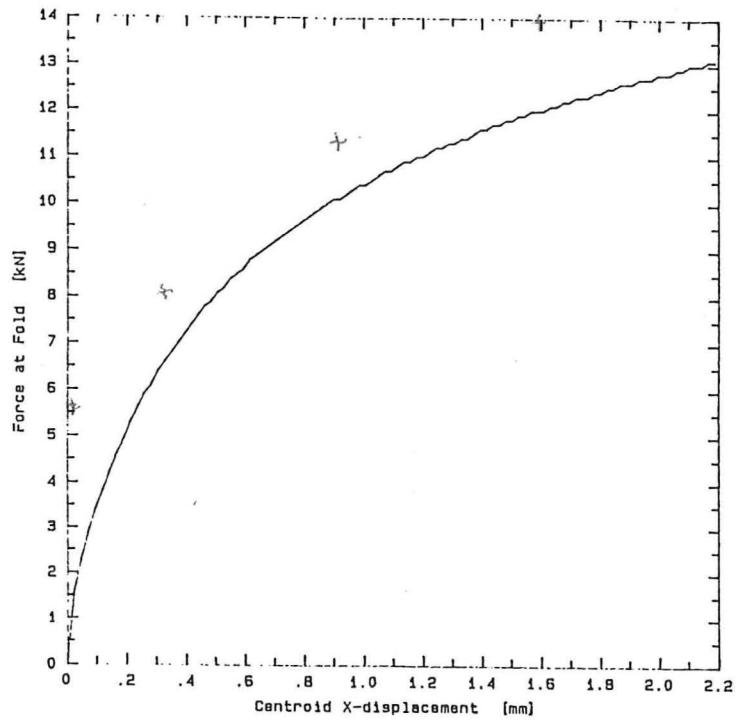


Figure 7.4 Results from computer model and testing

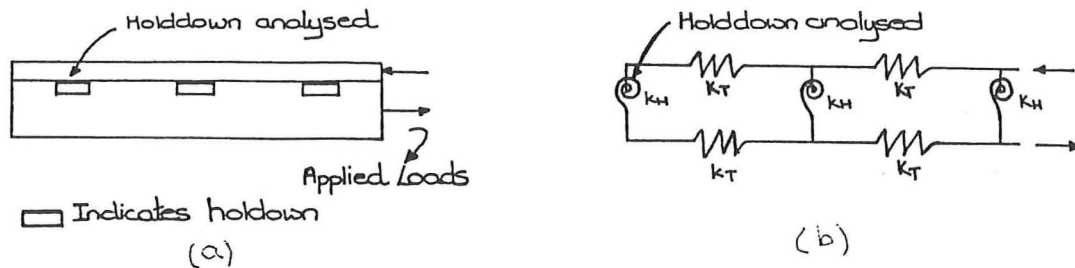


Figure 7.5 a) Real and b) Idealized components of the angle shearplate structure.

The second reason is that there was a measured displacement in the y-direction as well as in the x-direction. This displacement was caused by the members holding the frame in the reaction frame not allowing unconstrained movement to occur.

4. ANGLE SHEARPLATE PROPERTIES

In this section the effects of changing the pattern and number of nails in the nailgroup and changing the position of the applied load are investigated.

For the computer model (Appendix E, with the first version of the subroutine NAILIN) the Nailon plate was divided up into a matrix of rows and groups to enable the computer input data to be simplified. Figure 7.6 shows the definition of a ROW and GROUP of nails. The nailgroup in the model has ROWS rows of nails and GROUPS groups of nails.

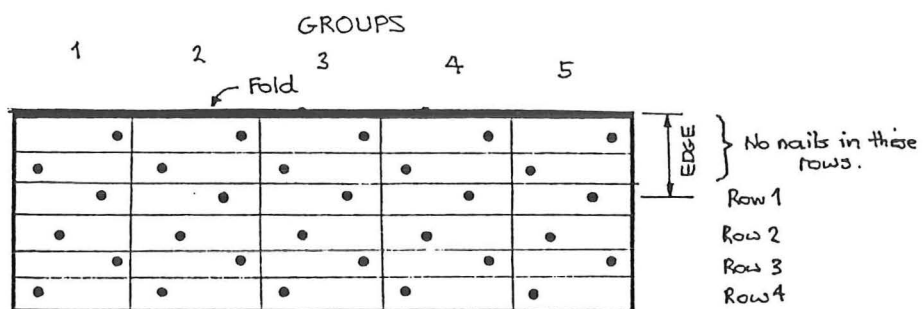
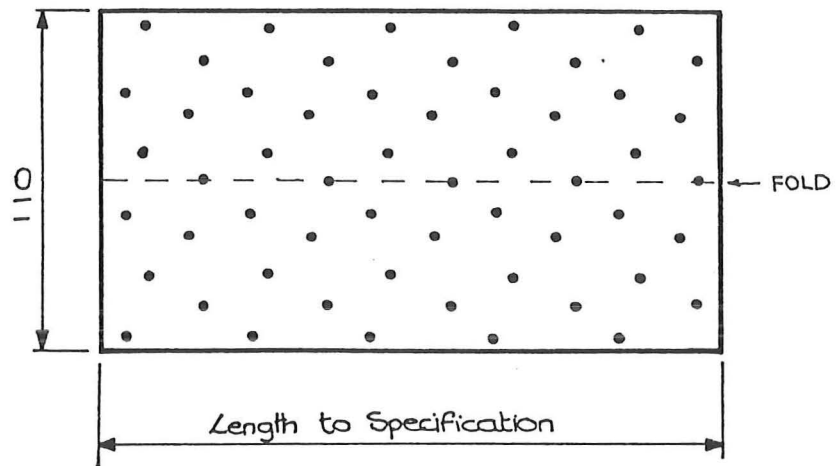


Figure 7.6 Definition of terms for angle shearplate

The first property of angle shearplate investigated is that of the number of GROUPS in a nailgroup. The number of ROWS was kept constant, and hence the value of ARM. The number of GROUPS was varied from 2 to 7. The maximum nail displacement has been plotted against the centroid displacement in Figure 7.7. The almost linear relationship between the centroid displacement and the maximum nail displacement for each nailgroup implies that each nail moves approximately in a straight line as the plate is loaded. This was not expected to occur with only a small number of nails because of the non-linear load-displacement relationship for the nails. The rotational component of the total nail displacement decreases as the number of nails in the nailgroup is increased.

The second property investigated was that of varying ARM. This models an increase in the edge distance EDGE (fig. 7.6) which is governed by minimum distances in design codes. The minimum distance EDGE is limited to 10 mm in practice by the difficulty of hammering nails close to the fold.

A constant nailgroup with 3 ROWS and 5 GROUPS was used for this investigation. Figure 7.8 shows the Load plotted against the displacement of the angle shearplate centroid. The curve for ARM (A) = 0 has been plotted in Figure 7.8 for comparison. The curves are terminated where the maximum nail displacement exceeds 5 mm.

Increasing ARM causes a reduction in the load carrying capacity of the angle shearplate and reduces the stiffness of the connection.

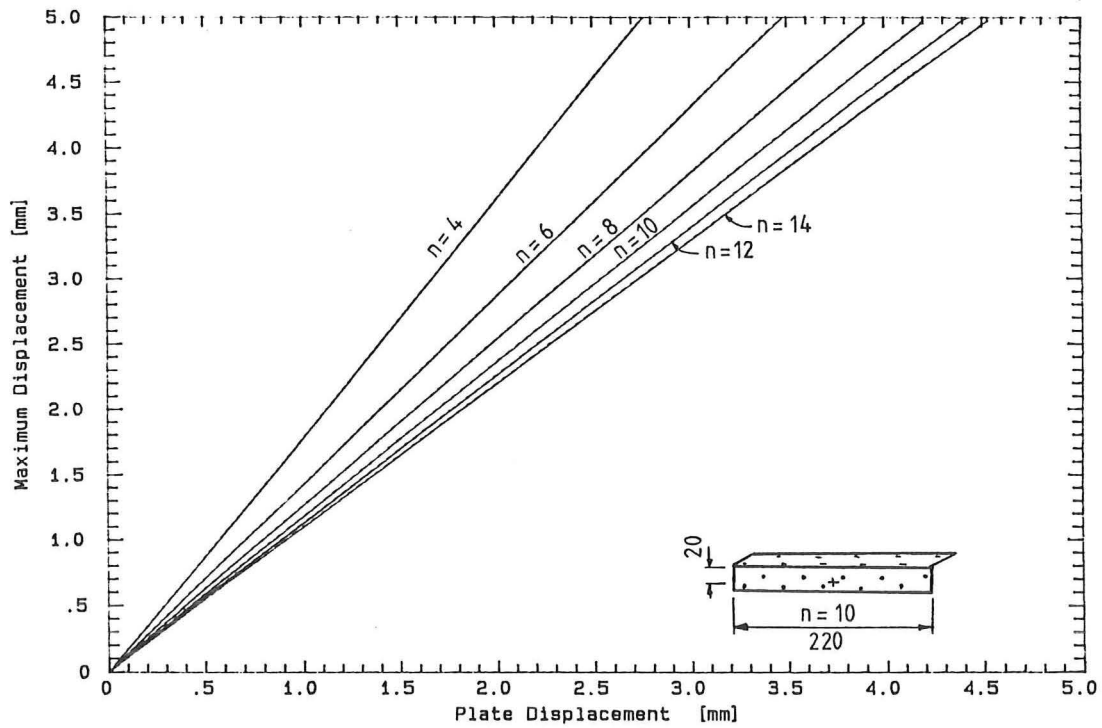


Figure 7.8 Curves from variation in number of GROUPS.

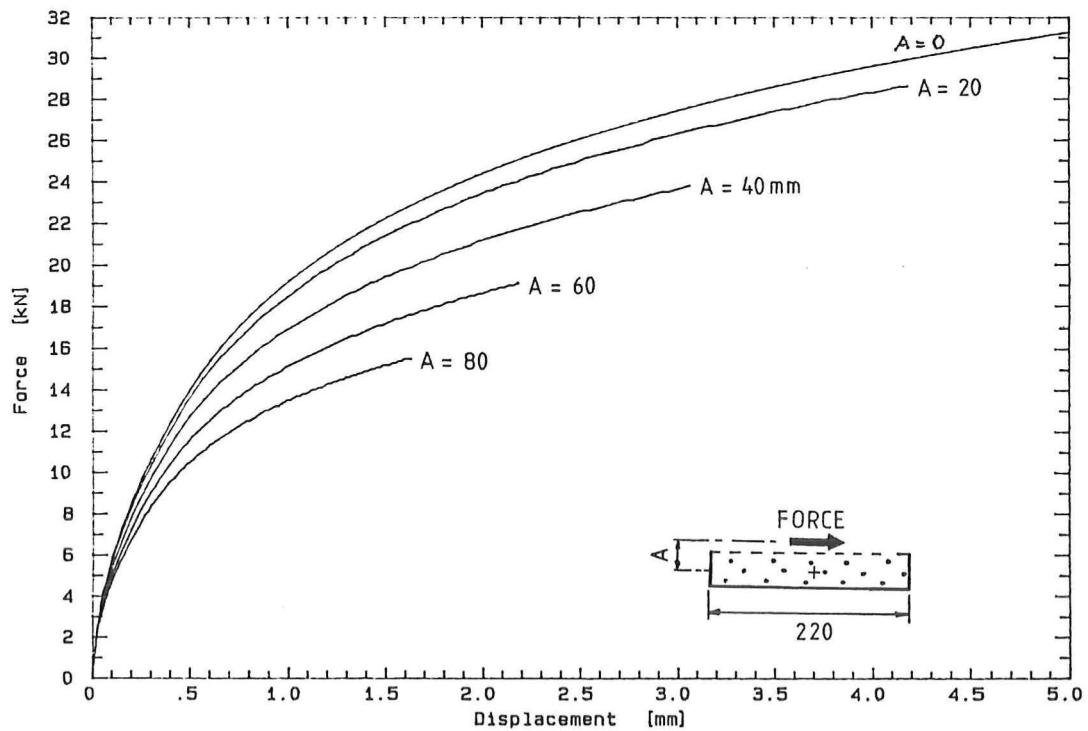


Figure 7.9 Curves from variation in ARM (A).

5. ANGLE SHEARPLATE LOAD-DISPLACEMENT CURVES

Two series curves (fig 7.9) have been produced for the applied force at the fold and the fold displacement. The force is plotted as the force per ROW of nails. The number of ROWS of nails is represented by different types of line. Figure 7.9(a) is for a timber edge distance of 10 mm and Figure 7.9(b) is for an edge distance of 15 mm. The 10 mm edge distance is the minimum and this will normally apply to a nailgroup in the centre of the timber member (e.g. in the restraining columns of the frames described in Chapter 5). The 15 mm edge distance is for a nailgroup which is close to the edge of the timber member. Figure 7.10 shows the nailgroup positions for these two edge values.

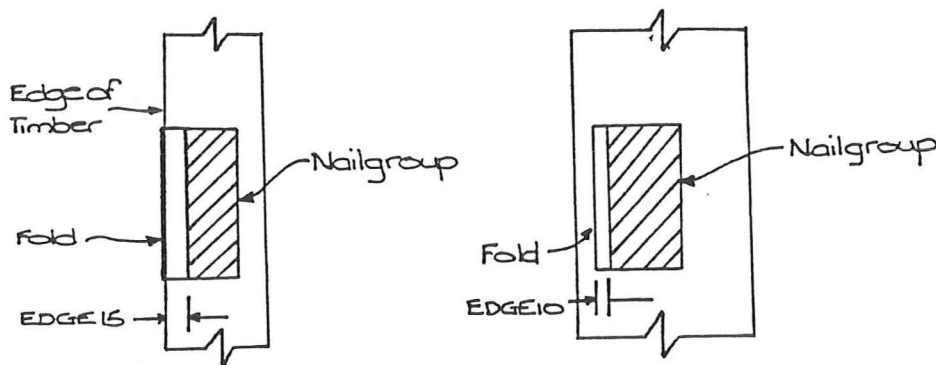


Figure 7.10 Nailgroup positions for curves in Fig. 7.9

The stiffness and design load for the connection increases with an increase in the number of ROWS and GROUPS. The stiffest connection has a small value of ARM and a large number of GROUPS.

All of the curves in Figure 7.9 have a similar shape so it may be possible to predict the displacement of the fold using one dimensionless variable which is dependent upon ARM, ROWS and GROUPS.

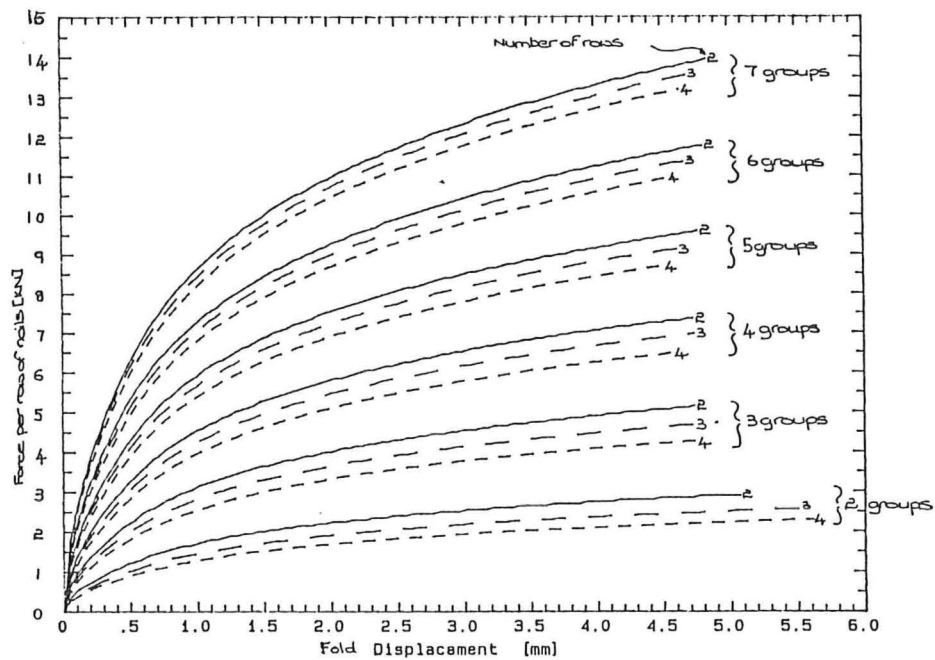
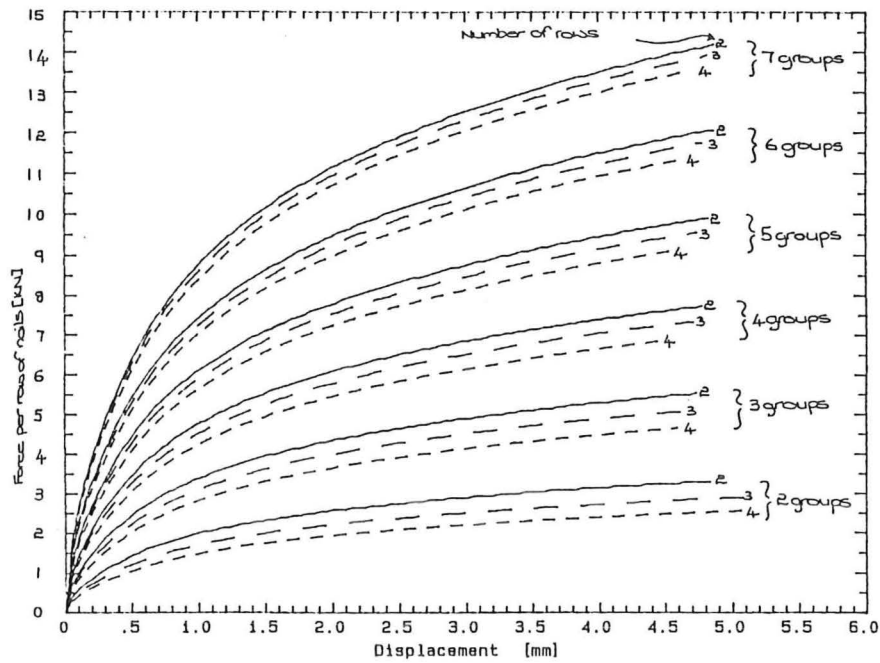


Figure 7.10 Load-displacement curves for edge distances of
a) 10 mm and b) 15 mm.

CHAPTER VIII

CONCLUSIONS AND RECOMMENDATIONS

1. CONCLUSIONS

A type of bracing frame to resist lateral force in timber structures has been proposed.

The shape of the hysteretic loop for Nailon plated joints is typical of those of nailed joints. The joint exhibits slackness and the load-displacement curve is bounded by the monotonic curve after cyclic loading. Thus good seismic behaviour can be expected from this type of joint.

The nail loads for nails in Nailon plate connections appear to be conservative in Lumberlok data and NZS 3603:1981.

Sawn timber diagonally braced frames with Nailon plate connections are strong, stiff and ductile.

The actual stiffness of timber frames is less than their calculated stiffness, a significant portion of this reduction arises from displacements at the hold-down connections.

One millimetre thick Nailon plate is suitable for diagonally braced frames. Two millimetre thick Nailon plate is only required when short lengths of plate across the joint are subject to a high shear stress.

Detailing of joints must take into account the combination of perpendicular-to-grain tension and shear as this may produce a brittle failure of the timber.

Design must take into account the out-of-plane buckling of the timber members. This buckling produces a ductile behaviour if the members do buckle but the rotations produced at the joints are undesirable.

Strip brace and toothplates exhibit brittle failure mechanisms. They should not be expected to have any ductility.

Folded Nailon plate connections have been investigated and design guidelines have been proposed.

2. RECOMMENDATIONS

More investigation is required on joints in which shear and perpendicular-to-grain tension are likely.

The design proposals for folded Nailon plate could be refined and extended to other uses for Nailon plate.

The design loadings for nails in Nailon plate should be revised as they appear to be conservative.

REFERENCES

- 1) Dean, J.A., Buchanan, A.H. Seismic Design Loadings for Timber Structures, Pacific Conference on Earthquake Engineering, Wairakei, N.Z. August 5-8, 1987, Vol 2, pp 141-152.
- 2) Dean, J.A., Stewart, W.G., Carr, A.J. The seismic behaviour of Plywood Sheathed Shearwalls. Bulletin of the New Zealand National Society of Earthquake Engineering, Vol 19, No. 1, March 1986, pp 48-63.
- 3) Edwards, M.R. Cyclic Properties of Nail Plated Timber Joints. ME Thesis (1985), University of Auckland.
- 4) Gang-Nails N.Z. Ltd. The Gang-Nail System Manual. Section V, Technical Information. Revised July 1985
- 5) Hunt, R.D., Bryant, A.H. Nailed Joints for Timber Structures. Proc. of Pacific Timber Eng. Conf., May 1984, Auckland, pp 616-621
- 6) Lumber-lok N.Z. Ltd. Lumberlok Timber Connector Catalogue 83/15
- 7) Standards Association of Australia, AS1649- 1974. Methods for the Determination of Basic Working Loads For Metal Fasteners for Timber. SAA, Sydney, Australia.
- 8) Standards Association of New Zealand, NZS 3603: 1981. Code of Practice for Timber Design. SANZ, Wellington N.Z.
- 9) Standards Association of New Zealand, NZS 4203: 1984. Code of Practice for General Structural Design and Design Loadings for Buildings. SANZ, Wellington N.Z.
- 10) Stewart W.G. The Seismic Design of Plywood Sheathed Shearwalls. Submitted in partial fulfillment of PhD degree, University of Canterbury 1987.
- 11) Thurston, S.J., Flack, P.F. Monotonic and Cyclic Testing of Timber Connections Using Nailed Steel Side Plates. Report 5-79/4, Central Laboratories, Ministry of Works and Development.
- 12) Yap, K.K. An Investigation of Damping Characteristics and Seismic Response of Ply-Box and Nail-Plate Portal Frames. Report 5-84/12, Central Laboratories, Ministry of Works and Development.

APPENDIX A

BASIC NAIL LOAD COMPUTATION

The basic working load for metal fasteners is determined by the requirements set out in AS 1649-1974 and NZS 3603:1981 Appendix A.

The joint load for a joint slip of 0.8 mm (column. 1, Table A.1) and the maximum joint load (column. 2) is measured from Figure 2.10(b). AS 1649 cl 6.3.3(b) requires that a log-normal distribution be used, so the average and standard deviation of the logarithm of the joint loads are computed as shown in table A.1.

0.8mm Slip (x1)	Ultimate Slip (x2)	y1 ln (x1)	y2 ln (x2)
2.12	4.25	0.751	1.45
2.25	4.1	0.811	1.41
2.34	4.1	0.850	1.41
2.44	4.0	0.892	1.39
2.50	4.1	0.916	1.41
2.52	4.1	0.924	1.39
		=====	=====
Average	\bar{y}	0.858	1.41
Standard Deviation	s	0.0672	0.0084

Table A.1 Log-normal average and standard deviation of joint loads.

The formula given in Appendix B of AS 1649 is modified to give the 5 percentile load because the sample size is smaller than that for which values are tabulated in NZS 3603:cl A1.1. The 5 percentile lower probability limit (LPL) is thus computed using Formula A.1.

$$LPL = EXP(\bar{y} - s t_{0.05, n-1} \sqrt{1 + 1/n}) \quad (A.1)$$

where: \bar{y} = Average of $\ln(\text{load})$
 s = Standard Deviation of $\ln(\text{load})$
 n = Number of specimens
 t = Student t distribution value
 $t_{0.05, 5} = 2.02$

e.g. $LPL_1 = EXP(0.858 - 0.0672 * 2.02 \sqrt{1 + 1/6}) = 2.03$

This gives $LPL_1 = 2.03$ (for 0.8mm) and $LPL_2 = 3.94$ (for Maximum). These values are then used in the formulae from AS 1649:c1 6.3.3 (A.2) to obtain the unit lateral load (ULL); the smallest of the two is the required value. The ULL is the smaller of the two values so that the nails do not require too large a slip before resisting the applied load and that the load is sufficiently below that of the maximum load.

$$ULL_1 = \frac{LPL_1}{1.6n} \qquad ULL_2 = \frac{LPL_2}{2.5n} \quad (A.2)$$

This gives values of $ULL_1 = 630$ and $ULL_2 = 790$ N / nail, therefore the load is based on the 0.8 mm slip value and $ULL = 630$. This value has to be modified to the reference density for the timber species used as specified in NZS 3603:c1 A1.2. The average density for the test specimens was 527 kg/m^3 , the Test density for 12 % moisture content is 486 kg/m^3 . This gives a Basic Working Load (BWL) of 580 N per nail.

$$BWL = 630 * \frac{486}{527} = 580 \text{ N}$$

This value is only representative of joints constructed dry and under dry service conditions. A loading rate of 2 mm/min was used for the testing which is greater than the rate of 1.25 mm/min specified by AS 1649, but the Basic Working Load obtained is only for comparison with other nail load data.

APPENDIX B

PROGRAM FOR COMPUTER MODEL

This is a copy of the computer program, described in Chapter 7, used for modelling Nailon plate connections. The program, for a series of 100 increments of plate rotation, computes the centroid displacement, maximum nail displacement, and the corner displacement relative to the timber as well as the applied X-force. The co-ordinates of the nails and the distance between the centroid and the position at which the force is applied are required as input data. The computed values may then be graphed to obtain the plots given in Chapter 7.

The program is written in the FORTRAN programming language and runs on a VAX 11/750 but should run without modification on most machines. The program is divided into subroutines to simplify the logic and to enable two different sources of nail co-ordinate data to be used.

The subroutine NAILIN is given in two versions. The first version reads the input data from a file stored in the computer and the data should be formatted as follows:-

```
Line: 1  up to 80 characters describing the nailgroup data
      2  NNAILS - the number of nails in the nailgroup
      3  x,y of the centroid of the nailgroup (0.0 0.0) if unknown
      4
      .    x,y co-ordinates of the NNAILS nails
      .
```

The second version of NAILIN is for a length of Nailon plate with a total of GROUPS * ROWS nails in it.

The computer input and output files are as follows:-

File No.	File
1	Data input file - co-ordinates of the nailgroups
2	Data output file - data which is to be processed further i.e. by a plotting subroutine
5	Terminal input - input of variables by operator
6	Screen output - for monitoring program progress and prompts

The subroutines are called in the following order from the MAIN program, each indentation showing a new level of subroutine nesting.

MAIN	
NAILIN	- Nail input or co-ordinate computation
CENTR	- Computation of the centroid of the nailgroup
TMAX	- Computes value of THETA to give 100 points
SOLVE	
SOLVE	- Secant method of equilibrating forces
SUM	- Computes total forces acting on plate
STIFF	- Computes tangent stiffness for nail disp.

```

C
C   Program computes force-displacement relationship for Nailon plate.
C   Calculatess out 100 points on curve up to a maximum nail
C   displacement of 5 mm. Loops on THETA, computing the centroid
C   displacement of the Nailon plate, the maximum nail displacement,
C   the displacement of the fold and the force on the plate.
C
C   B.L.Deam v1.0 February 1987
C
C   INTEGER I
C   REAL    ARM,DISX,FORX,MAXDIS,THETA,THETMAX,TOTDIS
C   REAL    NAILS(100,2)
C
C   WRITE(6,600)
C                                     Input nail co-ordinates
C   CALL NAILIN(NAILS,ARM)
C                                     Compute maximum theta required
C   THETMAX = TMAX(NAILS,ARM)
C
C   WRITE(6,630)
C                                     Scale all the curves to a common size
C   READ(5,*)SCALE
C   WRITE(2,640)0.0,0.0,0.0,6.0,SCALE
C   WRITE(2,640)0.0,0.0,0.0,6.0,0.0
C   DO 10 I=0,100
C       THETA = THETMAX * FLOAT(I) / 100.0
C       CALL SOLVE(THETA,ARM,NAILS,FORX,DISX,MAXDIS)
C       TOTDIS = DISX + ARM * THETA
C       WRITE(6,640)THETA,DISX,MAXDIS,TOTDIS,FORX
C       WRITE(2,640)THETA,DISX,MAXDIS,TOTDIS,FORX
10  CONTINUE
C   STOP
C
600  FORMAT(/' Lumberlok Nailon plate Analysis v2.0' /
+      ' Rotation controlled; Please enter:-' /)
630  FORMAT( ' Rotation X-Displ  Max-Dis  Tot-Dis  X-Force' /
+      '      rad      mm      mm      mm      kN' )
640  FORMAT( 1X,F7.5,3F9.3,F10.1)
END

```

```

SUBROUTINE NAILIN(NAILS,ARM)
C
C   Compute nail positions
C
REAL    NAILS(100,2),XCOORD(8),YCOORD(8),XSPAC,ARM
INTEGER II,ROWS,GROUPS,ROW,GROUP
C
DATA XCOORD / 5., 30., 10., 25., 5., 30., 10., 25. /
DATA YCOORD / 5., 15., 25., 35., 45., 55., 65., 75. /
DATA XSPAC  / 39.5 /
DATA EDGE   / 10.0 /
C
WRITE(6,600)
READ(5,*)ROWS,GROUPS
C
IND = 2
DO 10 GROUP = 1,GROUPS
  DO 20 ROW = 1,ROWS
    IND = IND + 1
    NAILS(IND,1)=XCOORD(ROW) + XSPAC * FLOAT(GROUP - 1)
    NAILS(IND,2)=YCOORD(ROW)
20  CONTINUE
10  CONTINUE
NAILS(1,1) = INT(IND - 2)
CALL CENTR(NAILS)
ARM = EDGE + YCOORD(ROWS) - NAILS(2,2)
RETURN
600  FORMAT(' ROWS GROUPS'/)
END

```

```

SUBROUTINE CENTR(NAILS)
C
C Find centroid of nail group and alter co-ordinates to be
C about that centroid
C
C v1.0 25-Oct-87
C 1.1 5-Nov Relpaced variables with a single array
C
INTEGER      NNAILS,II
REAL         NAILS(100,2)
DOUBLE PRECISION XX,YY
C
NNAILS = INT(NAILS(1,1))
XX = 0.0
YY = 0.0
DO 10 II =3,NNAILS + 2
      XX = XX + NAILS(II,1)
      YY = YY + NAILS(II,2)
10 CONTINUE
X = SNGL(XX) / NAILS(1,1)
Y = SNGL(YY) / NAILS(1,1)
DO 20 II = 3,NNAILS + 2
      NAILS(II,1) = NAILS(II,1) - X
      NAILS(II,2) = NAILS(II,2) - Y
20 CONTINUE
NAILS(2,1) = X
NAILS(2,2) = Y
RETURN
END

```

```

      REAL FUNCTION TMAX(NAILS,ARM)
C
C      Function to compute the value of theta which will give
C      a maximum nail displacement of 5 mm.
C
      REAL    ARM,NAILS(100,2)
      REAL    D,DISX,DM1,DMAX,DP1,EPS,ERR,FORX,MAXDIS,T,TH1,TP1
      INTEGER ITT
C
      DATA  MAXDIS,EPS / 5.0, 0.005 /
C
      TH1 = .0003
      CALL SOLVE(TH1,ARM,NAILS,FORX,DISX,DMAX)
      DM1 = DMAX - MAXDIS
C
      T    = .0005
      CALL SOLVE(T ,ARM,NAILS,FORX,DISX,DMAX)
      D    = DMAX - MAXDIS
C
      ITT = 0
10  CONTINUE
      TP1 = (D*TH1 - DM1*T) / (D - DM1)
      CALL SOLVE(TP1,ARM,NAILS,FORX,DISX,DMAX)
      DP1 = DMAX - MAXDIS
      ERR = DP1 / MAXDIS
      IF(ITT.GT.6) WRITE(6,600)ERR,ITT
      IF(ABS(ERR).LT.EPS) GOTO 20
      DM1 = D
      TH1 = T
      T    = TP1
      D    = DP1
      ITT = ITT + 1
      GOTO 10
20  CONTINUE
      TMAX = TP1
      RETURN
600  FORMAT(' Error of',F10.7,' at itteration',I4,' in function TMAX')
      END

```



```

SUBROUTINE SOLVE(THETA,ARM,NAILS,FORX,DISXP1,DMAX)
C
C   This routine solves for FORX and DISX given the co-ordinates of
C   the nailgroup in array NAILS. The secant method of approximation
C   is used, solving for the x-displacement by applying equilibrium
C   equations to the values returned from subroutine SUM.
C
C   B.L.Deam          v1.0  3-February-1987
C
REAL    THETA,ARM,FORX,DISXP1,DMAX,NAILS(100,2)
REAL    DISX,DISXM1,EPS,ERR,MOM,RSLT,RSLTM1,RSLTP1
INTEGER ITT
C
DATA    EPS / 0.004 /
C
C                                     Return if very small rotation
FORX    = 0.0
DISXP1  = 0.0
DMAX    = 0.0
IF(ABS(THETA).LE.1.0E-5) GOTO 20
C
C                                     Compute the initial value
DISXM1  = 0.0
CALL SUM(THETA,DISXM1,NAILS,FORX,FORY,MOM,DMAX)
RSLTM1  = FORX * ARM - MOM
C
C                                     Second initial value
DISX    = 0.1
CALL SUM(THETA,DISX ,NAILS,FORX,FORY,MOM,DMAX)
RSLT    = FORX * ARM - MOM
C
C                                     Begin iterative solution
ITT     = 0
10      CONTINUE
        DISXP1    = (RSLT*DISXM1 - RSLTM1*DISX)/(RSLT - RSLTM1)
        CALL SUM(THETA,DISXP1,NAILS,FORX,FORY,MOM,DMAX)
        RSLTP1    = FORX * ARM - MOM
        IF(MOM.GT.0.0001) THEN
            ERR    = RSLT / MOM
        ELSE
            ERR    = RSLT
        ENDIF
C
C                                     Print message if not converging
        IF(ITT.GT.5) WRITE(6,600)ERR,ITT
        IF(ABS(ERR).LT.EPS) GOTO 20
        DISXM1    = DISX
        RSLTM1    = RSLT
        DISX      = DISXP1
        RSLT      = RSLTP1
        ITT      = ITT + 1
        GOTO 10
20      CONTINUE
        RETURN
600     FORMAT(1X,'Error of',F10.7,' at itteration'
+          ,I4,'in subroutine SOLVE')
END

```

```

SUBROUTINE SUM(THETA,DX,NAILS,FORCEX,FORCEY,MOMENT,DMAX)
C
C   This subroutine computes the summed forces and moment of the
C   group of nails passed in the array NAILS by displacing each
C   nail by DX and rotating the whole joint through angle THETA.
C
C   B.L.Deam          v1.0  3-February-1987
C
REAL          THETA,DX,FORCEX,FORCEY,MOMENT,DMAX,NAILS(100,2)
REAL          DISP,K,SX,SY,X,Y
DOUBLE PRECISION FX,FY,SFX,SFY,SMOM
INTEGER       I,NNAILS
C
NNAILS = INT(NAILS(1,1))
DMAX   = 0.0
SFX    = 0.0
SFY    = 0.0
SMOM   = 0.0
C
C                                     Perform Summation over all nails
DO 10 I = 1,NNAILS
  X   = NAILS(I+2,1)
  Y   = NAILS(I+2,2)
  SX  = Y * THETA + DX
  SY  = -X * THETA
  DISP = SQRT(SX*SX + SY*SY)
C
C                                     Find maximum nail displacement
  IF(DISP.GT.DMAX) DMAX = DISP
  K   = STIFF(DISP)
  FX  = DBLE(SX * K)
  FY  = DBLE(SY * K)
  SFX = SFX + FX
  SFY = SFY + FY
  SMOM = SMOM + FX*Y - FY*X
10  CONTINUE
C
FORCEX = SNGL(SFX)
FORCEY = SNGL(SFY)
MOMENT = SNGL(SMOM)
C
WRITE(6,600)THETA,DX,FORCEX,FORCEY,MOMENT,DMAX
RETURN
C 600  FORMAT(1X,'SUM',6F10.5)
END

```

```

REAL FUNCTION STIFF(XX)
C
C   Stiffness derived from Gang-Nail 1mm thick plate tests
C
REAL    FORCE,DISP,XX,S
DISP    = ABS(XX)
IF(DISP.GT.0.001) THEN
  IF(DISP.LT.0.5)THEN
    FORCE = 1.357 * DISP ** 0.54
  ELSE
    FORCE = 0.933 + 0.5 * ALOG(2*DISP)
  ENDIF
  STIFF = FORCE / DISP
ELSE
  STIFF = 0.0
ENDIF
RETURN
END

```

```

      SUBROUTINE NAILIN(NAILS,ARM)
C
C      Input matrix NAILS from input file FOR001, and compute the centroid
C      if necessary
C
      REAL    ARM,NAILS(100,2)
      INTEGER II,NNAILS,MAXRAD
      CHARACTER TITLE*80
C
C      Write out description of nailgroup
      READ(1,600)TITLE
      WRITE(6,601)TITLE
C
      READ(1,*)NAILS(1,1)
      DO 10 II = 2,INT(NAILS(1,1))+2
        READ(1,*)NAILS(II,1),NAILS(II,2)
10    CONTINUE
C      Compute centroid if X and Y centroids are equal to zero
C
      IF(NAILS(2,1).EQ.0.0.AND.NAILS(2,2).EQ.0.0) CALL CENTR(NAILS)
C
C      Input ARM for solution from operator
      WRITE(6,603)
      READ(5,*)ARM
      RETURN
600  FORMAT(A)
601  FORMAT(1X,80A)
603  FORMAT(' ARM')
      END

```

Bent Nailon plate as used for hold-down test

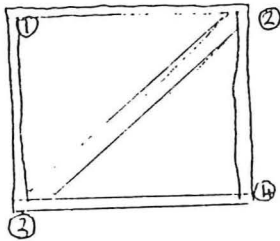
```

11
0.0  0.0
5  10
25 15
45 10
65 15
85 10
105 15
15 30
35 35
55 30
75 35
95 30

```

APPENDIX C

The following is the method of computing the failure load of a toothplate connector. The failure loads are computed from the Gang-Nail System Manual [4] by dividing the working load for the plate by 0.6.

FRAME F3 /1Tooth Loads

Wind/Seismic Loadings

Connection ①④

- Tensile load = Compressive load

30 pairs of teeth @ 1.5×200 N/tooth

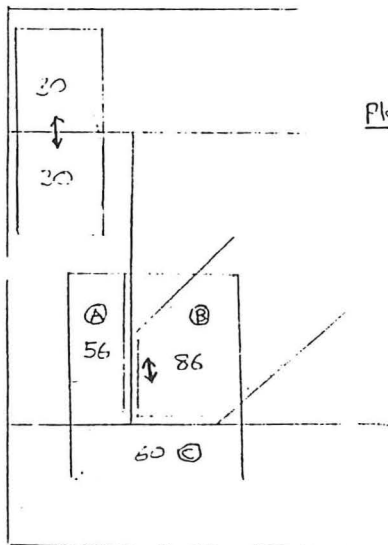
9 kN \updownarrow

Connection ②③

$$\begin{aligned} A \updownarrow & 1.5 \times 56 \times 270 = 22.7 \text{ kN} \\ \rightarrow & 1.5 \times 56 \times 230 = 19.3 \text{ kN} \end{aligned}$$

$$\begin{aligned} B \updownarrow & 1.5 \times 86 \times 220 = 28.4 \text{ kN} \\ \rightarrow & 28.4 \text{ kN} \end{aligned}$$

$$\begin{aligned} C \updownarrow & 1.5 \times 60 \times 200 = 18.0 \text{ kN} \\ \rightarrow & 1.5 \times 60 \times 220 = 19.8 \text{ kN} \end{aligned}$$

Plate Loads

Connection ①④

Assumed no shear

Tension (low density)

$$320 / 0.6 \times 68 \text{ mm} = 36.3 \text{ kN}$$

connection ②③

$$\begin{aligned} AB-C \text{ Shear} & 136 \text{ mm} \times 71 / 0.6 = 16.1 \text{ kN} \\ \text{Tension} & 136 \text{ mm} \times 260 / 0.6 = 58.9 \text{ kN} \end{aligned}$$

$$\begin{aligned} A-C \text{ Shear} & 50 \times 71 / 0.6 = 5.9 \text{ kN} \\ \text{Tension} & 50 \times 260 / 0.6 = 21.7 \text{ kN} \end{aligned}$$

$$\begin{aligned} B-C \text{ Shear} & 10.2 \text{ kN} \\ \text{Tension} & 37.2 \text{ kN} \end{aligned}$$

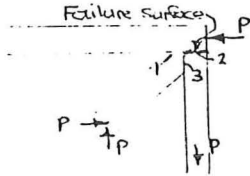
$$\begin{aligned} A-B \text{ Shear} & 121 \times 91 / 0.6 = 18.4 \text{ kN} \\ \text{Tension} & 121 \times 143 / 0.6 = 28.8 \text{ kN} \end{aligned}$$

FRAME F3 /2

Joint 2 Plate Failure Loads

$$\left(\frac{t}{T}\right)^2 + \left(\frac{V}{V}\right)^2 < 1 \quad (\text{failure})$$

Assume stresses distributed according to proportion of allowable



$$\begin{aligned} V_1 &= 10.2 \text{ kN} \\ V_2 &= 5.9 \text{ kN} \\ V_3 &= 18.4 \text{ kN} \\ T_2 &= 21.7 \text{ kN} \end{aligned}$$

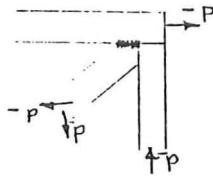
Failure on (2) First

$$t_2 = \frac{21.7}{21.7+18.4} P = 0.54 P$$

$$v_2 = \frac{5.9}{5.9+10.2} P = 0.37 P$$

$$\left(\frac{0.37 P}{5.9}\right)^2 + \left(\frac{0.54 P}{21.7}\right)^2 < 1 \Rightarrow \boxed{P < 14.8 \text{ kN}}$$

$$\begin{aligned} \text{Check } V_1 & \quad V_1 = 0.63 P = 9.3 \text{ kN} < 10.2 \text{ OK} \\ V_3 & \quad V_3 = 0.46 P = 6.8 \text{ kN} < 18.4 \text{ OK} \end{aligned}$$



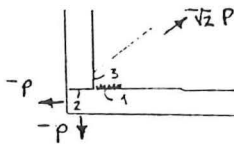
$$\begin{aligned} V_1 & \\ V_2 & \\ V_3 & \\ T_1 &= 37.2 \text{ kN} \end{aligned}$$

$$t_1 = 0.67 P \quad V_1 = 0.63 P$$

$$\left(\frac{0.67 P}{37.2}\right)^2 + \left(\frac{0.63 P}{10.2}\right)^2 < 1 \Rightarrow \boxed{P < 15.5 \text{ kN}}$$

$$\begin{aligned} \text{Check } V_2 &= 0.37 \times 15.5 = 5.7 < 5.9 \\ V_3 &= 0.33 \times 15.5 = 5.1 < 18.4 \end{aligned}$$

Joint 3 Plate Failure Loads



$$\begin{aligned} V_1 &= 10.2 \\ T_1 &= 37.2 \\ V_2 &= 5.9 \\ T_2 &= 21.7 \\ V_3 &= 18.4 \\ T_3 &= 28.8 \end{aligned}$$

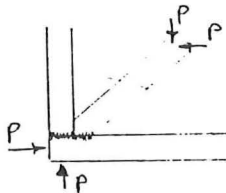
$$\begin{aligned} v_1 &= 0.68 P \\ t_1 &= 0.79 P \\ v_2 &= 0.32 P \\ t_2 &= v_3 \\ v_3 &= 0.21 P \\ t_3 &= v_2 \end{aligned}$$

see next page

$$1: \left(\frac{0.79 P}{37.2}\right)^2 + \left(\frac{0.68 P}{10.2}\right)^2 < 1 \Rightarrow \boxed{P < 14.3 \text{ kN}}$$

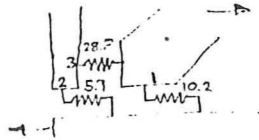
$$2: \left(\frac{0.21 P}{37.2}\right)^2 + \left(\frac{0.32 P}{10.2}\right)^2 = 0.46 \quad \checkmark$$

$$3: \left(\frac{0.21 P}{18.4}\right)^2 + \left(\frac{0.32 P}{28.8}\right)^2 = 0.23 \quad \checkmark$$



$$\begin{aligned} V_1 &= 0.63 P \\ t_1 &= 0 \\ V_2 &= 0.37 P \\ t_2 &= 0 \\ V_3 &= 0 \\ t_3 &= 0 \end{aligned}$$

$$0.63 P = 10.2 \Rightarrow \boxed{P < 16.1 \text{ kN}}$$

FRAME F3 / 3Distribution of forces in joint 3Horizontal

$$\begin{aligned}
 f_1 &= 10.2 \Delta_1 \\
 f_2 &= 5.9 \Delta_2 \\
 f_3 &= 28.8 (\Delta_1 - \Delta_2)
 \end{aligned}
 \quad
 \delta = \frac{\Delta_1}{\Delta_2} \Rightarrow \begin{cases} f'_1 = 10.2\delta \\ f'_2 = 5.9 \\ f'_3 = 28.8(\delta - 1) \end{cases}$$

$$f_2 = f_3 \Rightarrow \delta = 1.205$$

$$\begin{aligned}
 f'_1 &= 12.3 = \frac{12.3}{12.3 + 5.9} P = 0.68 P \\
 f'_2 &= 5.9 = 0.32 P \\
 &= f'_3
 \end{aligned}$$

Vertical

$$\begin{aligned}
 f_1 &= 37.2 \Delta_1 \\
 f_2 &= 21.7 \Delta_1 \\
 f_3 &= 18.4 (\Delta_1 - \Delta_2)
 \end{aligned}$$

$$\begin{aligned}
 f'_1 &= 37.2\delta = 81.8 = 0.79 P \\
 f'_2 &= 21.7 = 0.21 P \\
 \delta &= 2.18
 \end{aligned}$$

Classn:

THE PERFORMANCE OF LATERALLY LOADED CROSS-BRACED TIMBER
FRAMES

B.L. Deam

ABSTRACT: Laterally loaded cross-braced frames are identified as being ductile or non-ductile. Load-displacement characteristics and strength of frames and individual joints are determined from tests. Nailon plate is suitable for joints. Design data is presented for a particular Nailon plate connector.

Department of Civil Engineering, University of Canterbury
Master of Engineering Report, 1988.